Diarylheptanoids from *Dioscorea villosa* (Wild Yam)†

Shi-Hui Dong, Dejan Nikolic, Charlotte Simmler, Feng Qiu, Richard B. van Breemen, Djaja D. Soejarto, Guido F. Pauli, Shao-Nong Chen*

UIC/NIH Center for Botanical Dietary Supplements Research, Department of Medicinal Chemistry and Pharmacognosy, College of Pharmacy, University of Illinois at Chicago, Chicago, IL 60612, United States

† *Residual Complexity and Bioactivity*, Part 16 (see S1.)

*To whom correspondence should be addressed.

Tel: +1 (312) 996-7253; Fax: +1 (312) 996-7107; E-mail: sc4sa@uic.edu

Supporting Information

Table of Contents

S1. Publication Series *Residual Complexity and Bioactivity*

The present publication forms *Part 16* in a series of communications on *Residual Complexity and Bioactivity*.

From a **chemical perspective**, residual complexity (RC) refers to the subtle but significant convolution of major and minor chemical species in materials that originate from reaction mixtures, such as natural products. Because natural products are formed biosynthetically, they inherit a certain portion of side products from the metabolomic cocktail. This RC is frequently conserved in highly purified materials, even after an elaborate analytical separation scheme has been applied. The relationship between the (bio)synthetic cocktail and the products is perpetuated by the RC of the samples. In principle, RC affects all "pure" materials. RCs can be divided into two main groups: static RC describes the thermodynamically stable cases, whereas dynamic RC refers to situations where the impurity patterns change over time due to reactivity or other chemical change that occurs during the timeframe and under the conditions of the observation (e.g., a bioassay).

From a **biological perspective**, RC can have a major impact on bioactivity. Numerous forms of bioassays are widely used for the biological assessment (in vitro, ex vivo, in vivo) of bioactive agents. As many of the bioassays are mechanistically complex by nature, biological evaluation also can be residually complex. This adds a biological layer to the overall RC of bioactive agents and applies to various levels of chemical and biological complexity. Accordingly, both the chemical RC of the agent and the biological RC of the bioassay have to be considered when interpreting information about bioactivity.

As discussed in detail in Part 12 of the publication series (Journal of Natural Products, *75*: 1243-1255 (**2012**); see also below), the recognition and analysis of **RC can help establishing links between the observed biological activity and the underlying chemistry of bioactive agents**. The following table lists the preceding publications since 2008 which establish the publication series *Residual Complexity and Bioactivity*.

Part	**Reference**	**Brief Synopsis Regarding *Residual Complexity and Bioactivity***
Part 1	Jaki BU, Franzblau SG, Chadwick LR, Lankin DC, Zhang F, Wang Y, Pauli GF Purity Bioactivity Relationships – The Case of Anti-TB Active Ursolic Acid Journal of Natural Products *71*: 1742-1748 (**2008**) dx.doi.org/10.1021/np800329j	Demonstrates the relationship between purity, RC and anti-TB activity of different batches of a natural product; uses qHNMR methodology to establish quantitative relationships between purity/RC and activity.

Part 2	Chen S, Turner A, Jaki B, Nikolic D, van Breemen R, Friesen B, Pauli GF An Experimental Implementation of Chemical Subtraction Journal of Pharmaceutical and Biomedical Analysis *46*: 692-698 (**2008**) dx.doi.org/10.1016/j.jpba.2007.12.014	Performs selective removal of a single, interfering phytoconstituent from a bioactive (*E. coli* anti-adherence) fraction and demonstrates the presence of RC in the removed ("subtracted") compound and its assessment by qNMR and MS methods.
Part 3	Schinkovitz A, Pro S, Main M, Chen SN, Jaki BU, Lankin DC, Pauli GF The Dynamic Nature of the Ligustilide Complex Journal of Natural Products *71*: 1606-1611 (**2008**) dx.doi.org/10.1021/np800137n	Shows how RC is generated and varies in purified samples of ligustilide, a designated bioactive marker present in *Angelica* and *Ligusticum* species; compares analytical methods suitable to assess dynamic RC.
Part 4	Gödecke T, Chen SN, Lankin D, Nikolic D, van Breemen R, Pauli GF Phytochemistry of Cimicifugic Acids and Associated Bases in *Cimicifuga racemosa* Root Extracts Phytochemical Analysis *20*: 120-131 (**2009**) dx.doi.org/10.1002/pca.1106	Establishes the new phytochemical methodology that leads to the LC-MS-driven discovery of trace amounts of N-Methyl-serotonin as serotonergic active principle in black cohosh; demonstrates the relevance of low-abundance constituents (RC) as potential bioactive markers for metabolomic mixtures such a botanical extracts.
Part 5	Chen SN, Lankin D, Chadwick L, Jaki B, Pauli GF Dynamic Residual Complexity of Natural Products by qHNMR: Solution Stability of Desmethylxanthohumol Planta Medica 75: 757-762 (**2009**) dx.doi.org/10.1055/s-0028-1112209	Exemplifies how the dynamic form of RC can lead to the generation of a highly potent phytoestrogen (8-PN) from the inactive precursor (DMX); institutes qHNMR methodology to assess RC in a time-resolved fashion, enabling correlation with bioassay outcome.
Part 6	Pauli GF, Friesen B, Goedecke T, Farnsworth N, Glodny B Occurrence of Progesterone and Related Animal Steroids in Two Higher Plants Journal of Natural Products *73*: 338-345 (**2010**) dx.doi.org/10.1021/np9007415	Unambiguously demonstrates the unexpected occurrence of the mammalian steroid, progesterone, in higher plants and shows that small amounts of this hormone as well as mammalian-like steroid metabolites (e.g., 3-O-sulfates) can form a small but integral part of the RC of plant metabolomes.
Part 7	Molina-Salinas G, Rivas-Galindo V, Said-Fernández S, Lankin D, Muñoz M, Joseph-Nathan P, Pauli GF*, Waksman N* [*corresponding authors] Stereochemical Analysis of Leubethanol, an Anti-TB Active Serrulatane, from *Leucophyllum frutescens*	Establishes the subtle but significant diastereomeric difference between elisabethanol, which had been isolated from a gorgonian organism, and leubethanol, the anti-TB active lead compound isolated from a plant; utilizes VCD for the determination of absolute

	Journal of Natural Products *74*: 1842-1850 (**2011**) dx.doi.org/10.1021/np2000667	stereochemistry and emphasizes ^{1}H iterative full spin analysis (HiFSA) as a dereplication tool and for the analysis of RC of natural products.
Part 8	Gödecke T, Napolitano J, Yao P, Nikolic D, Dietz B, Bolton J, van Breemen R, Chen SN, Lankin D, Farnsworth N, Pauli GF Integrated standardization concept for *Angelica* botanicals using quantitative NMR Fitoterapia *83*: 18-32 (**2012**) dx.doi.org/10.1016/j.fitote.2011.08.017	Establishes a qHNMR-based protocol for the simultaneous quantitation of multiple marker compounds in the bioactive fraction ([anti-]estrogenicity, cytotoxicity) of *Angelica sinensis* botanicals; demonstrates the advanced role qHNMR can have in botanical standardization and evaluation of RC of the plant extracts.
Part 9	Qiu F, Imai A, McAlpine J, Lankin D, Burton I, Karakach T, Farnsworth N, Chen SN, Pauli GF Dereplication, Residual Complexity and Rational Naming - the Case of the *Actaea* Triterpenes Journal of Natural Products *75*: 432-443 (**2012**) dx.doi.org/10.1021/np200878s	Determines the RC of purified botanical reference materials of triterpenes from black cohosh; demonstrates the assessment of RC by computer-aided dereplication using classification binary trees (CBTs) to derive both structural information and quantitative measures for minor components contained in residually complex samples.
Part 10	Napolitano J, Gödecke T, Rodriguez Brasco MF, Jaki BU, Chen SN, Lankin DC, Pauli GF The Tandem of Full Spin Analysis and qHNMR for the Quality Control of Botanicals Exemplified with *Ginkgo biloba* Journal of Natural Products *75*: 238-248 (**2012**) dx.doi.org/10.1021/np200949v	Establishes ^{1}H iterative full spin analysis (HiFSA)as the basis of a qHNMR approach for the parallel quantitation of eight bioactive markers in *Ginkgo biloba*; exemplifies how multi-target standardization can be achieved without the need for identical calibrants in (residually) complex samples including reference materials, fractions, and extracts; addresses the role of RC in reference materials of calibrants.
Part 11	Qiu F, Friesen JB, McAlpine JB, Pauli GF NMR-based Design of Countercurrent Separation of *Ginkgo biloba* Terpene Lactones Journal of Chromatography A *1242*: 26-34 (**2012**) dx.doi.org/10.1016/j.chroma.2012.03.081	Introduces the use of qHNMR for both the design and the analysis of countercurrent separation (CS) of bioactive botanical markers; demonstrates the measurement of partition coefficients of target markers in mixtures; performs the evaluation of chromatographic orthogonality in CS; establishes quantitative links between predicted and measured chromatographic CS performance and the RC of the purified markers.

Part 12	Pauli GF, Chen SN, Friesen JB, McAlpine J, Jaki BU Analysis and Purification of Bioactive Natural Products - The AnaPurNa Study Journal of Natural Products, *75*: 1243-1255 (**2012**) dx.doi.org/10.1021/np300066q	Comprehensive meta-analysis of the literature (1999-2010) focusing on the role of analytical methodology in the purification and characterization of bioactive compounds from natural sources; addresses the role of RC in their purification and characterization and discusses the impact of RC on the biological evaluation and validation of lead compounds.
Part 13	Napolitano J, Lankin D, Chen SN, Pauli GF Complete ^{1}H NMR Spectral Analysis of Ten Chemical Markers of *Ginkgo biloba* Magnetic Resonances in Chemistry *50*: 569-575 (**2012**) dx.doi.org/10.1002/mrc.3829	Establishes the methodology for the generation of unambiguous ^{1}H NMR fingerprints of bioactive markers, exemplified for terpene lactones and flavonoids from *Ginkgo biloba*; the fingerprints are suitable for both structural dereplication and qHNMR quantitation at various levels of RC, can be scaled to all existing NMR field strength and are independent of instrumentation.
Part 14	Riihinen K, Gödecke T, Pauli GF Purification of Berry Flavonoids by Long-bed Gel Permeation Chromatography Journal of Chromatography A, *1244*: 20-27 (**2012**) dx.doi.org/10.1016/j.chroma.2012.04.060	Establishes long-bed gel permeation chromatography (GPC) on Sephadex LH-20 as an efficient method for the purification of bioactive berry polyphenols; despite its capability to resolve closely related compounds, qHNMR analysis reveals an un expected degree of RC in the GPC fractions.
Part 15	Inui T, Wang Y, Pro S, Franzblau SG, Pauli GF Unbiased Evaluation of Bioactive Secondary Metabolites in Complex Matrices Fitoterapia *83*: 1218-1225 (**2012**) dx.doi.org/10.1016/j.fitote.2012.06.012	Establishes biochemometric methodology capable of identifying bioactive principles in crude metabolomic mixtures, as an alternative to bioassay-guided fractionation; establishes chemometric links between the bioassay and the preparative and analytical chemistry of (residually) complex natural products; exemplifies the concept for the anti-TB active principles of the ethnobotanical, *Oplopanax horridus*.

S2. LC-MS profiles for compound **11**: isolated compound (S1-1), and detection in the crude extracts of BC-601 (S1-2) and BC-630 (S1-3).

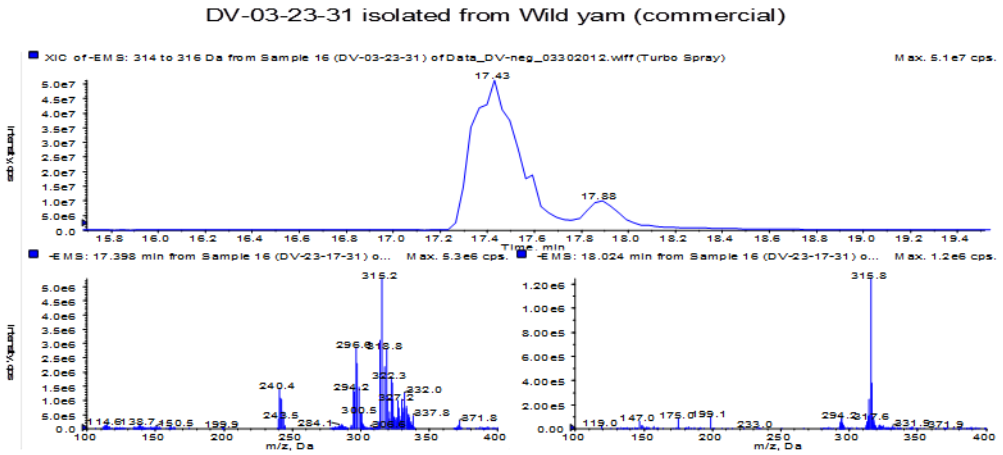

Figure S1-1. LC-MS profile for compound **11**

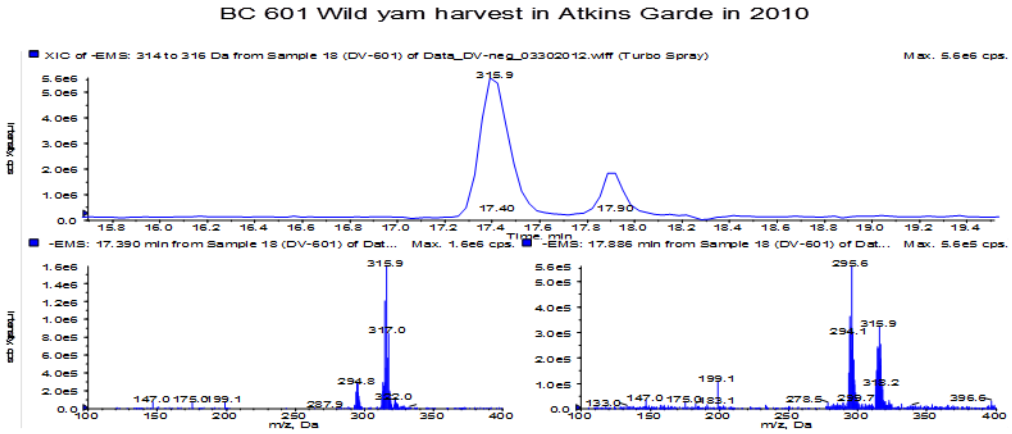

Figure S1-2. LC-MS profile for compound **11** in BC-601

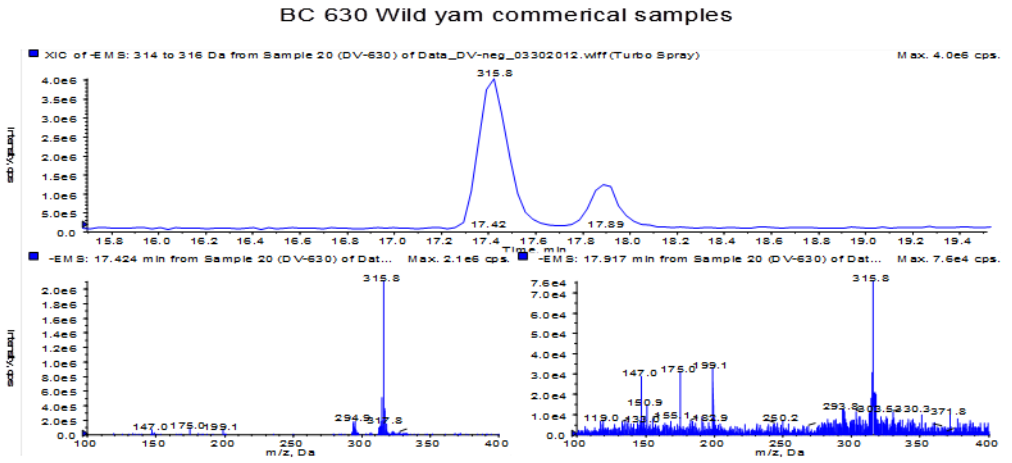

Figure S1-3. LC-MS profile for compound **11** in BC-630

S3. ^{1}H NMR spectra of all primary fractions obtained by C-18 SPE fractionation of the crude extract of *Dioscorea villosa*

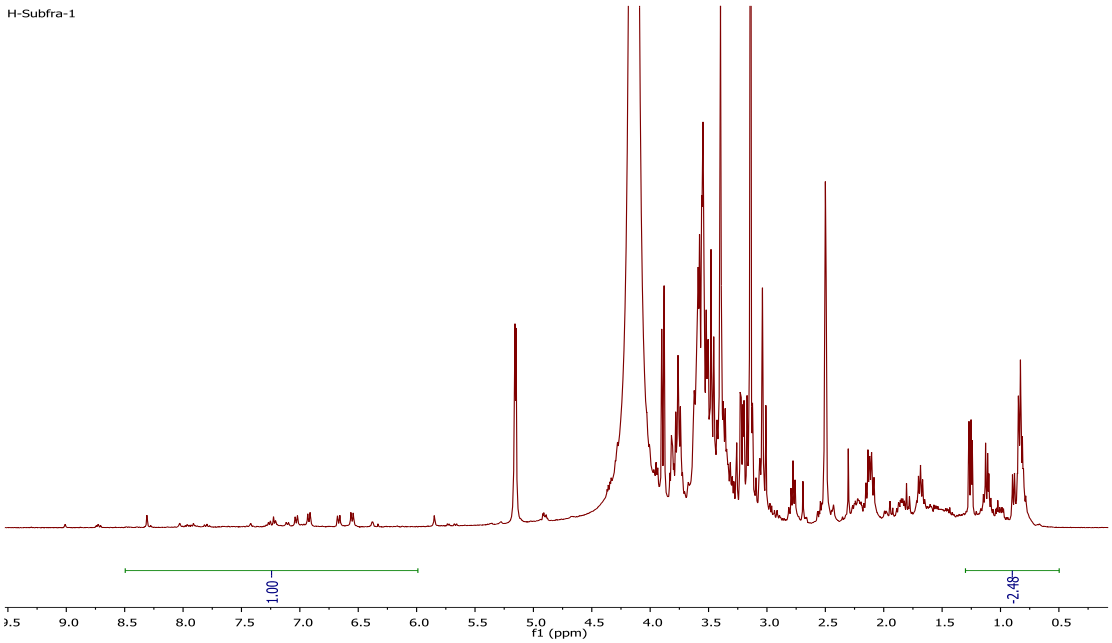

Figure S3-1. ^{1}H NMR spectrum of primary subfraction 1

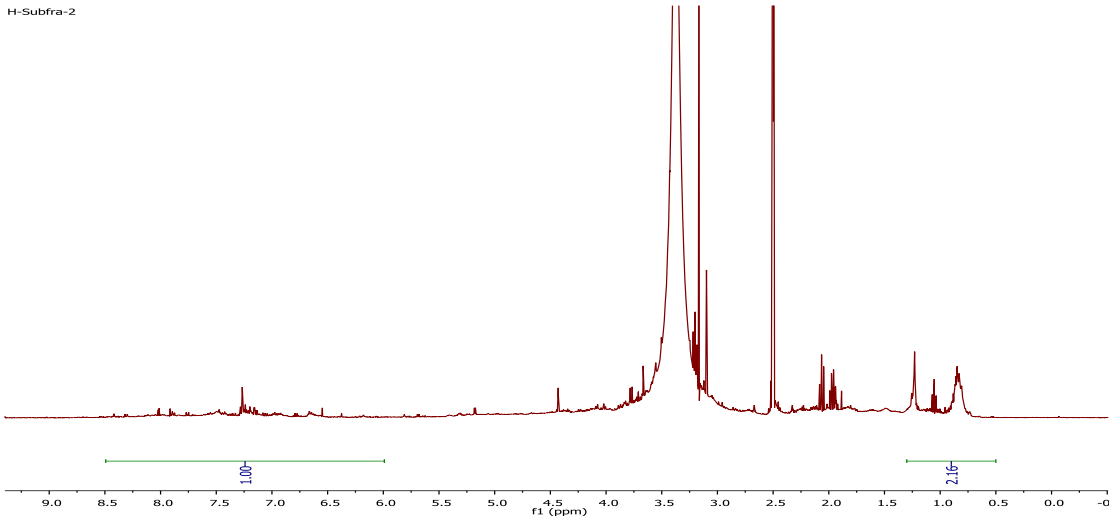

Figure S3-2. ^{1}H NMR spectrum of primary subfraction 2

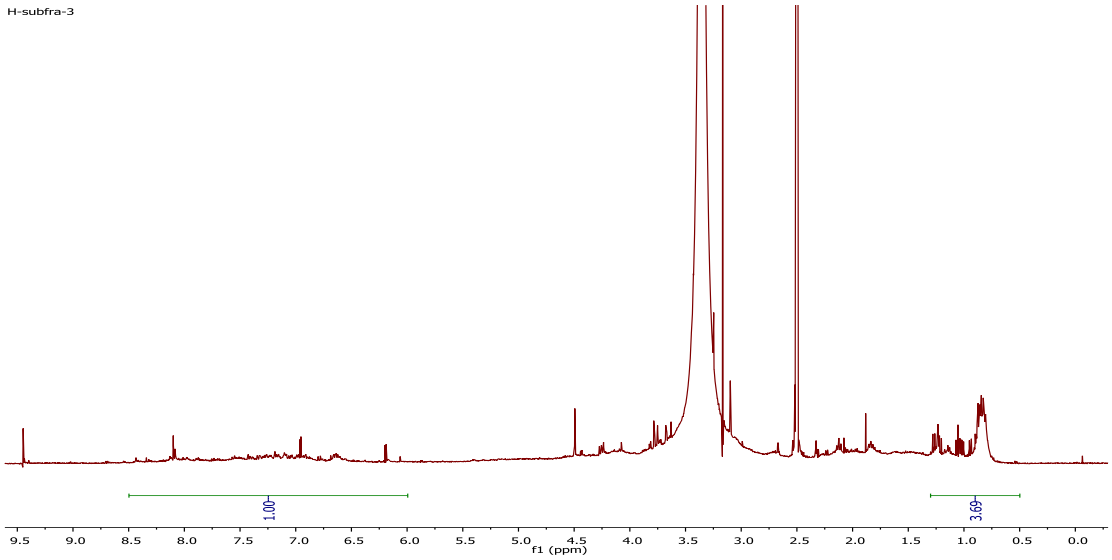

Figure S3-3. ^{1}H NMR spectrum of primary subfraction 3

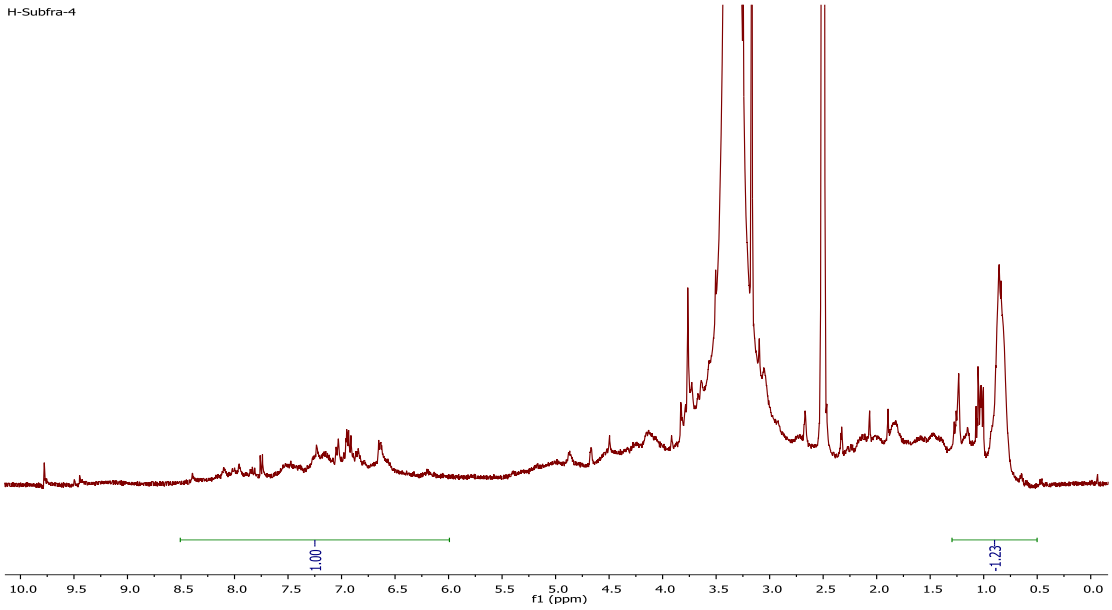

Figure S3-4. ^{1}H NMR spectrum of primary subfraction 4

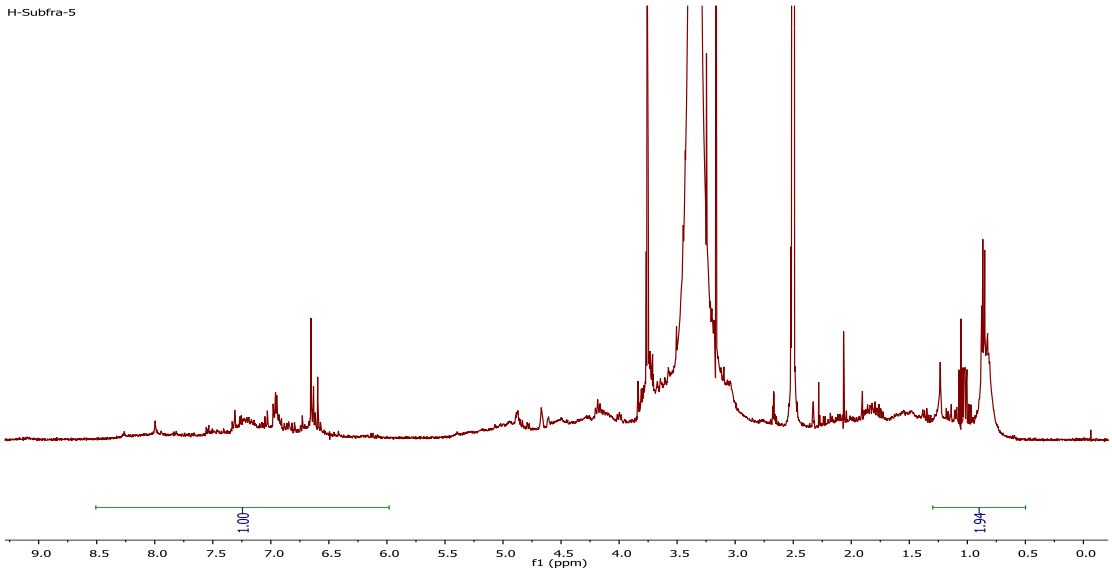

Figure S3-5. ^{1}H NMR spectrum of primary subfraction 5

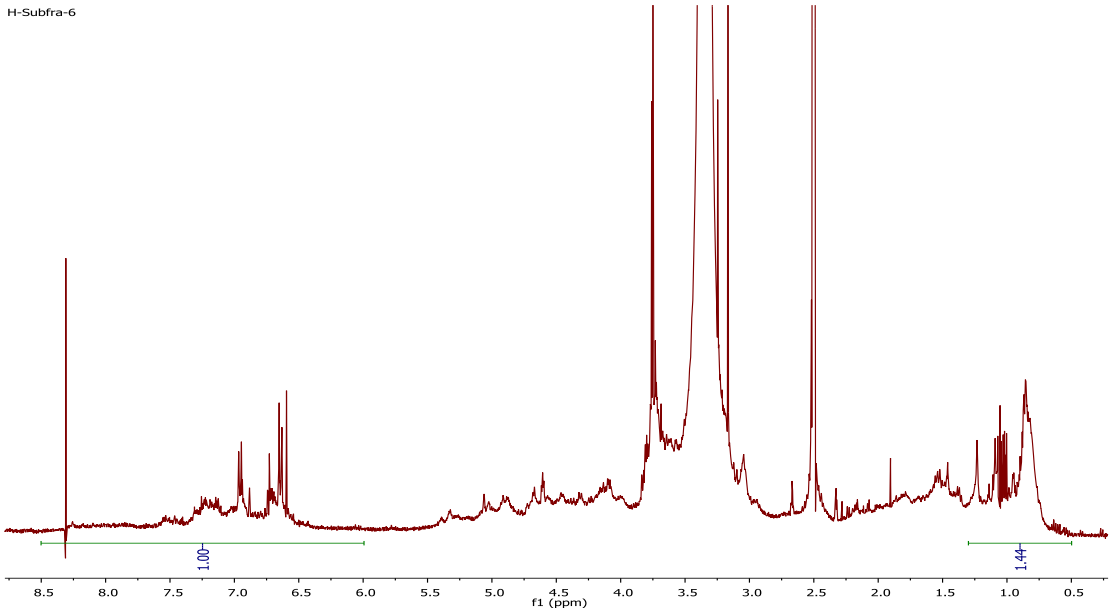

Figure S3-6. ^{1}H NMR spectrum of primary subfraction 6

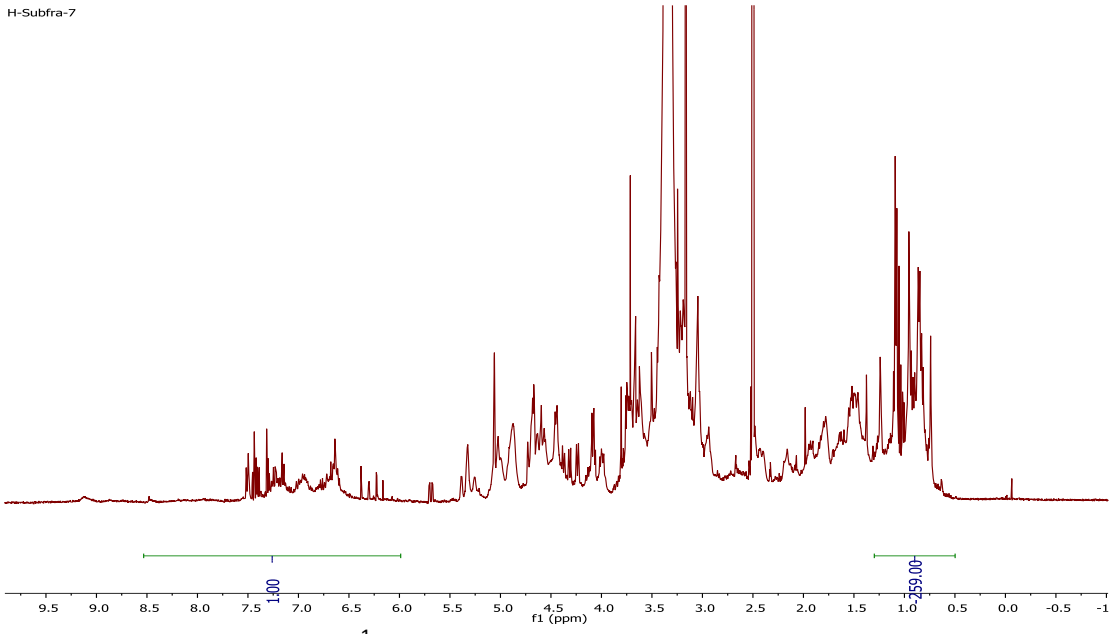

Figure S3-7. ^{1}H NMR spectrum of primary subfraction 7

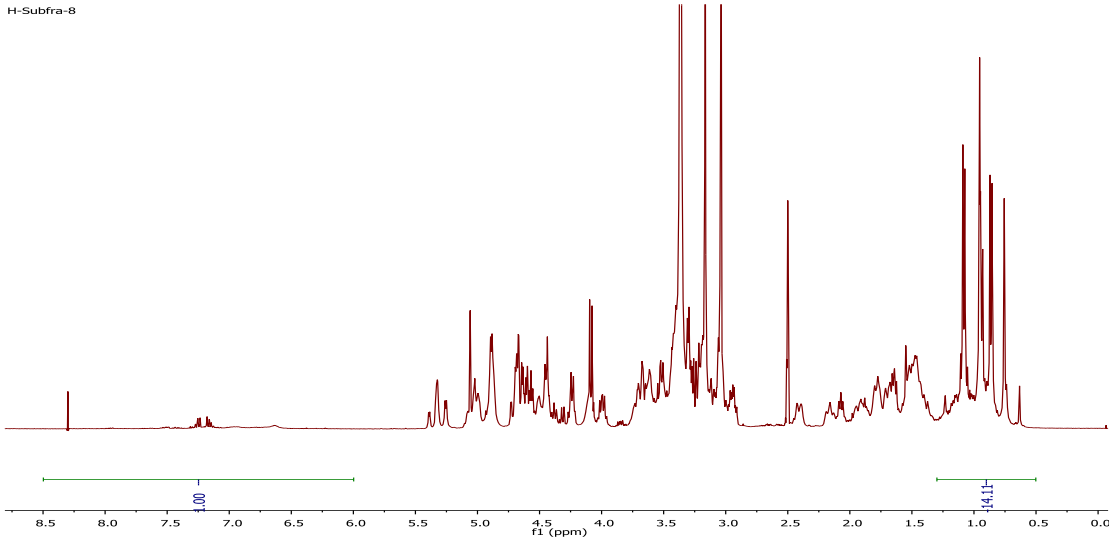

Figure S3-8. ^{1}H NMR spectrum of primary subfraction 8

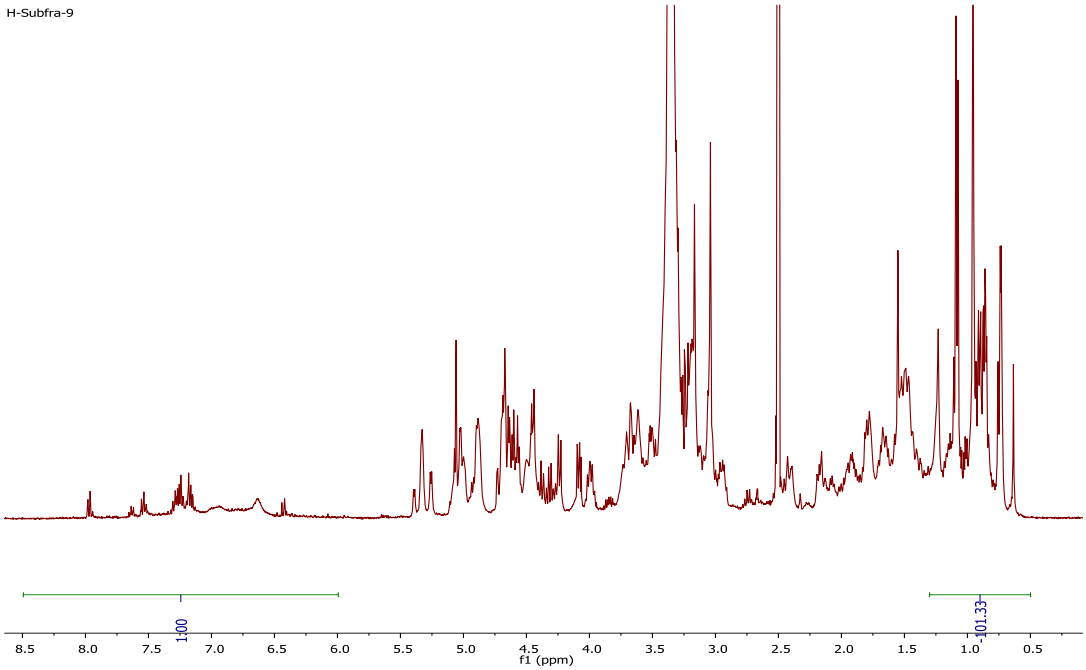

Figure S3-9. ^{1}H NMR spectrum of primary subfraction 9

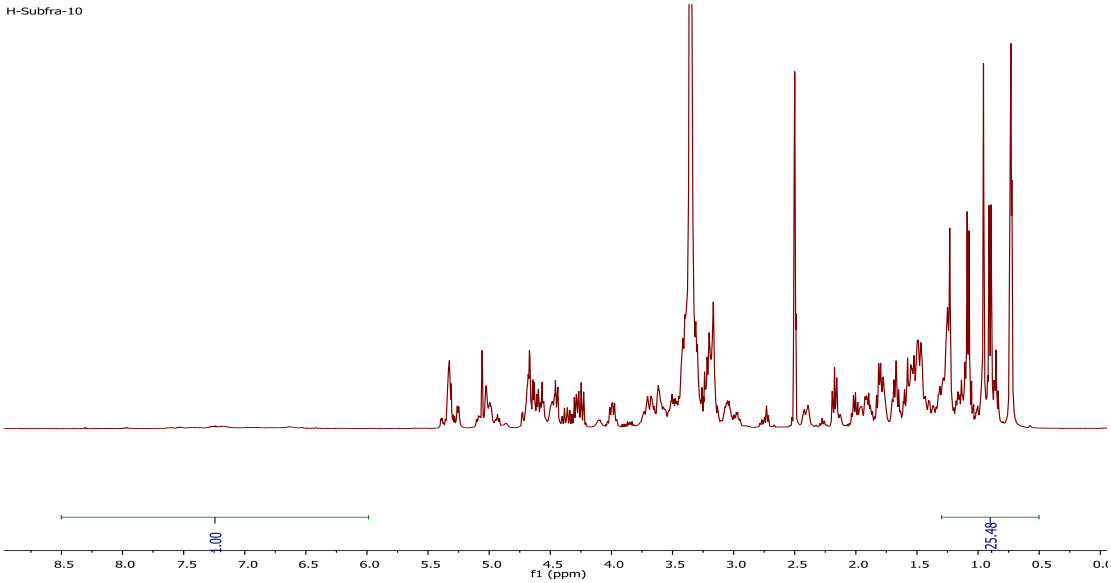

Figure S3-10. ^{1}H NMR spectrum of primary subfraction 10

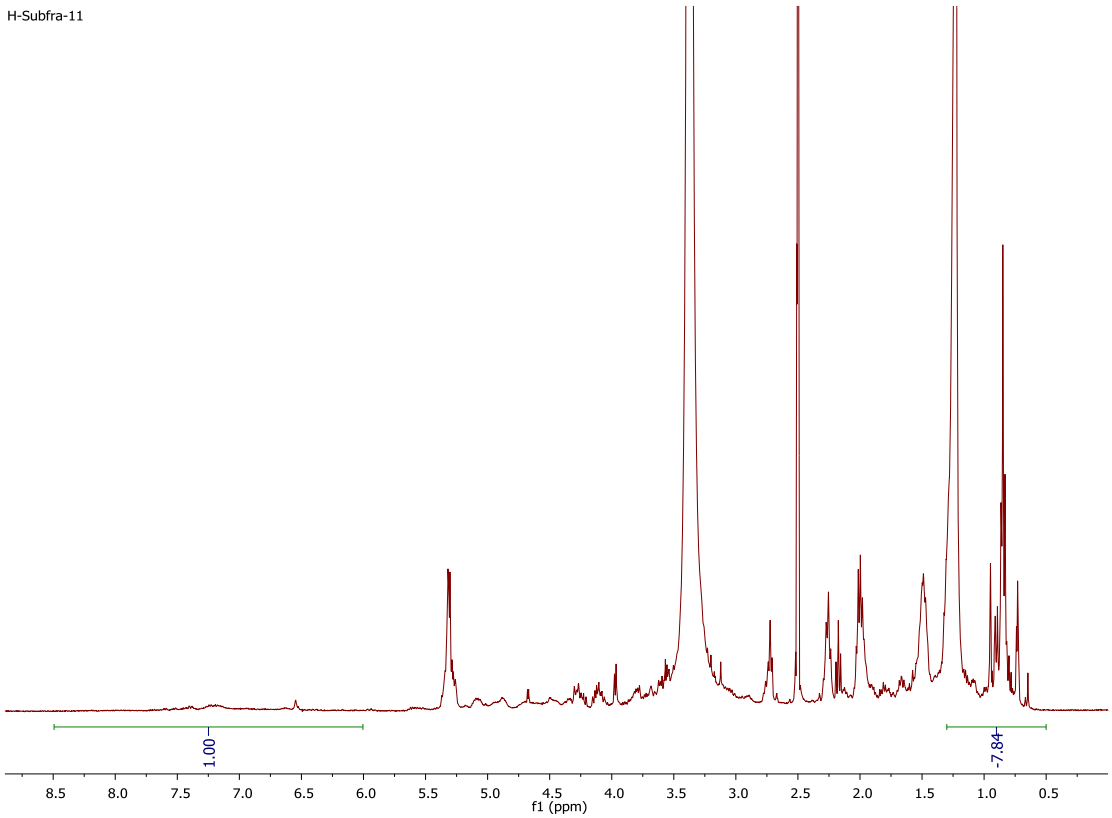

Figure S3-11. ^{1}H NMR spectrum of primary subfraction 11

S4. ^{1}H NMR iterative full spin analysis of **1**–**7** in CD_3OD

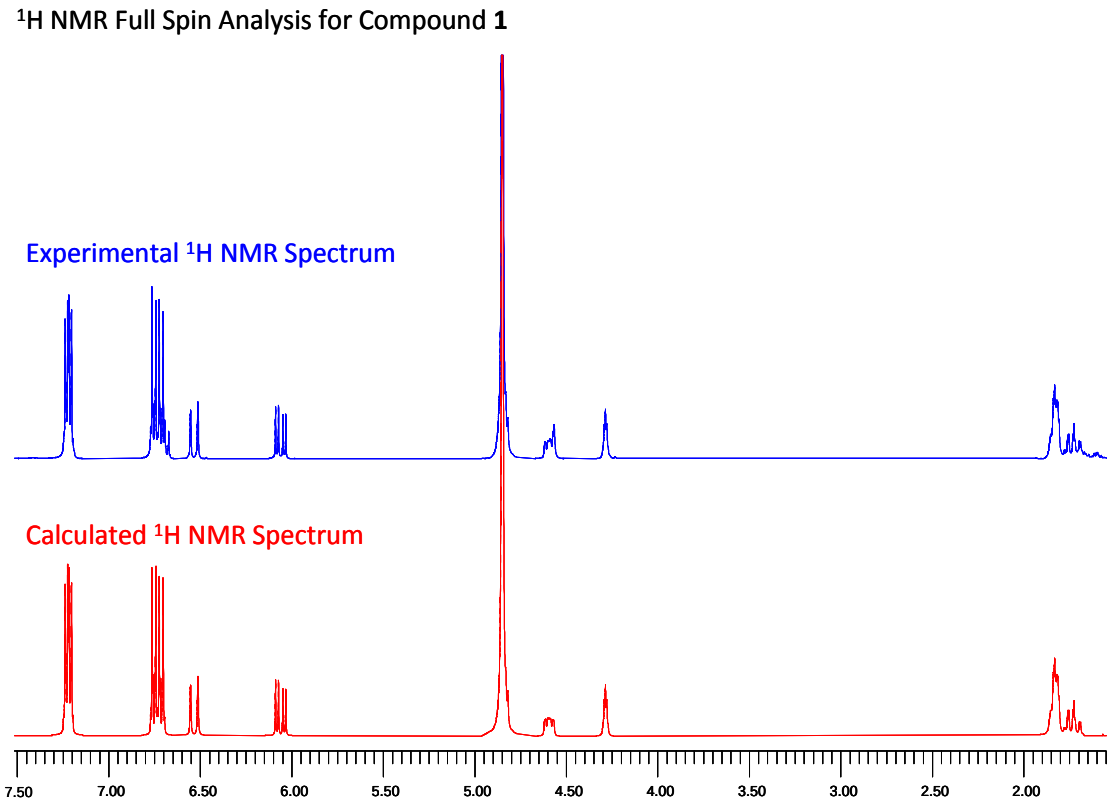

Figure S4-1. ^{1}H NMR iterative full spin analysis of **1** in CD_3OD

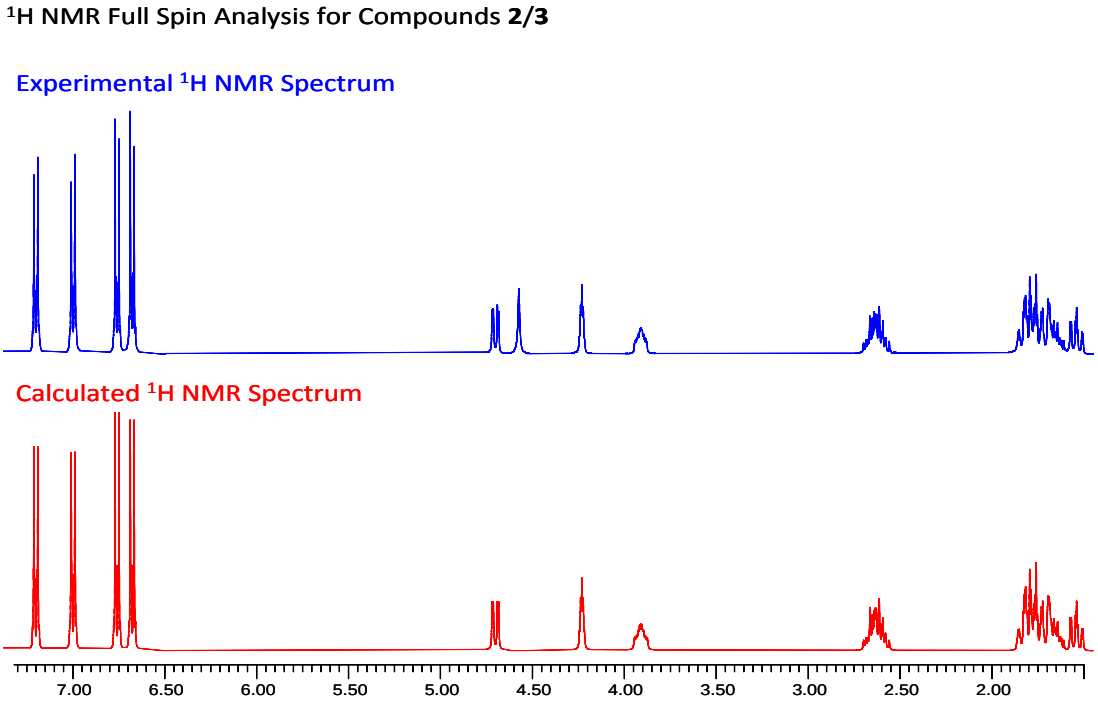

Figure S4-2. ^{1}H NMR iterative full spin analysis of **2**/**3** in CD_3OD

^{1}H NMR Full Spin Analysis for Compounds **4/5**

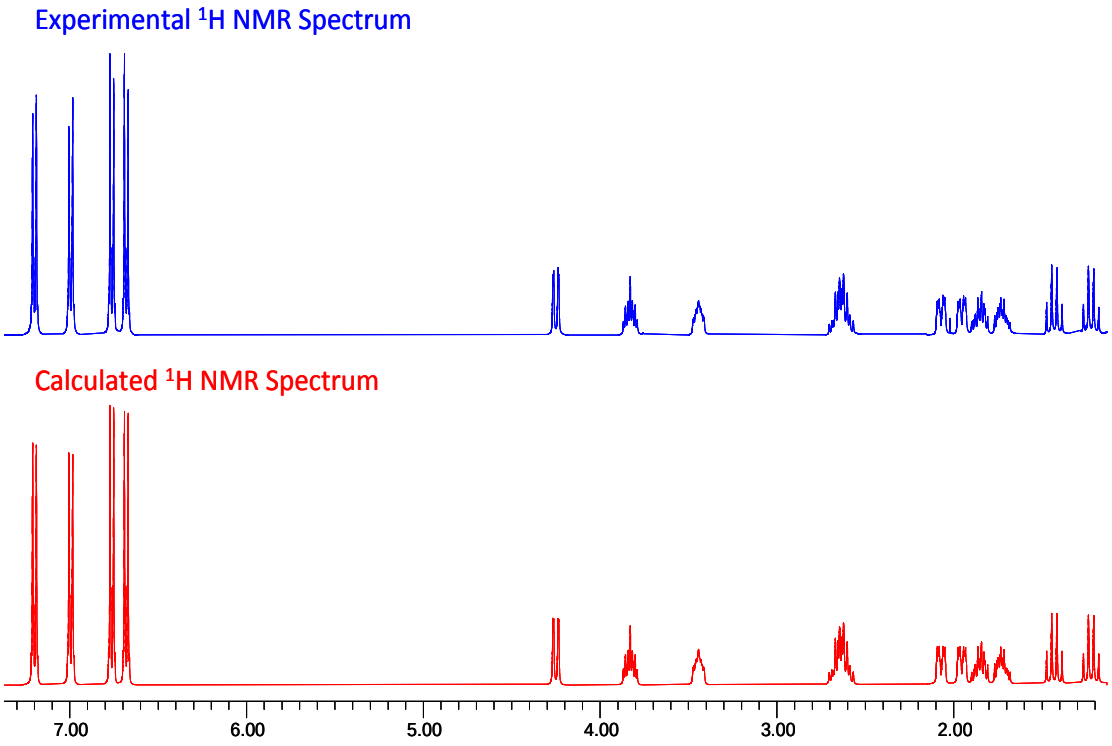

Figure S4-3. ^{1}H NMR iterative full spin analysis of **4/5** in CD_3OD

^{1}H NMR Full Spin Analysis for Compound **6/7**

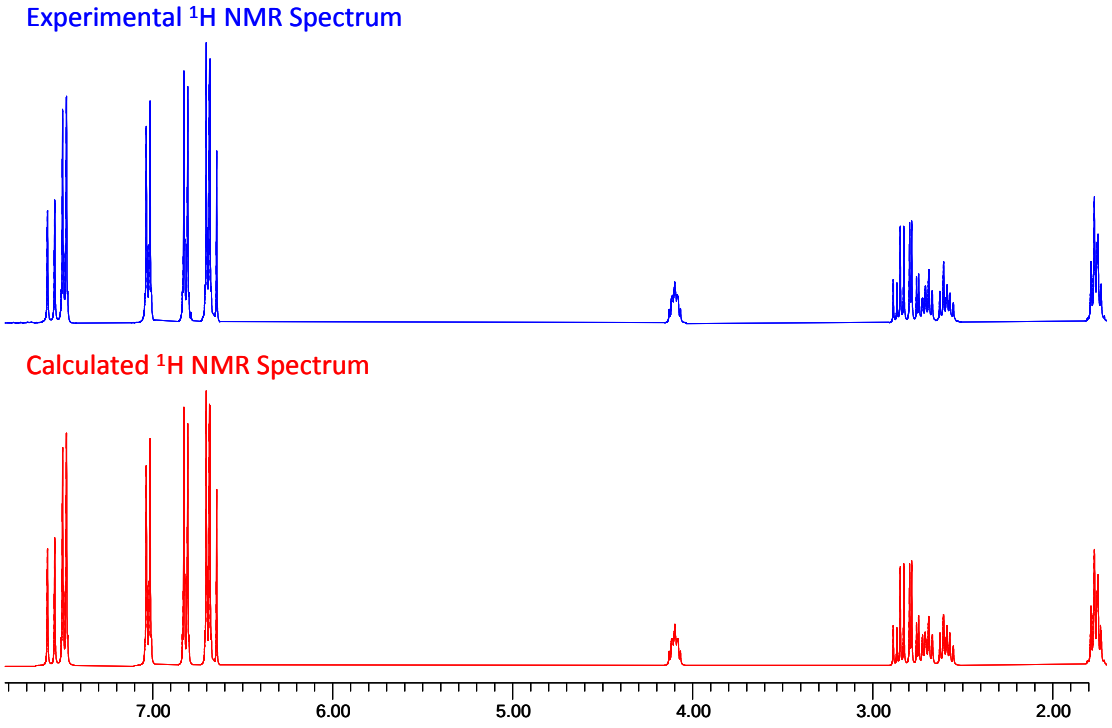

Figure S4-4. ^{1}H NMR iterative full spin analysis of **6/7** in CD_3OD

S5. ^{1}H NMR spectrum of **1** in $CD_3OD/CDCl_3$ (10:1)

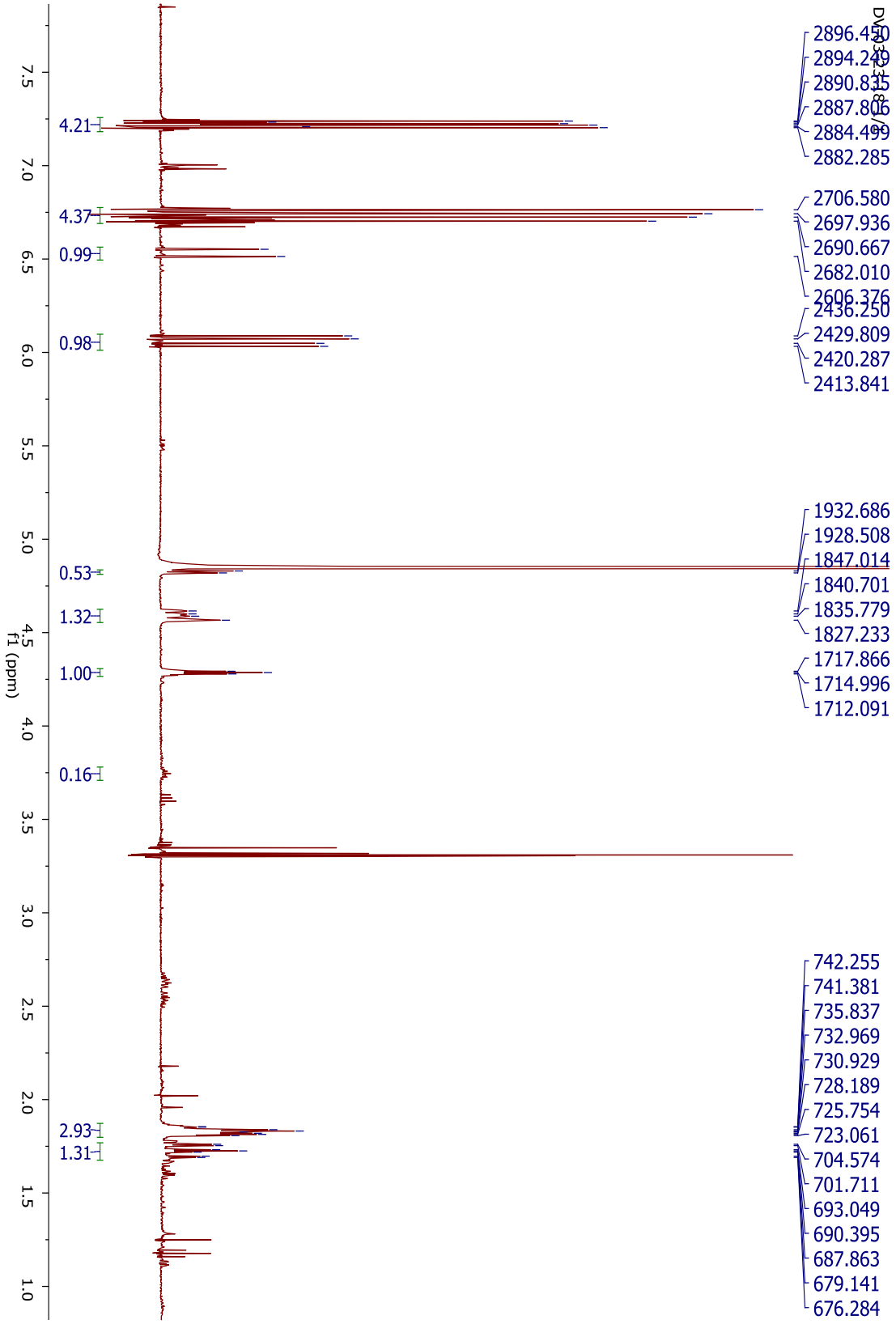

S6. ^{13}C NMR spectrum of **1** in $CD_3OD/CDCl_3$ (10:1)

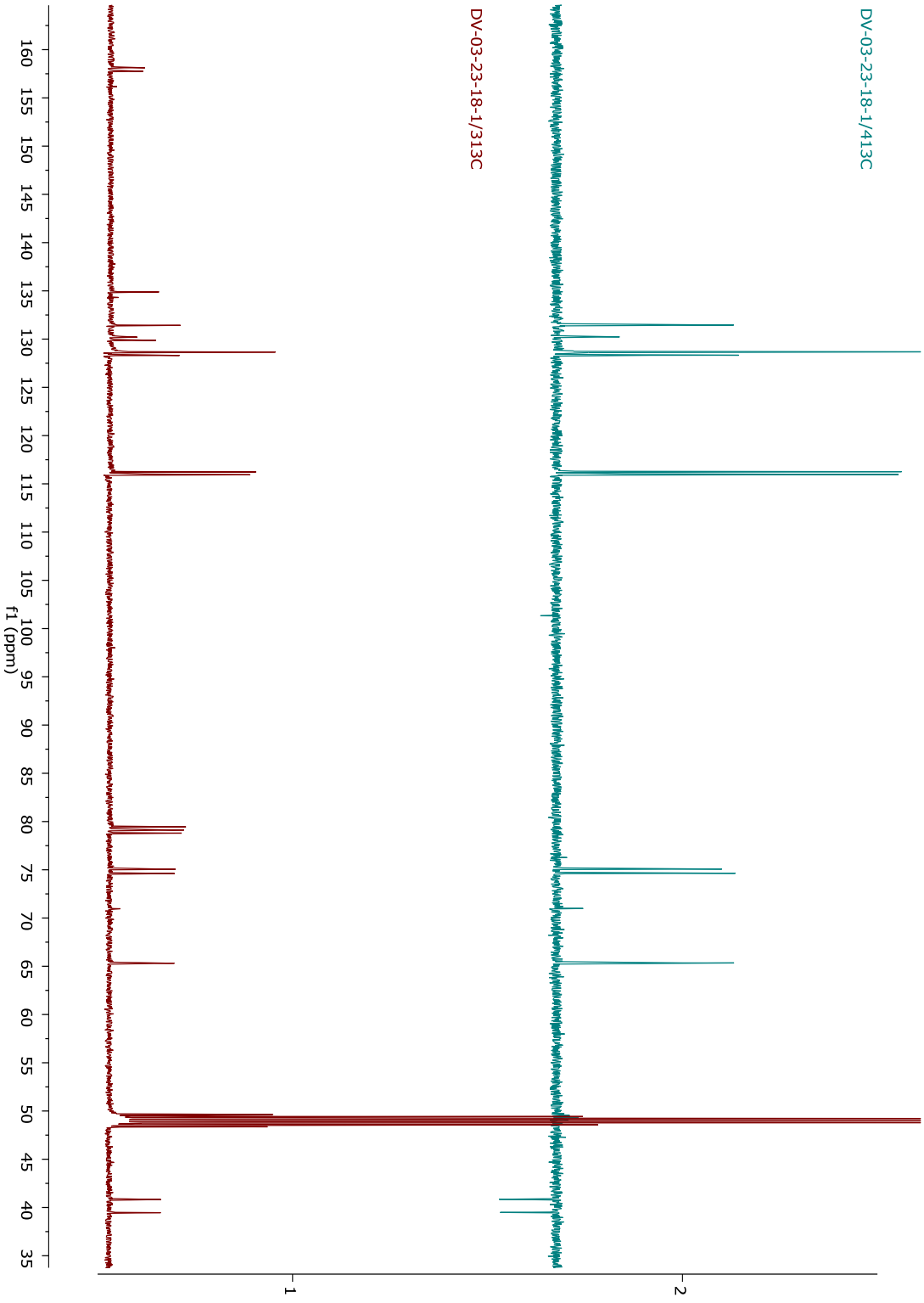

S7. $^{1}H–^{1}H$ COSY spectrum of **1** in $CD_3OD/CDCl_3$ (10:1)

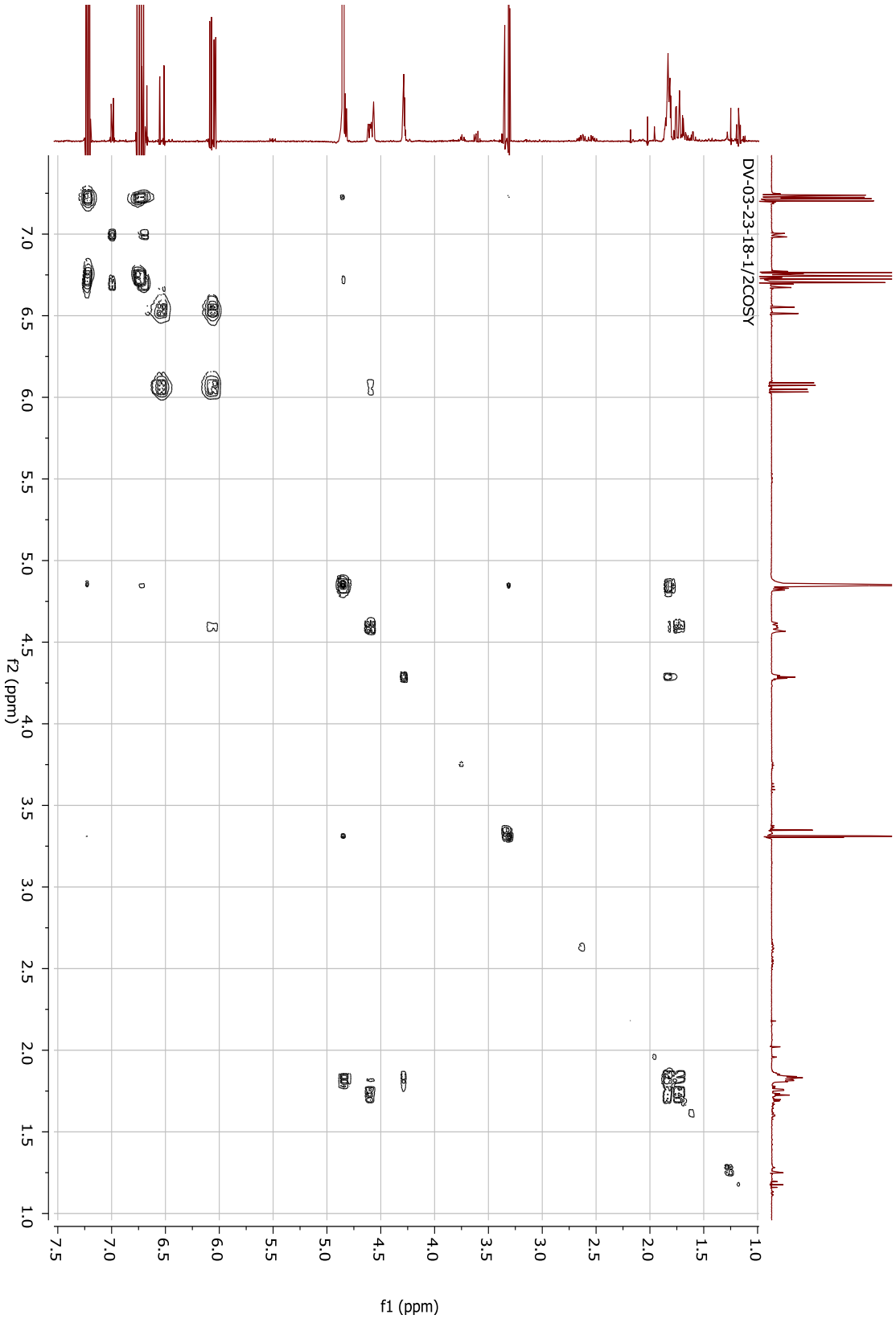

S8. HSQC spectrum of **1** in $CD_3OD/CDCl_3$ (10:1)

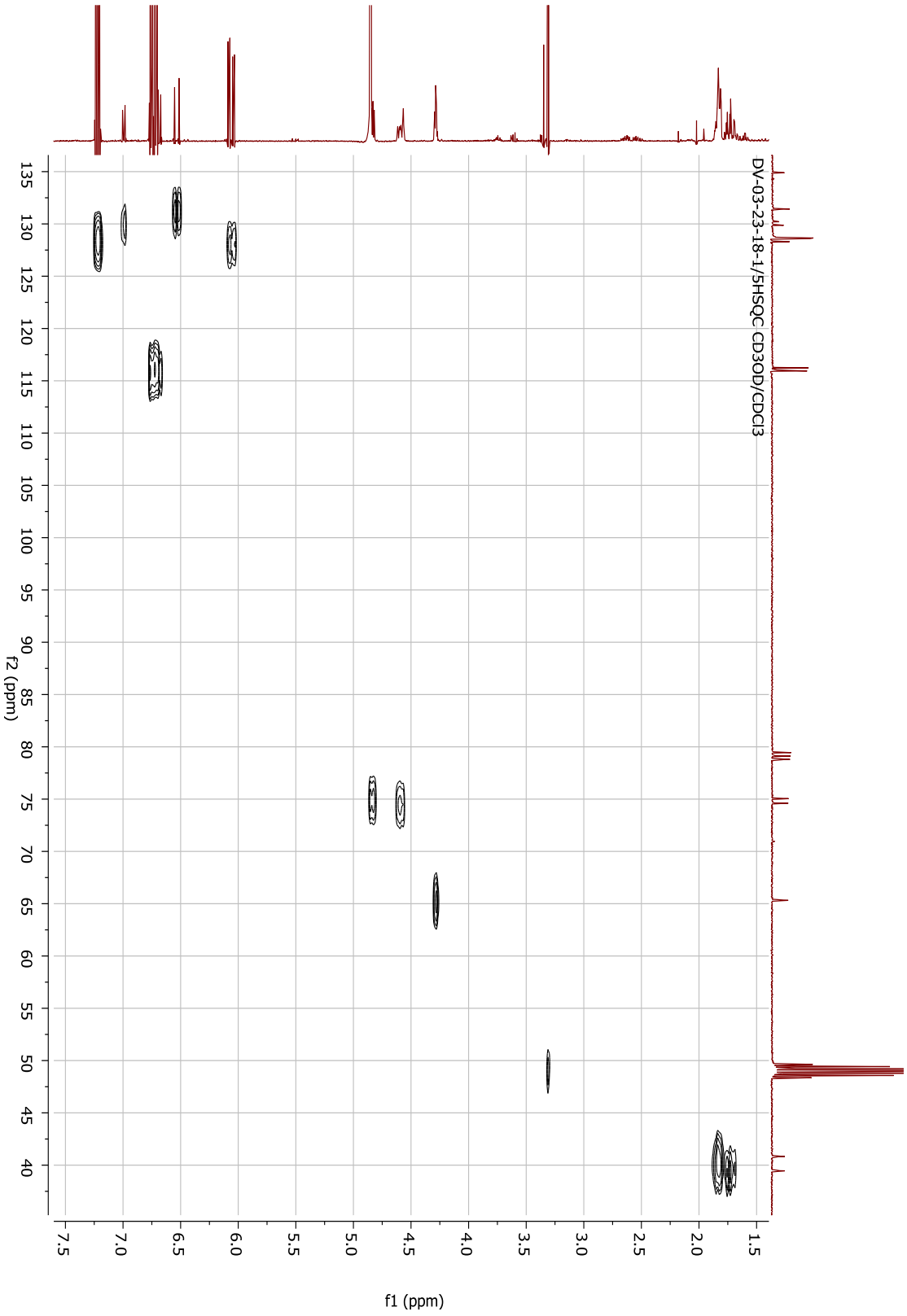

S9. HMBC spectrum of **1** in $CD_3OD/CDCl_3$ (10:1)

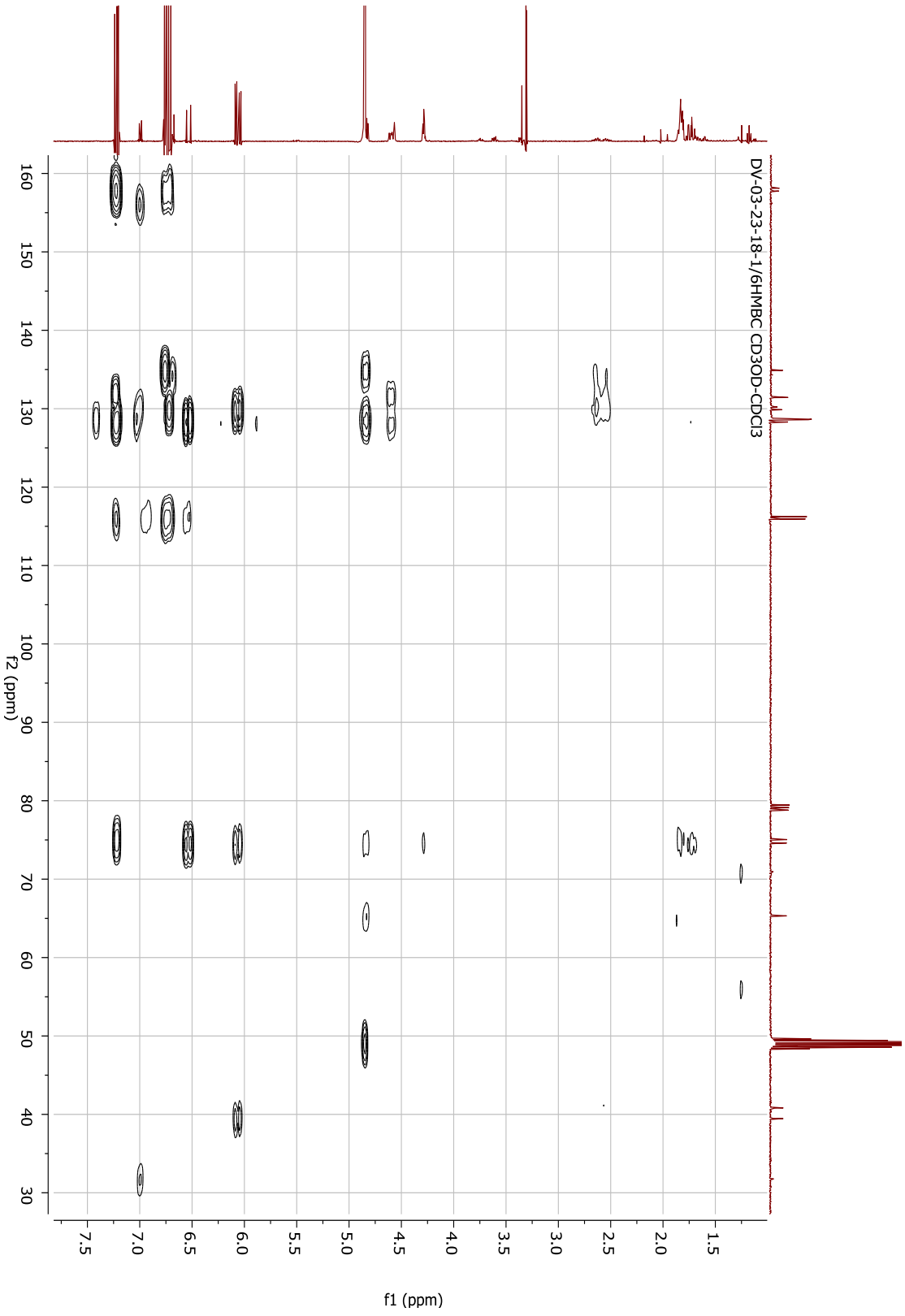

S10. ROESY spectrum of **1** in $CD_3OD/CDCl_3$ (10:1)

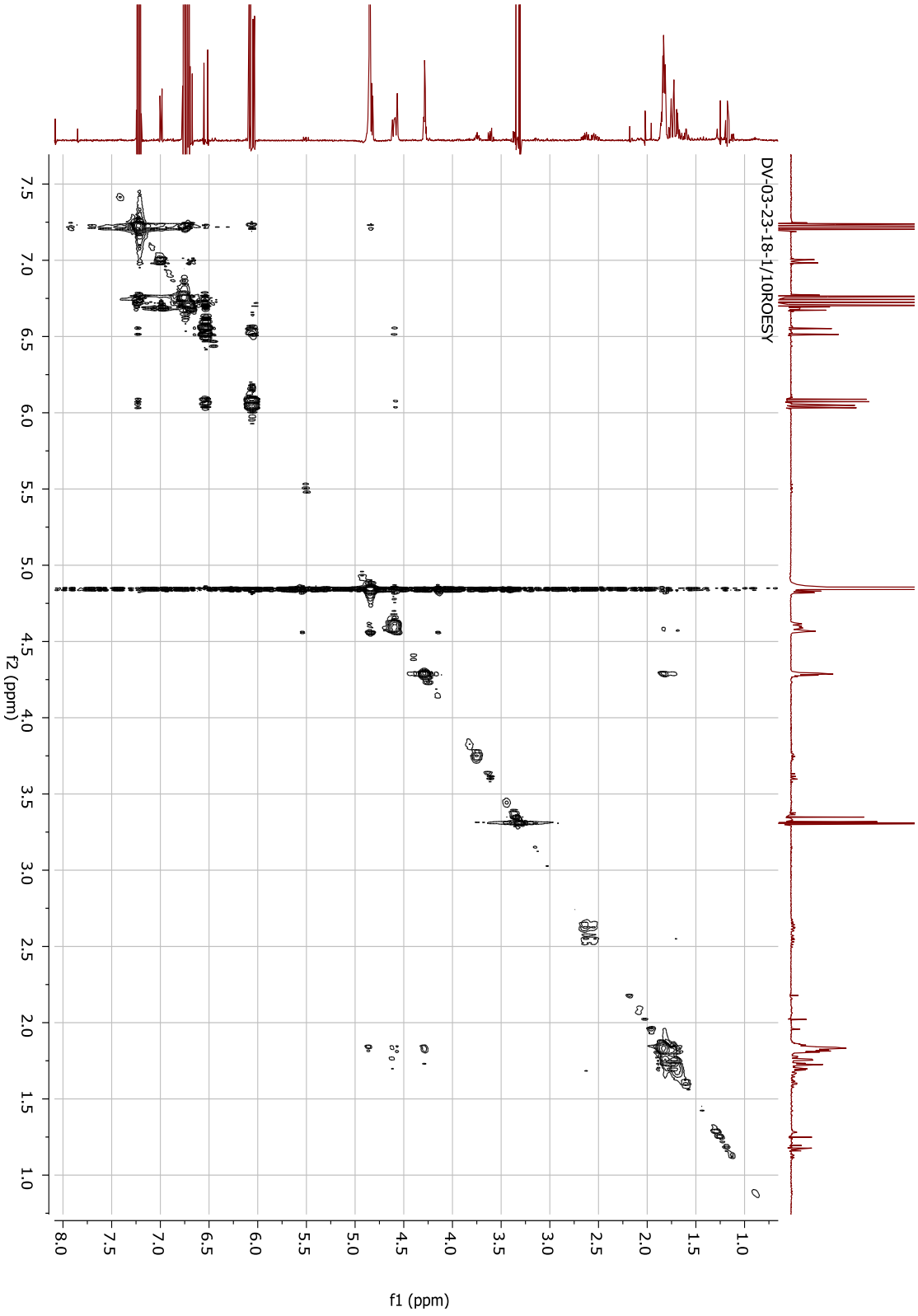

S11. IR (film/ATR) spectrum of **1**

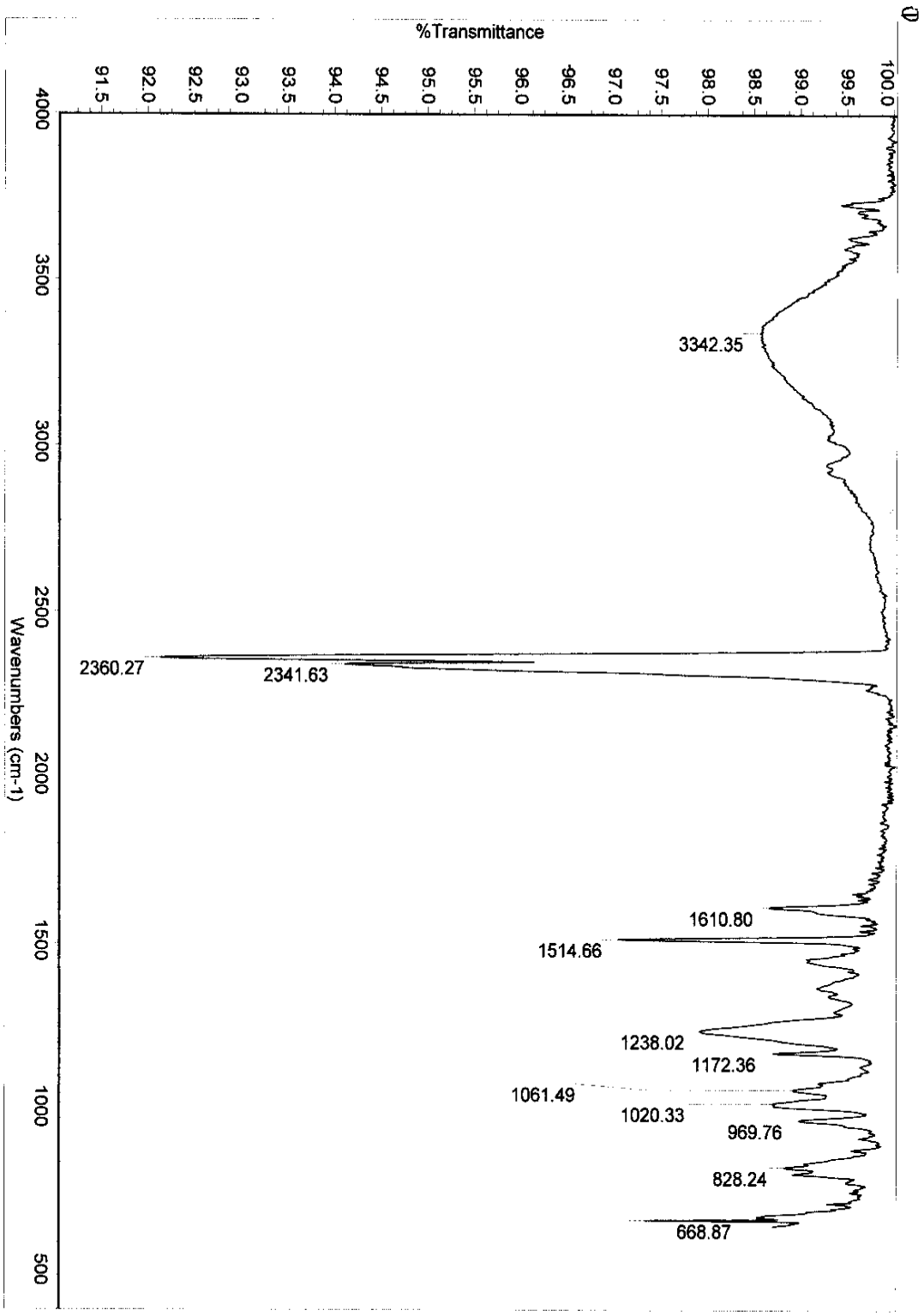

S12. ^{1}H NMR spectrum of **2**/**3** in CD_3OD

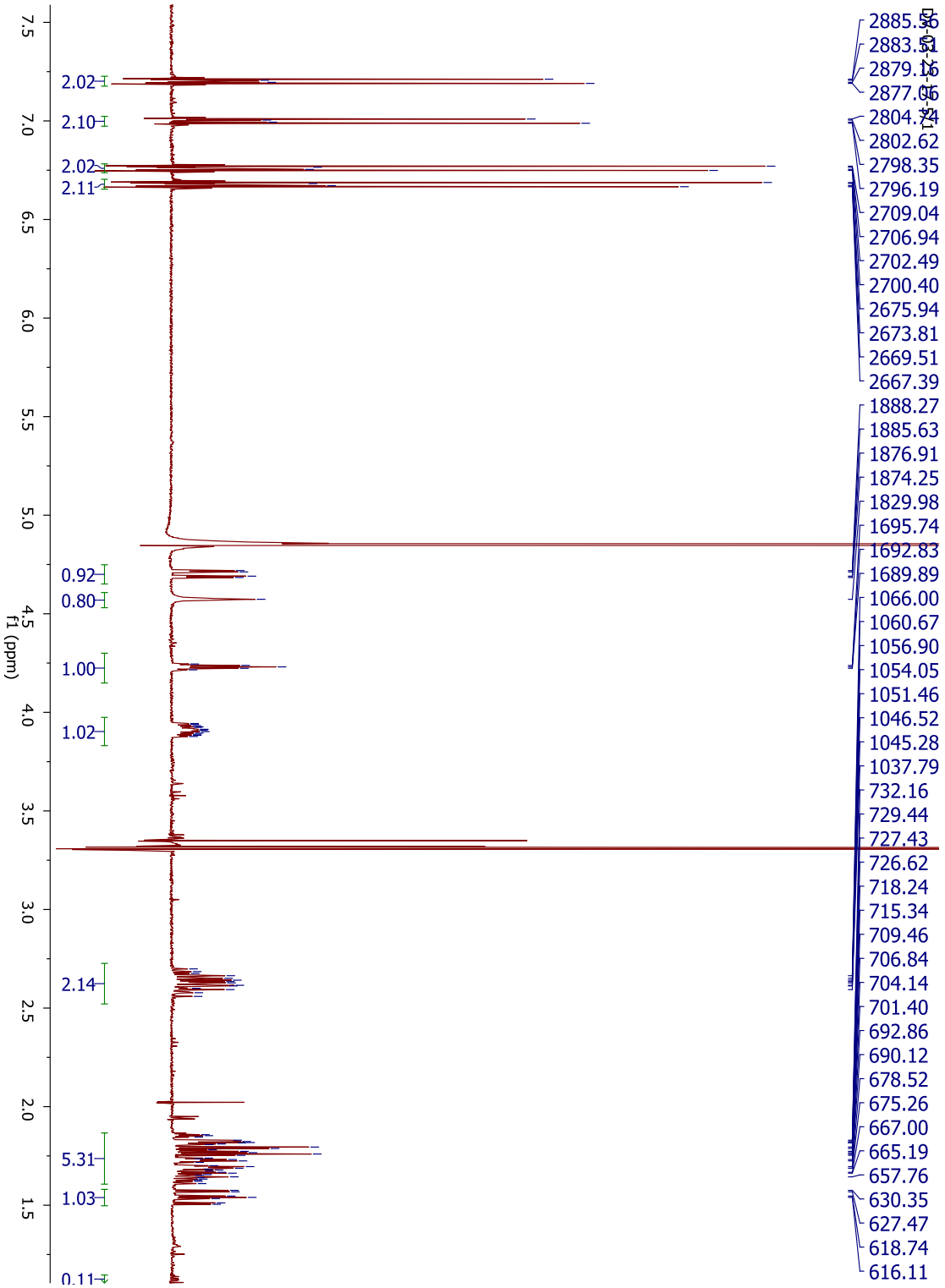

S13. ^{13}C NMR spectrum of **2/3** in CD_3OD

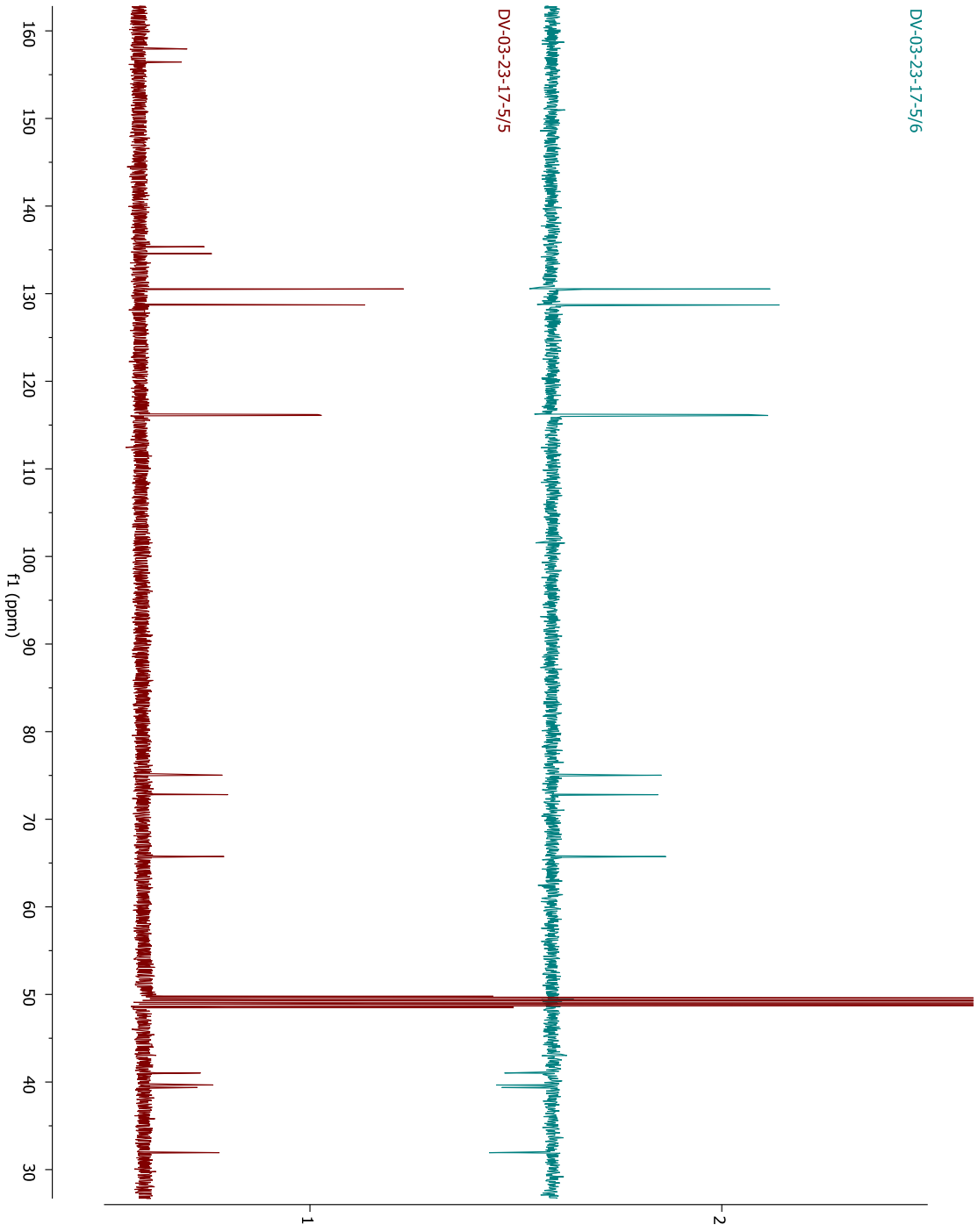

S14. ^{1}H–^{1}H COSY spectrum of **2**/**3** in CD_3OD

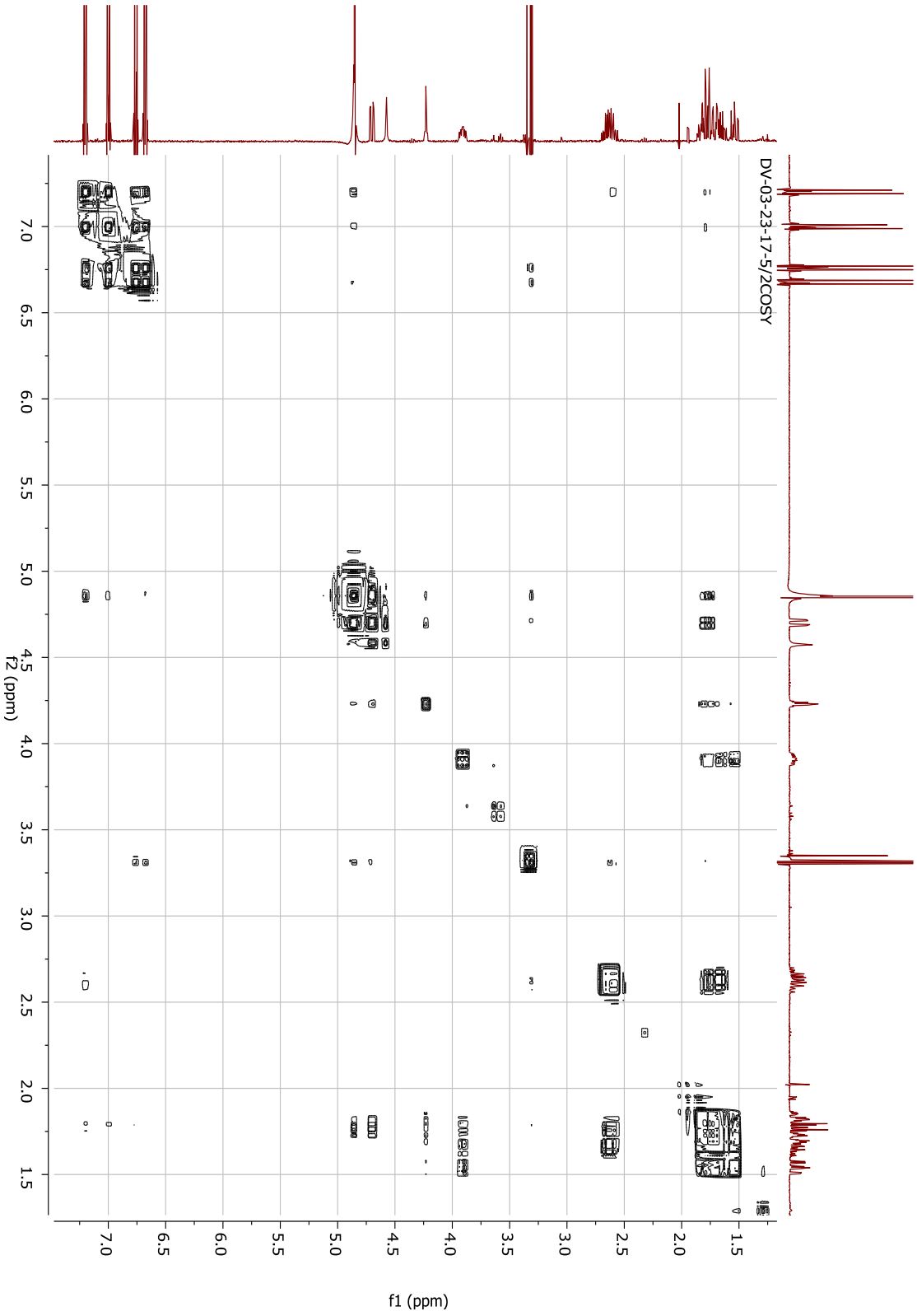

S15. HSQC spectrum of **2**/**3** in CD_3OD

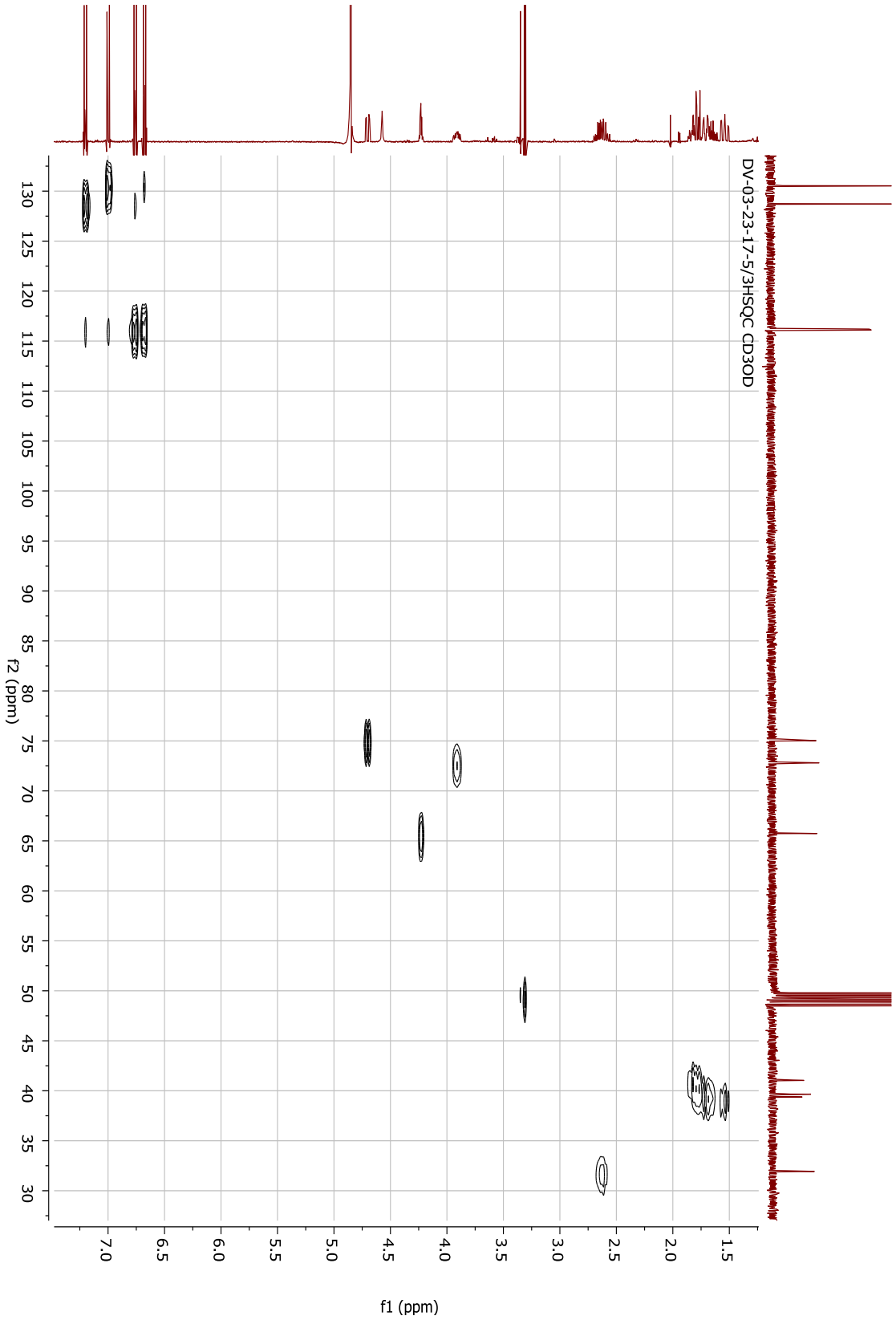

S16. HMBC spectrum of **2**/**3** in CD_3OD

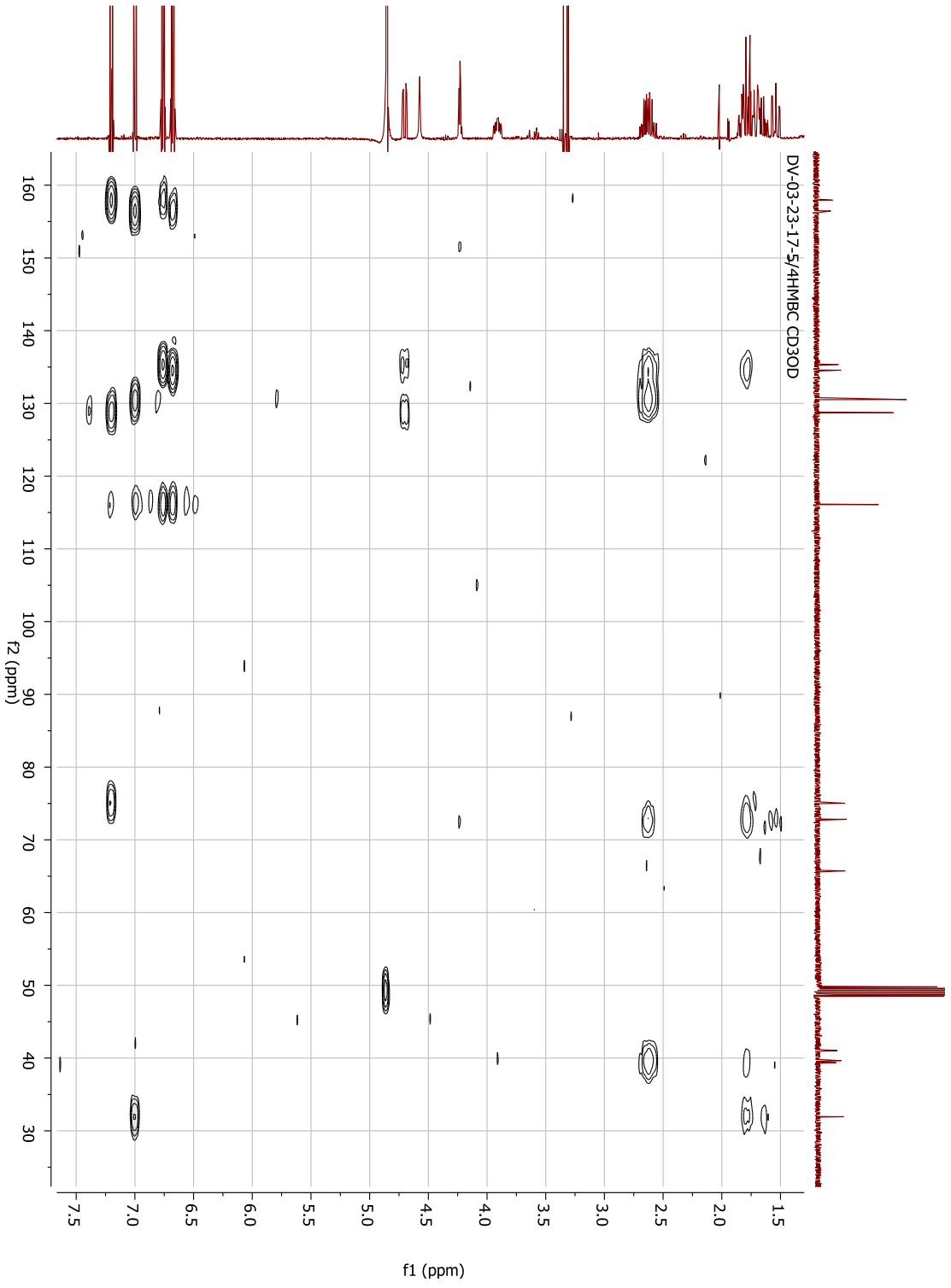

S17. ROESY spectrum of **2/3** in CD_3OD

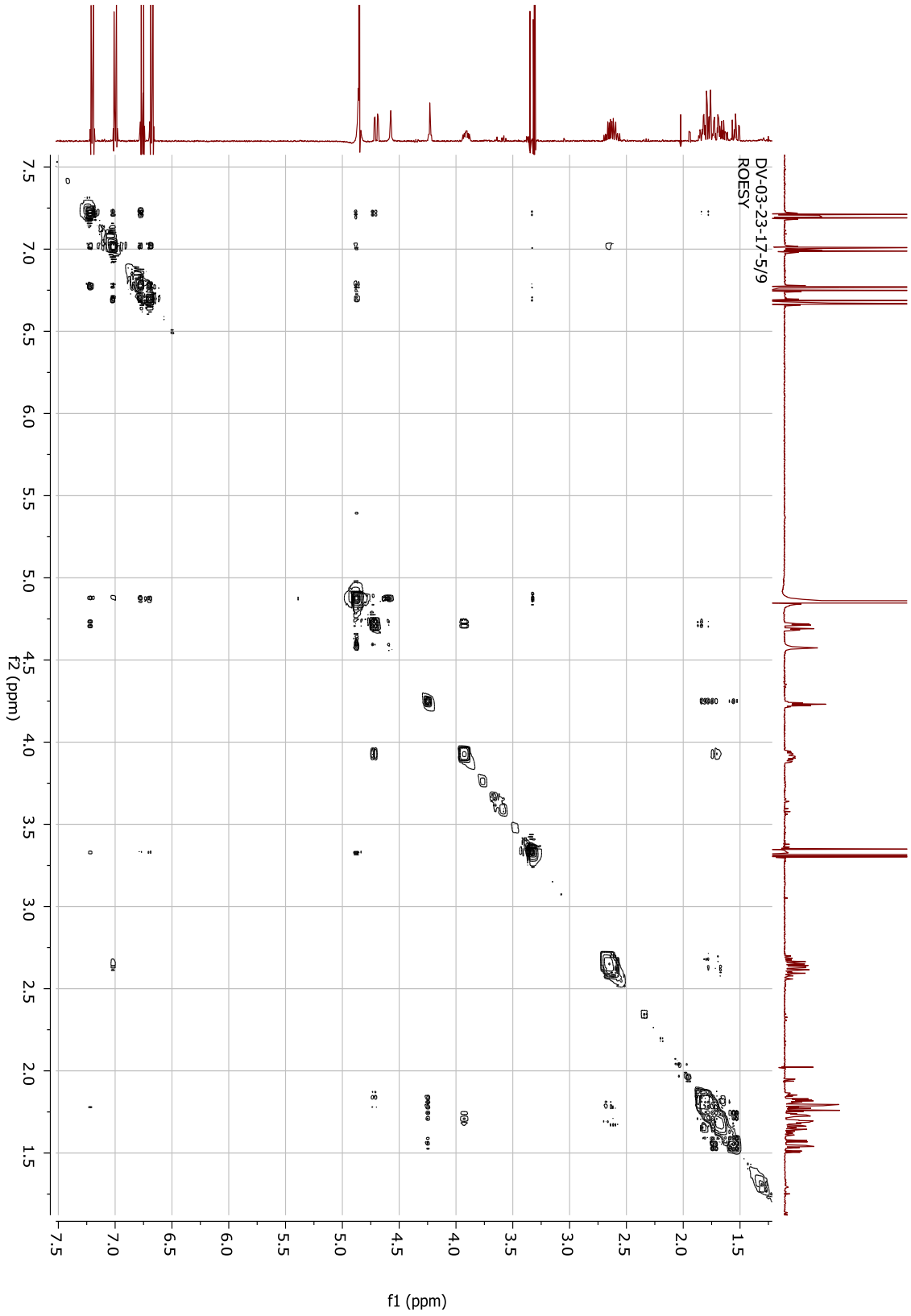

S18. IR (film/ATR) spectrum of **2** and **3**

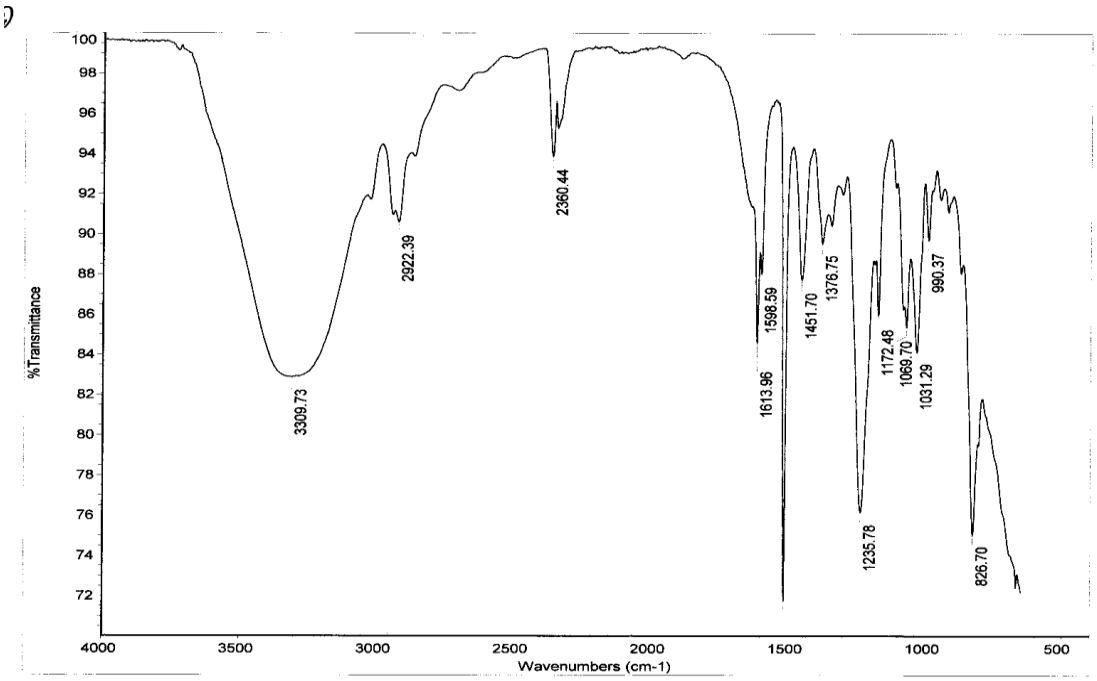

Figure S18-1. IR (film/ATR) spectrum of compound **2**

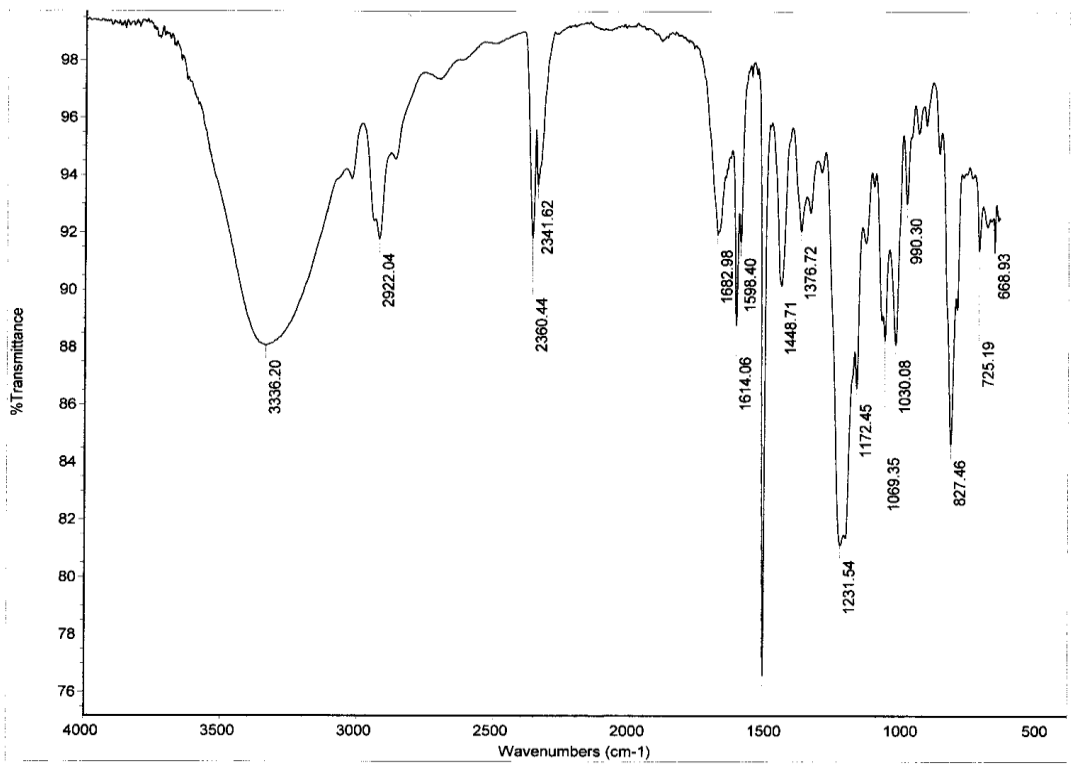

Figure S18-2. IR (film/ATR) spectrum of compound **3**

S19. ^{1}H NMR spectrum of **4**/**5** in CD_3OD

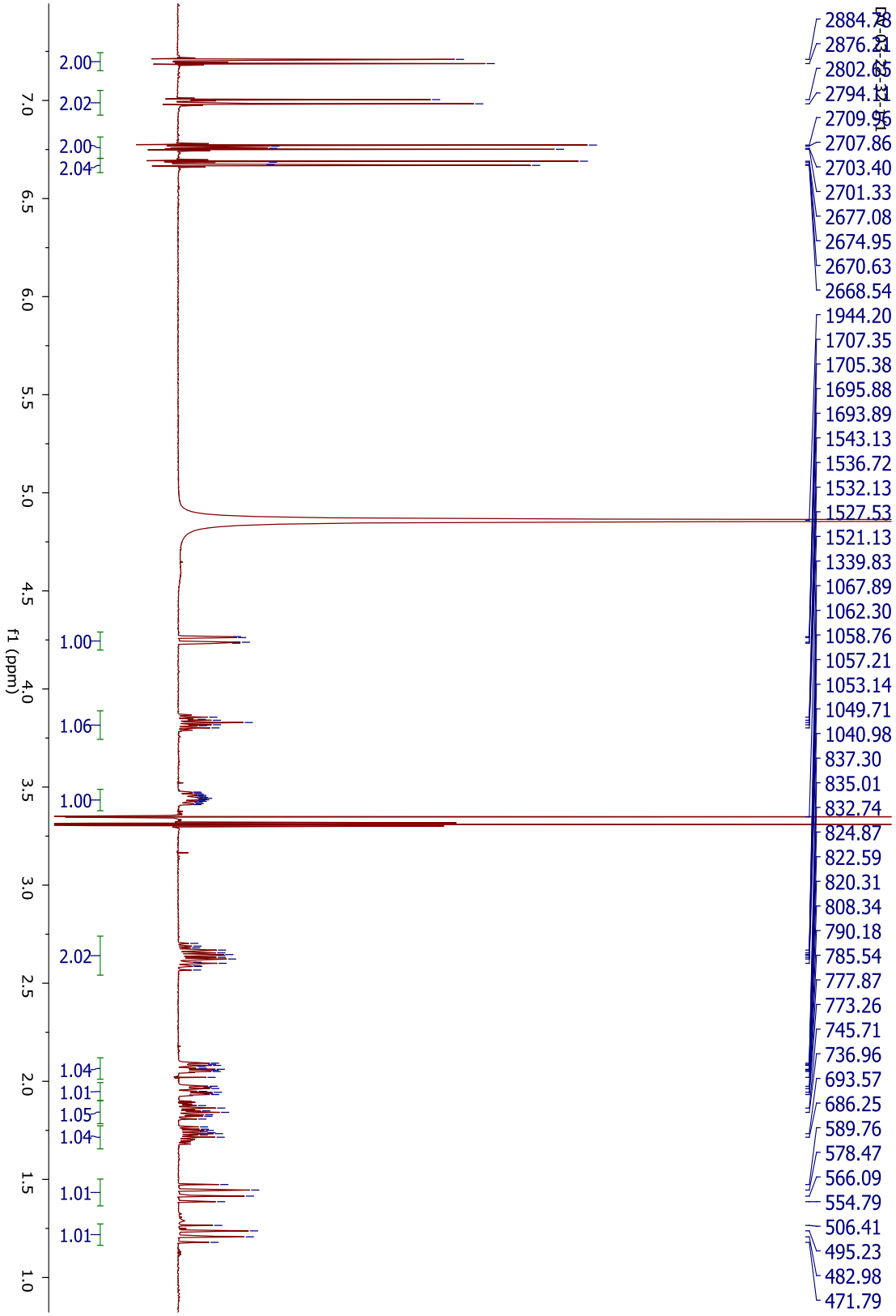

S20. ^{13}C NMR spectrum of **4/5** in CD_3OD

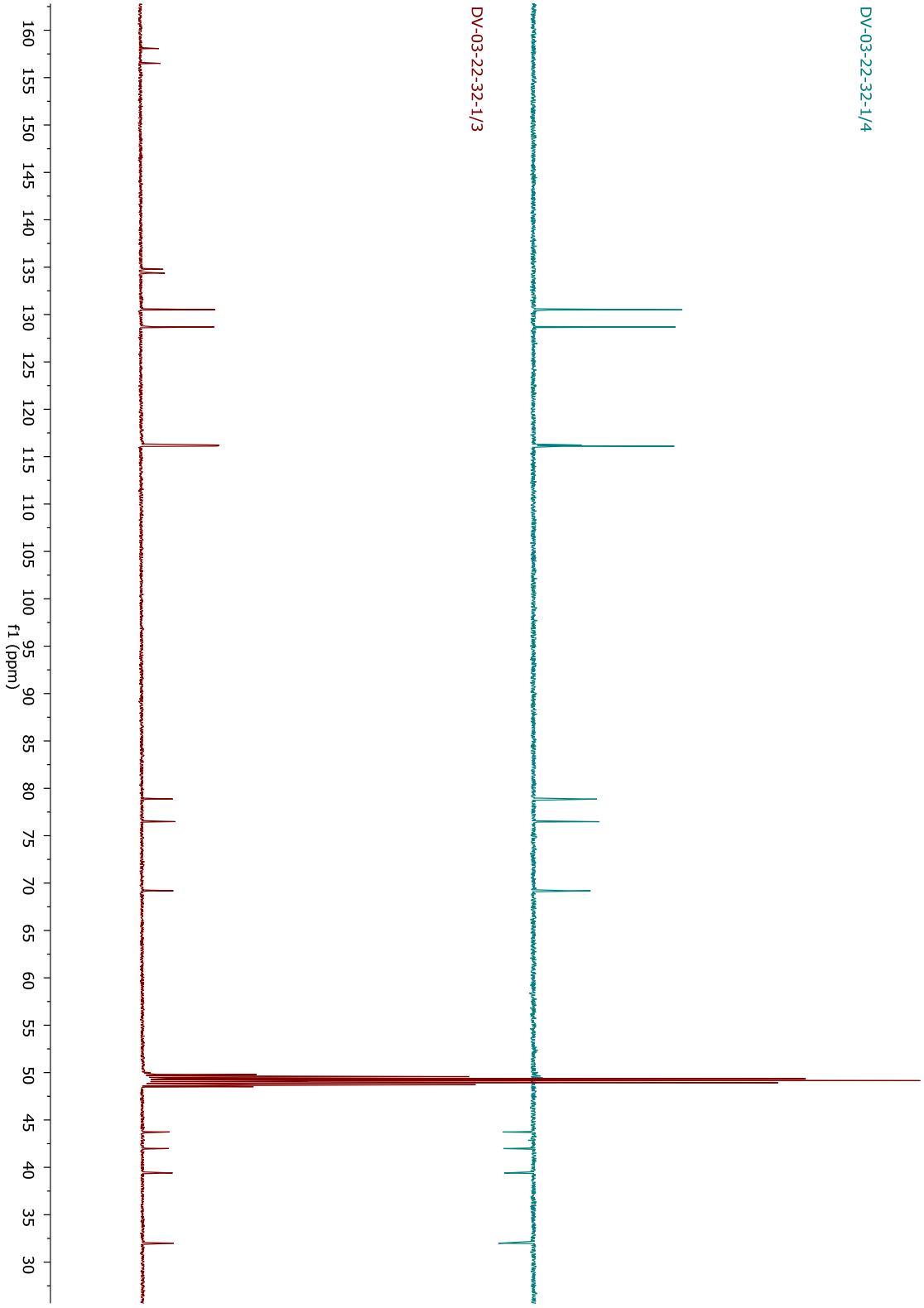

S21. $^{1}H–^{1}H$ COSY spectrum of **4/5** in CD_3OD

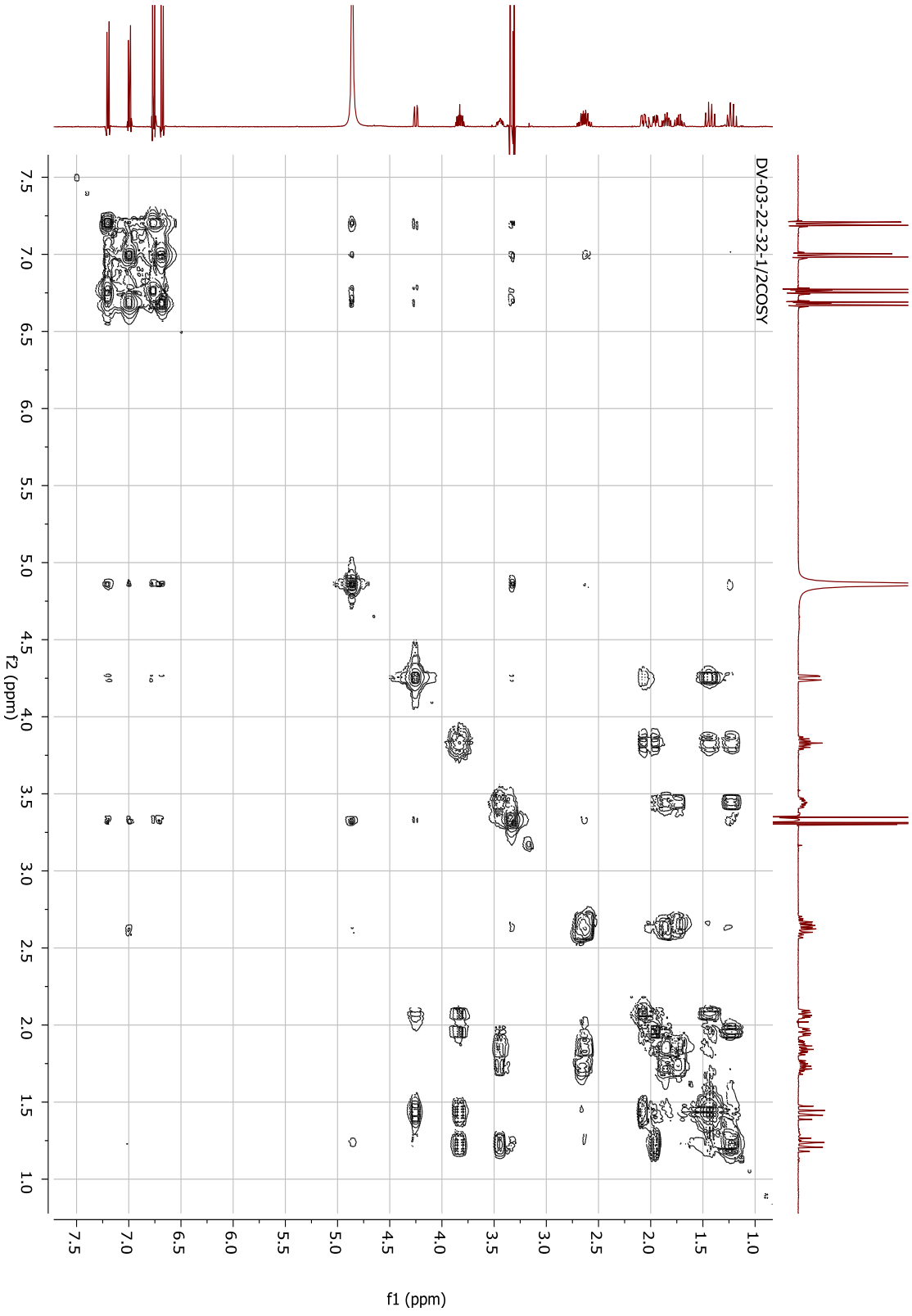

S22. HSQC spectrum of **4**/**5** in CD_3OD

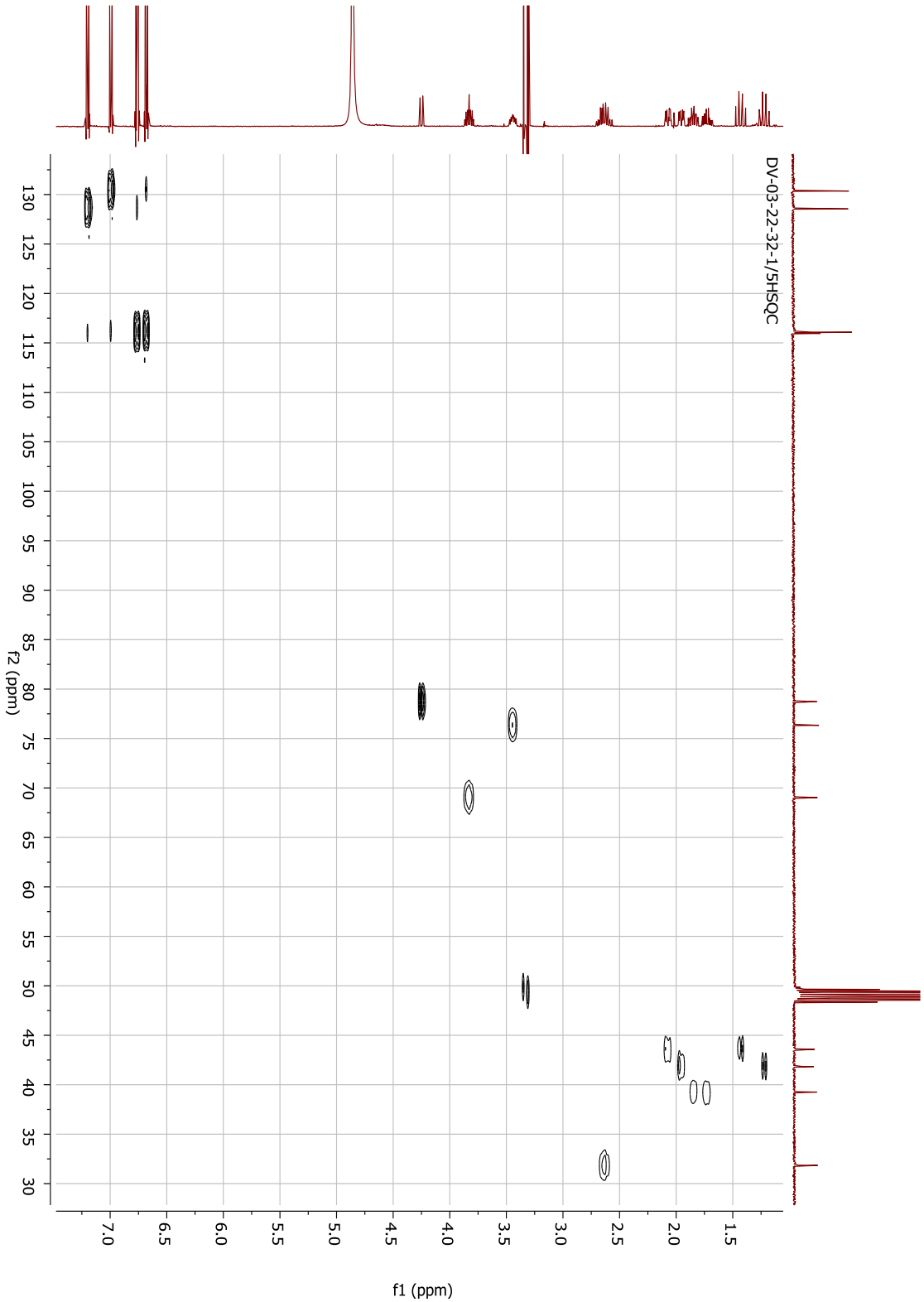

S23. HMBC spectrum of **4/5** in CD_3OD

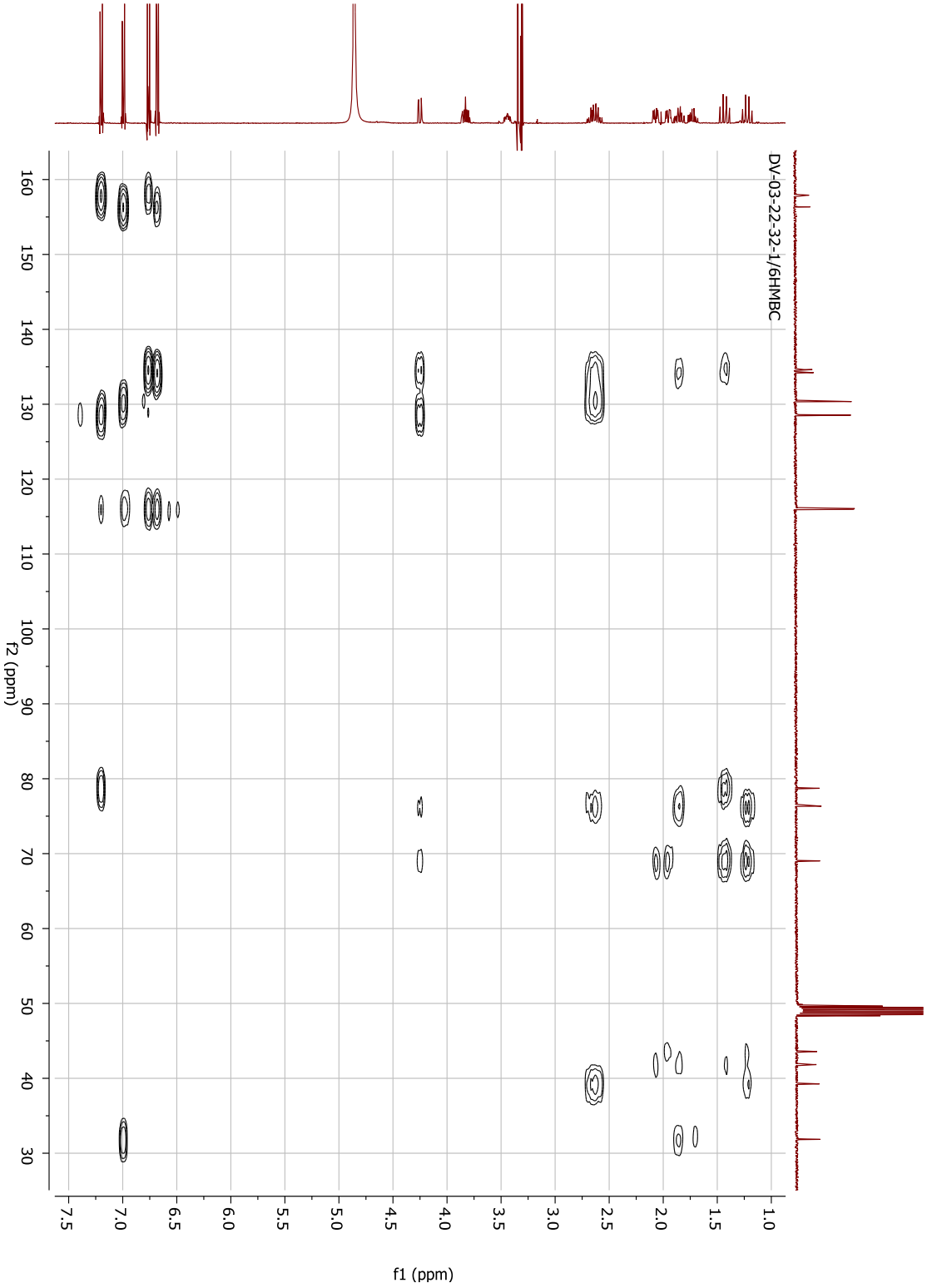

S24. NOESY spectrum of **4**/**5** in CD_3OD

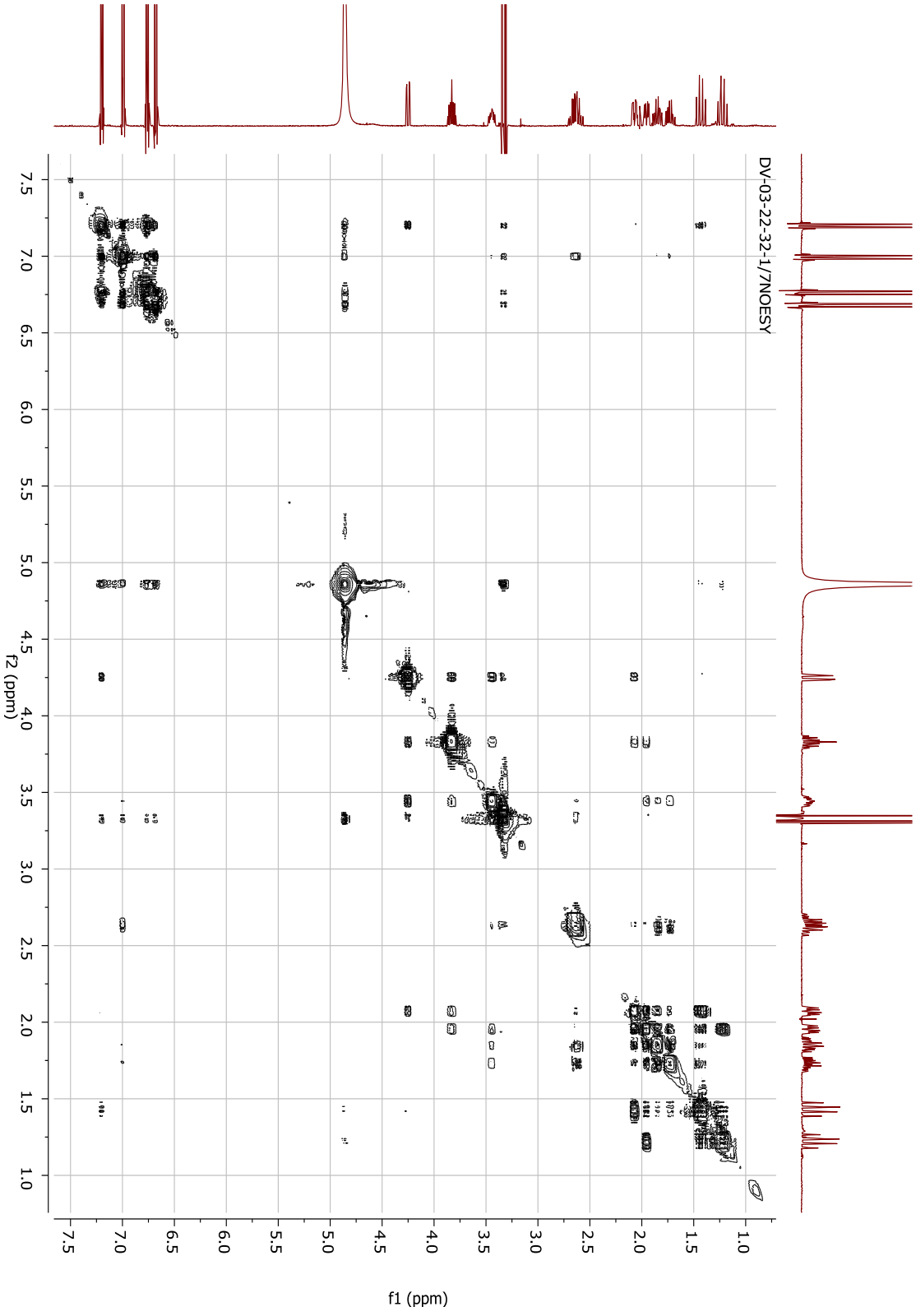

S25. IR (film/ATR) spectrum of **4**/**5**

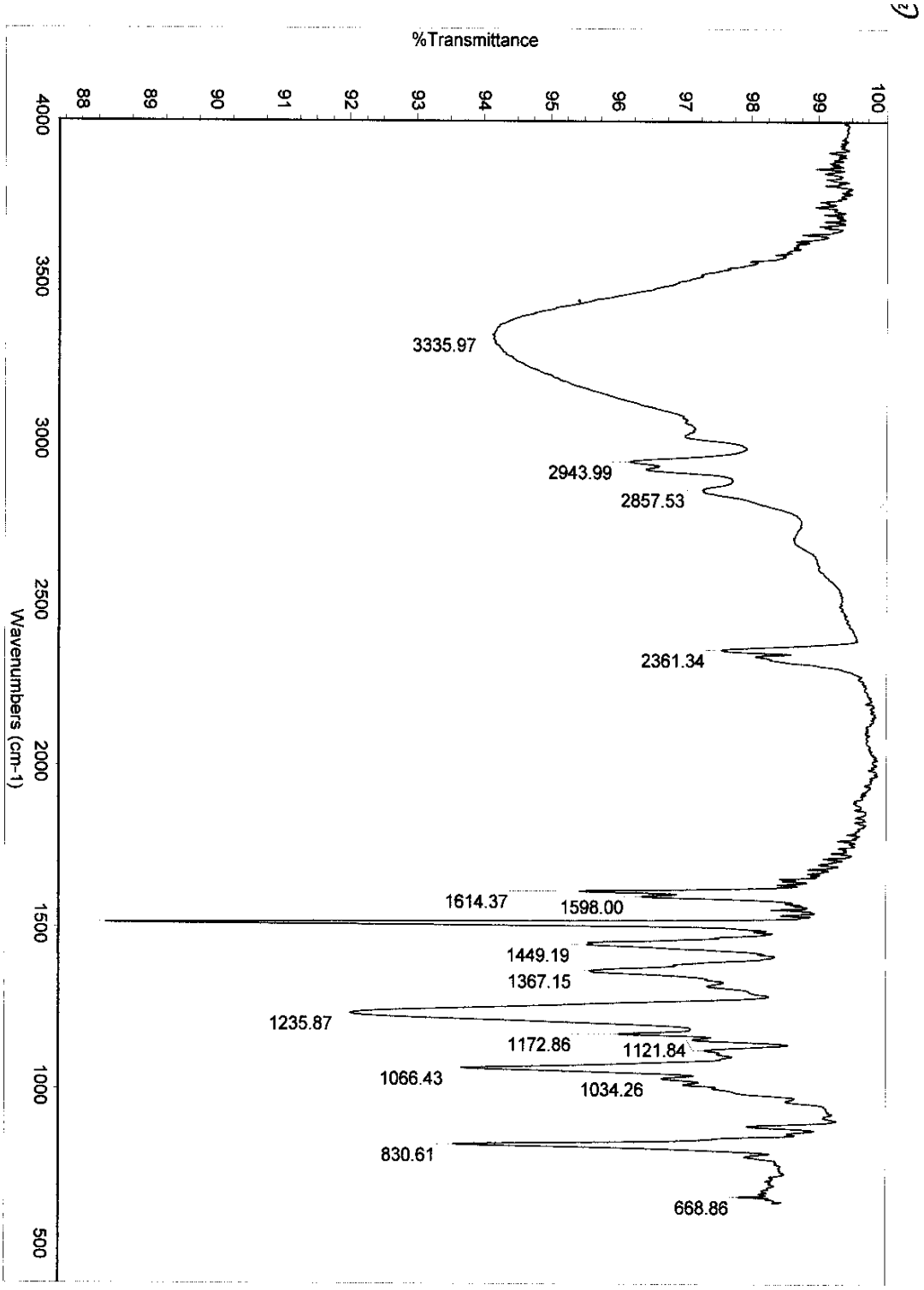

S**26**. ^{1}H NMR spectrum of **6**/**7** in CD_3OD

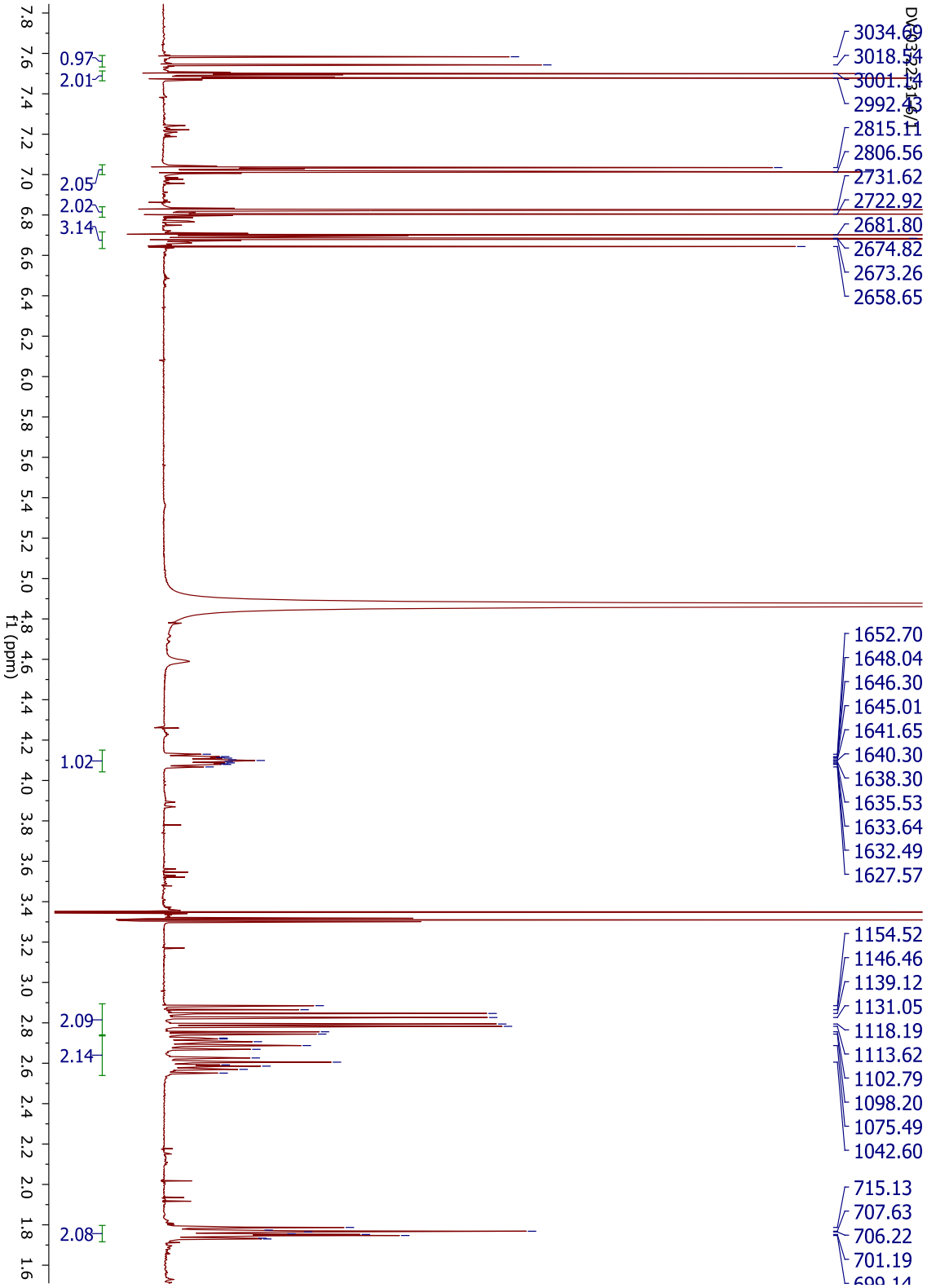

S27. ^{13}C NMR spectrum of **6**/**7** in CD_3OD

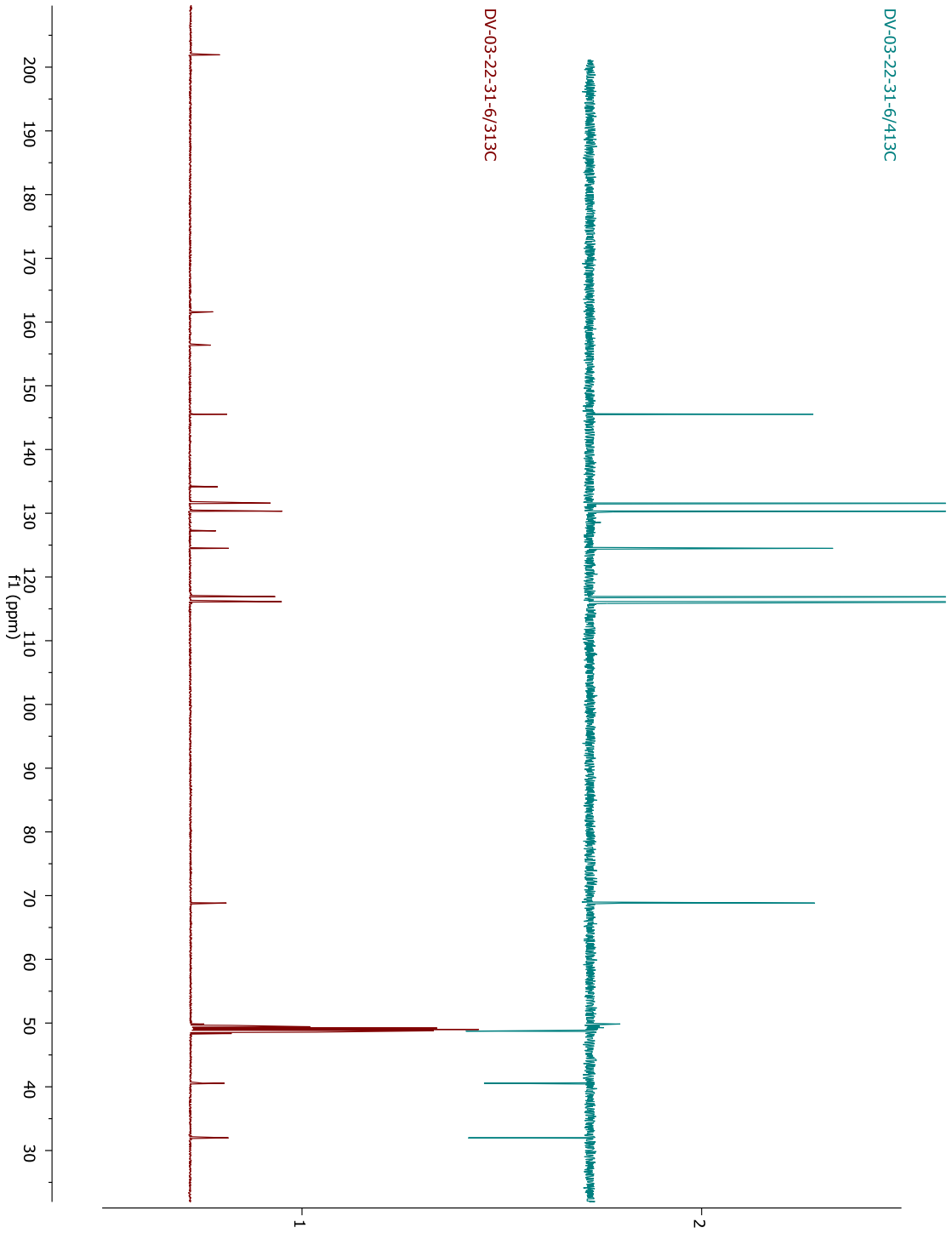

S28. $^{1}H–^{1}H$ COSY spectrum of **6**/**7** in CD_3OD

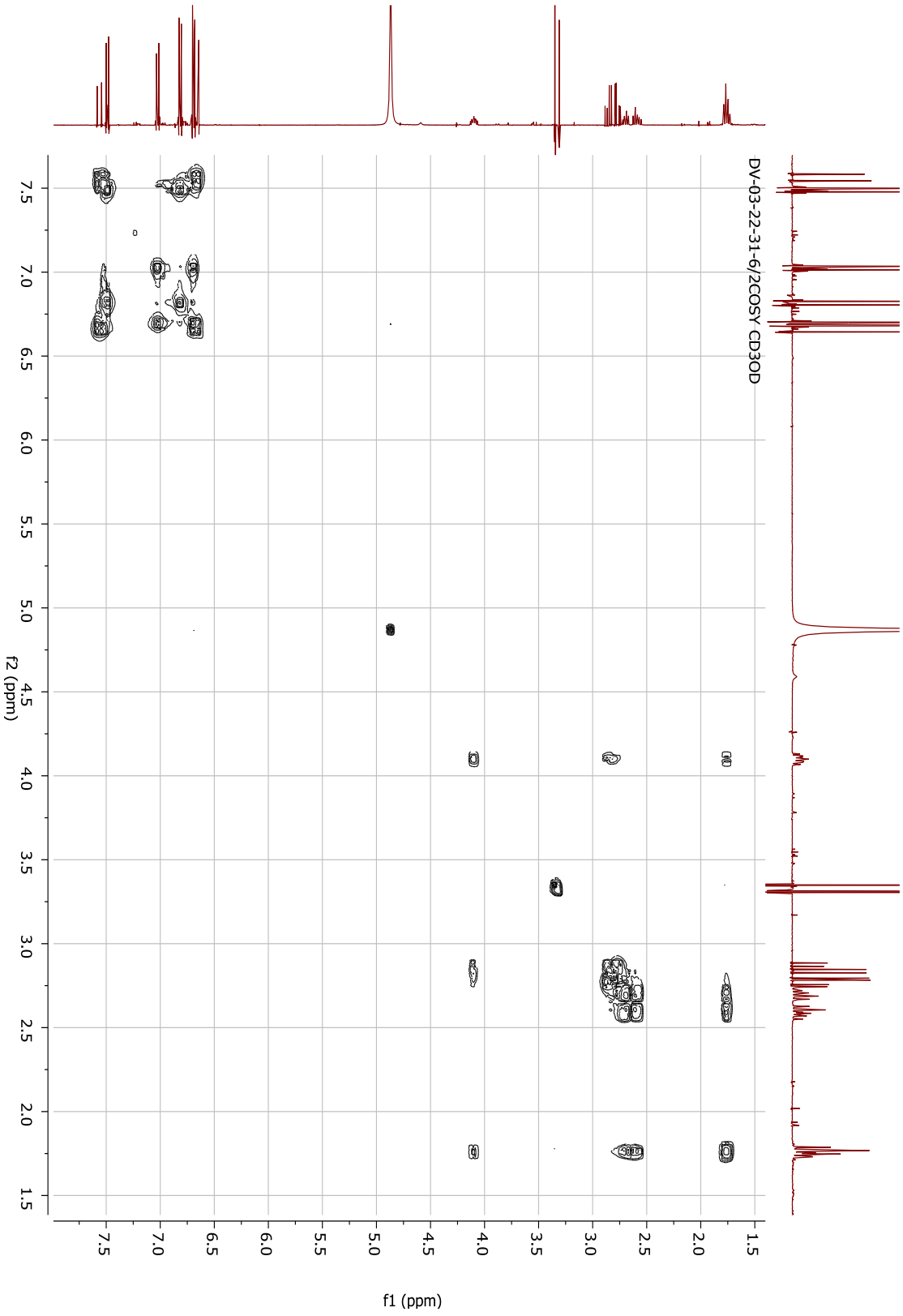

S29. HSQC spectrum of **6**/**7** in CD_3OD

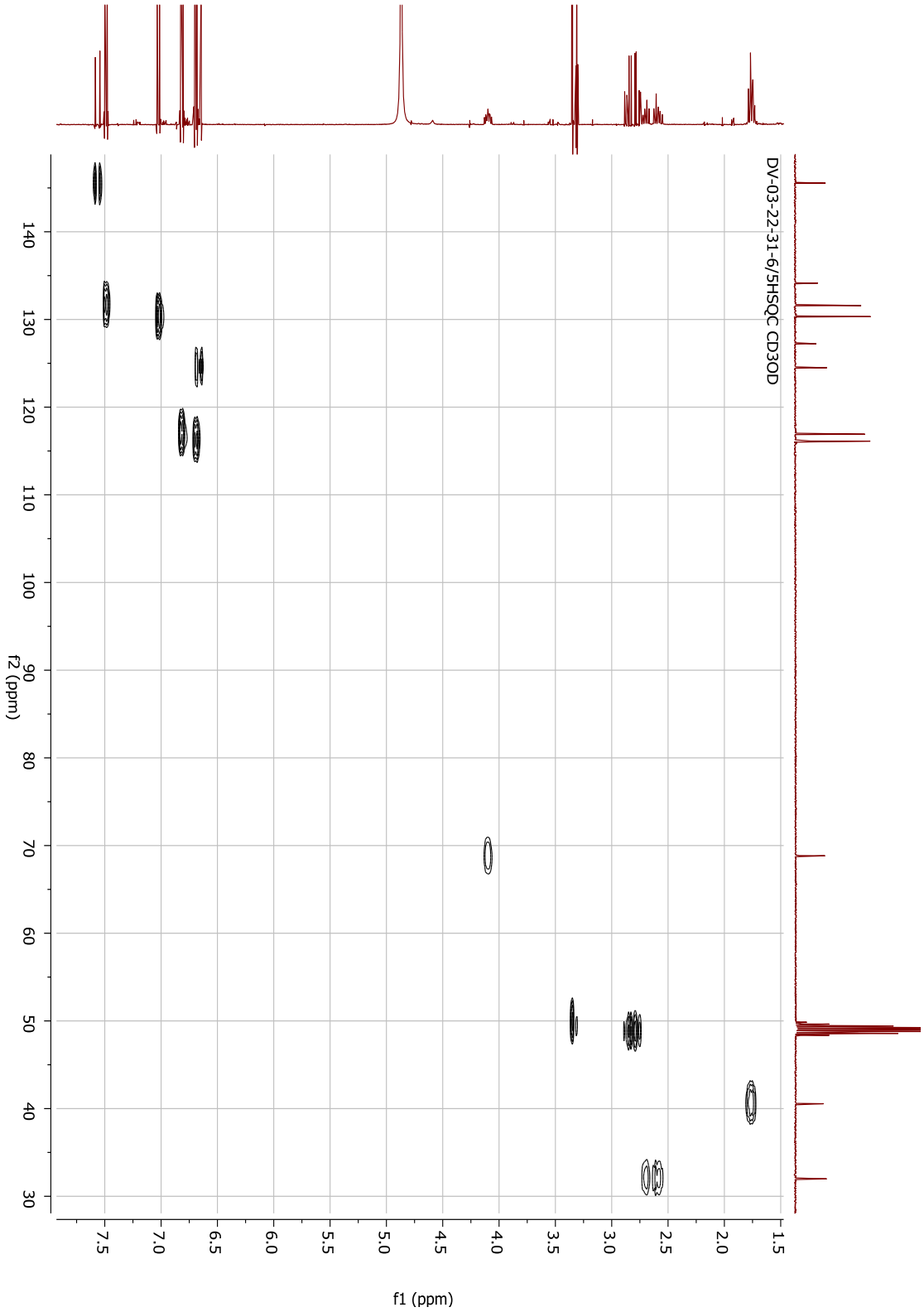

S30. HMBC spectrum of **6**/**7** in CD_3OD

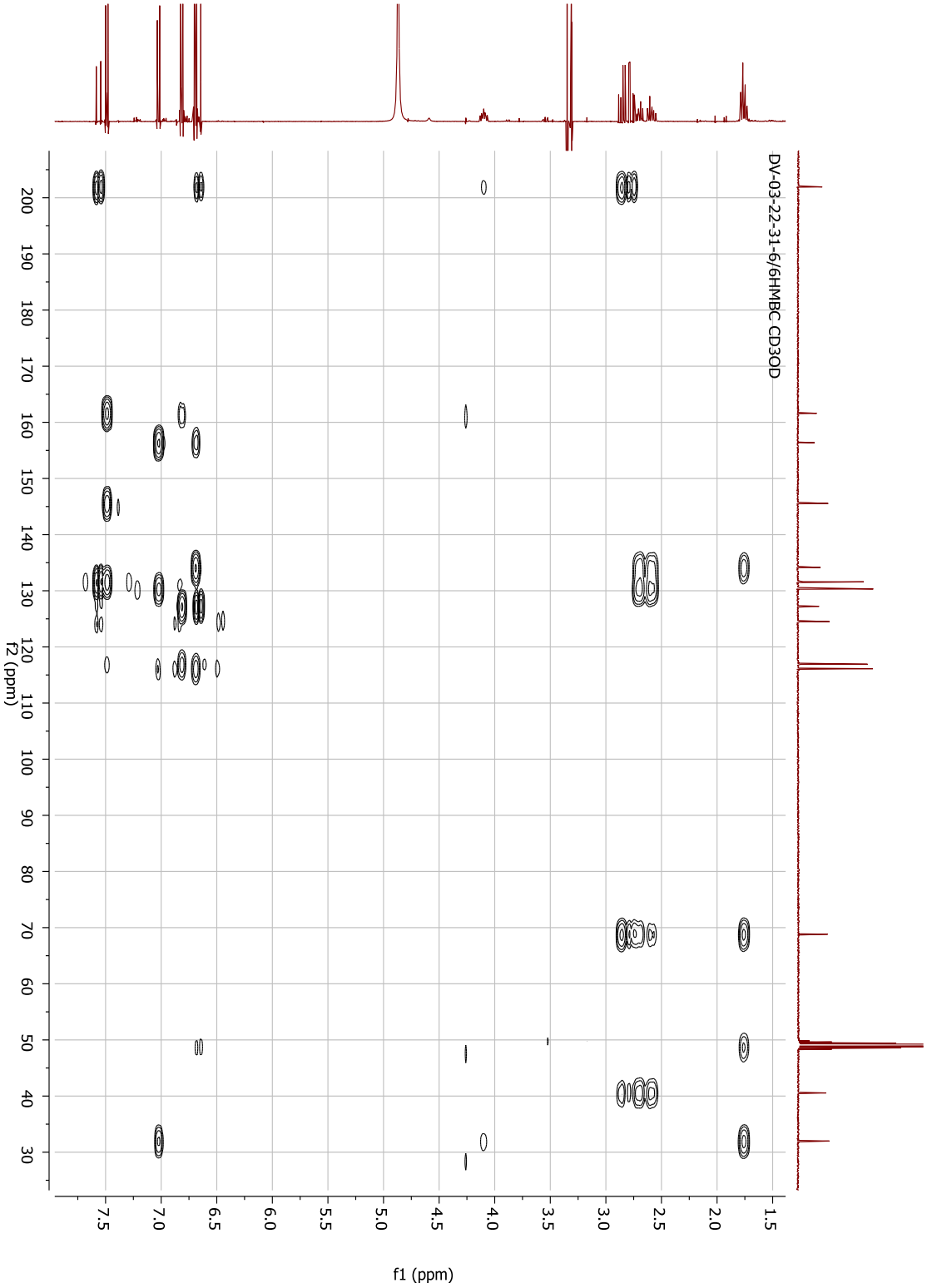

S31. IR (film/ATR) spectrum of **6** and **7**

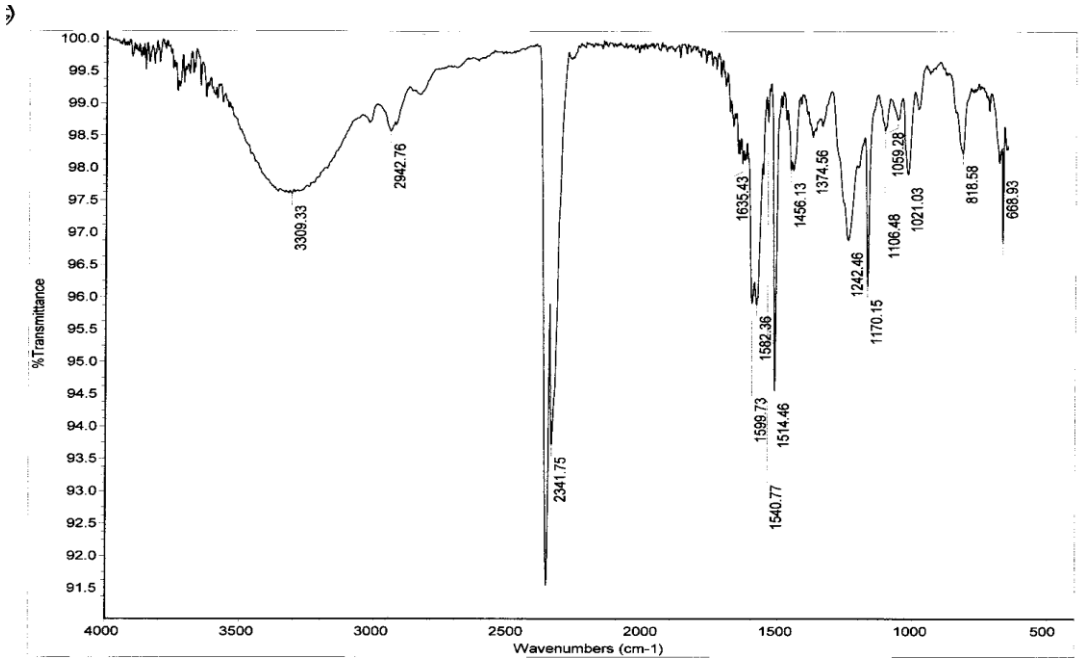

Figure S31-1. IR (film/ATR) spectrum of compound **6**

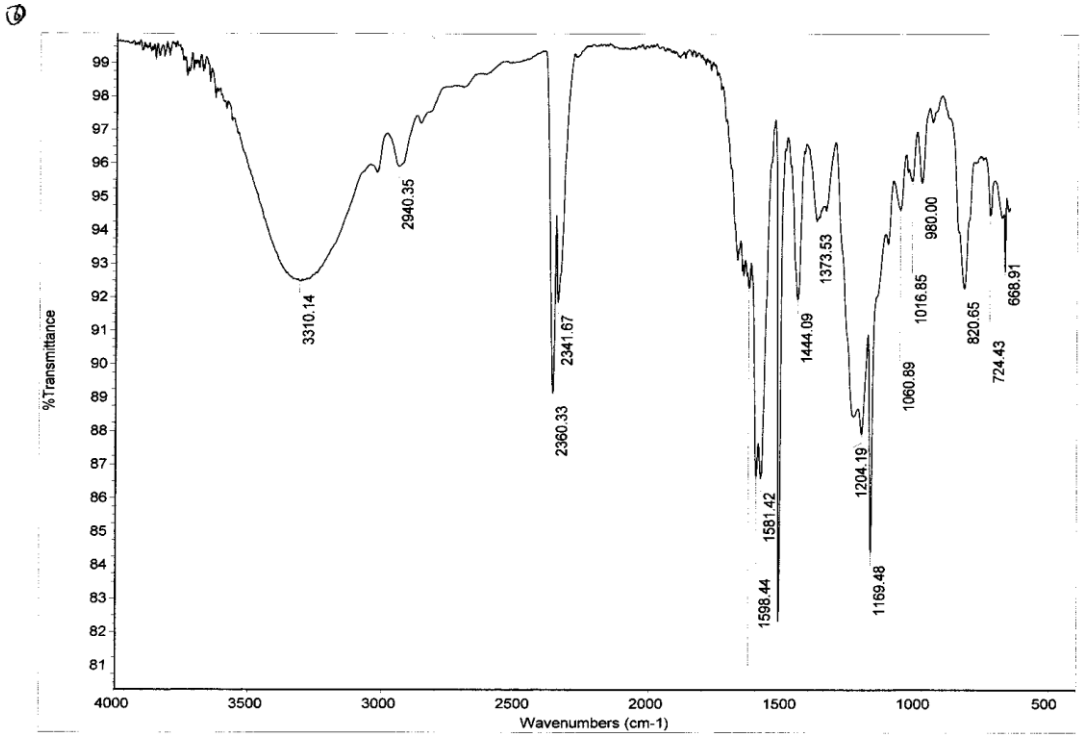

Figure S31-2. IR (film/ATR) spectrum of compound **7**

S32. ^{1}H NMR spectrum of **8**/**9** in CD_3OD

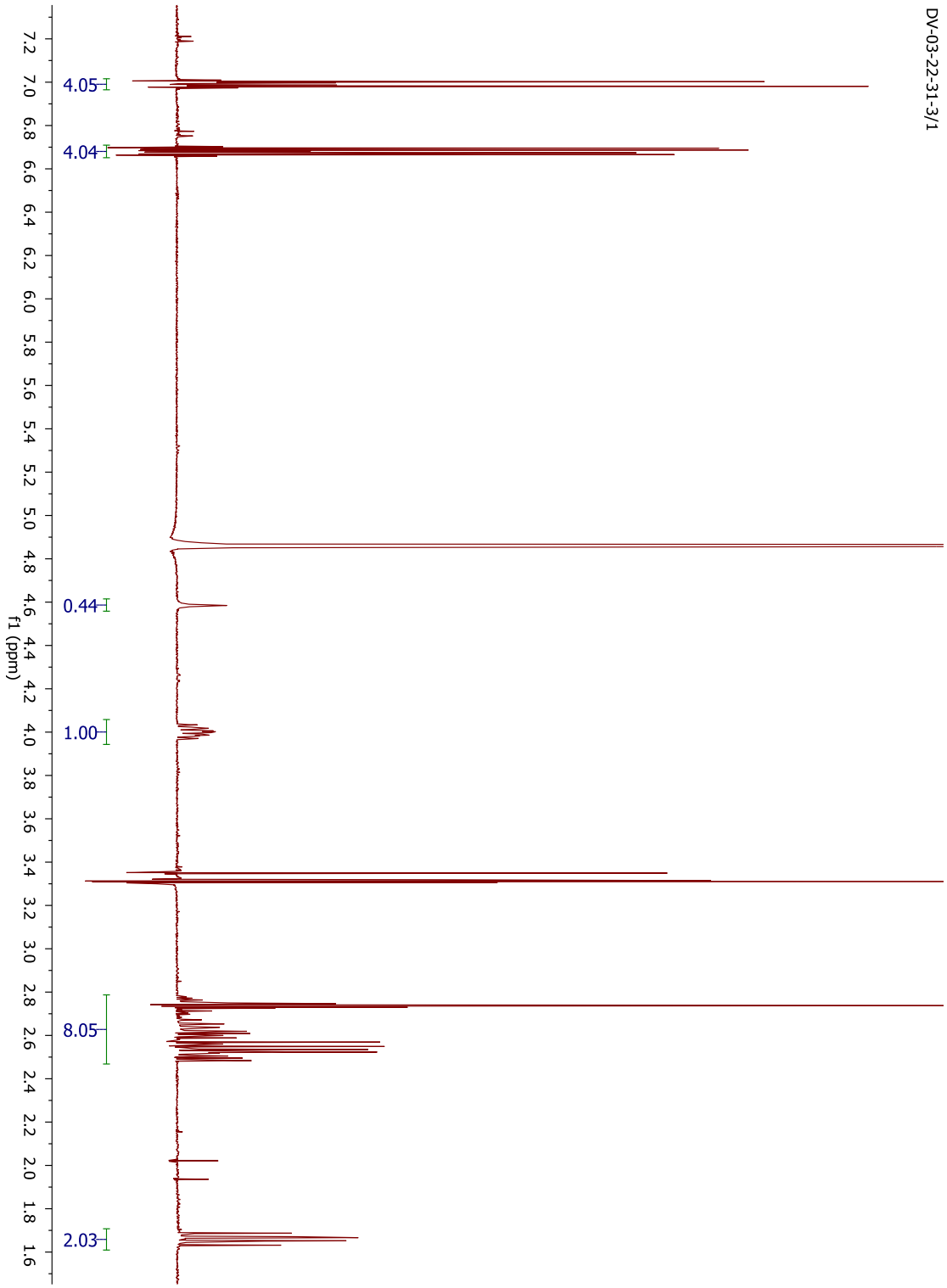

S33. ^{1}H NMR spectrum of **10** in DMSO-d_6

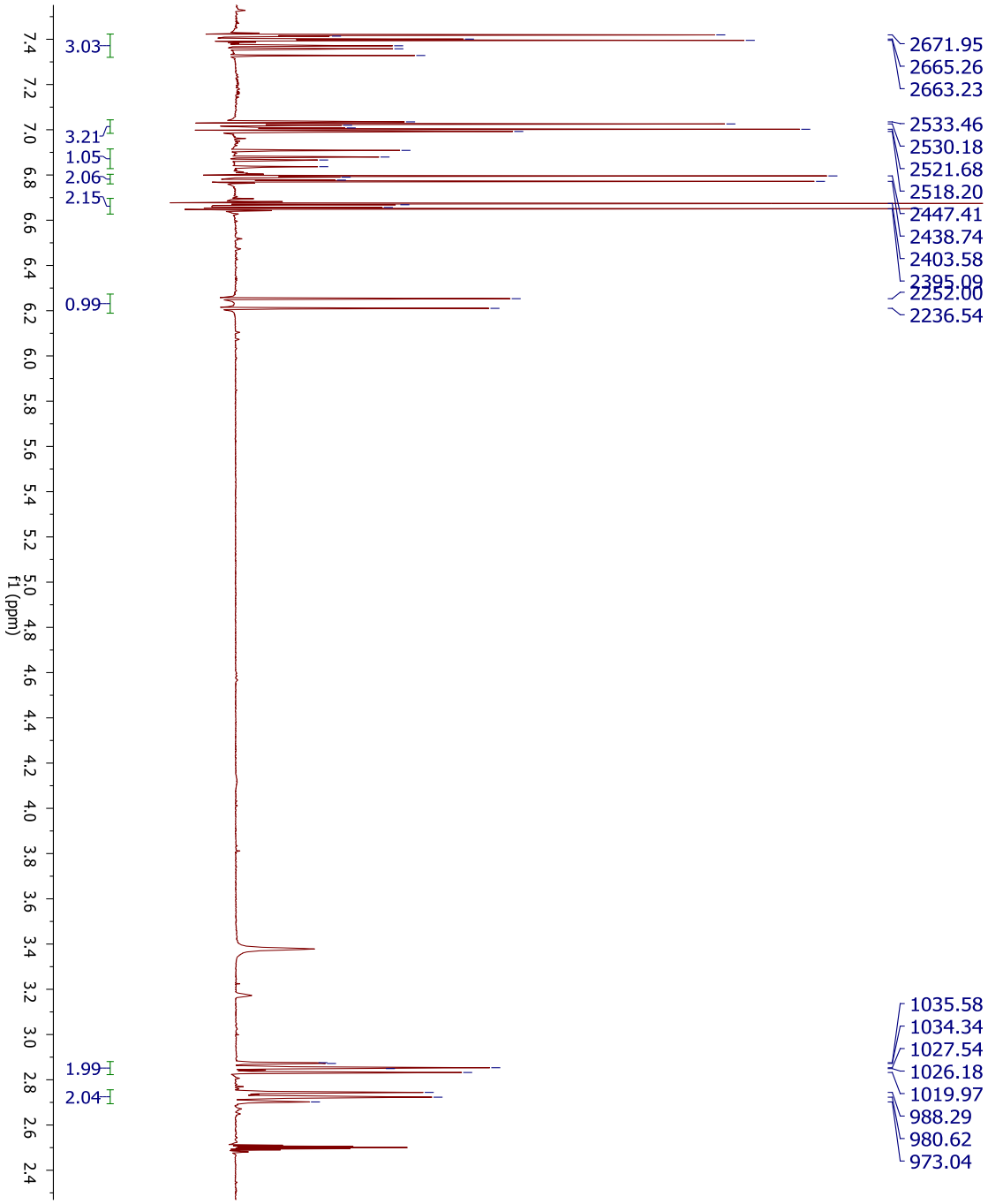

S34. ^{1}H NMR spectrum of **11** in CD_3OD

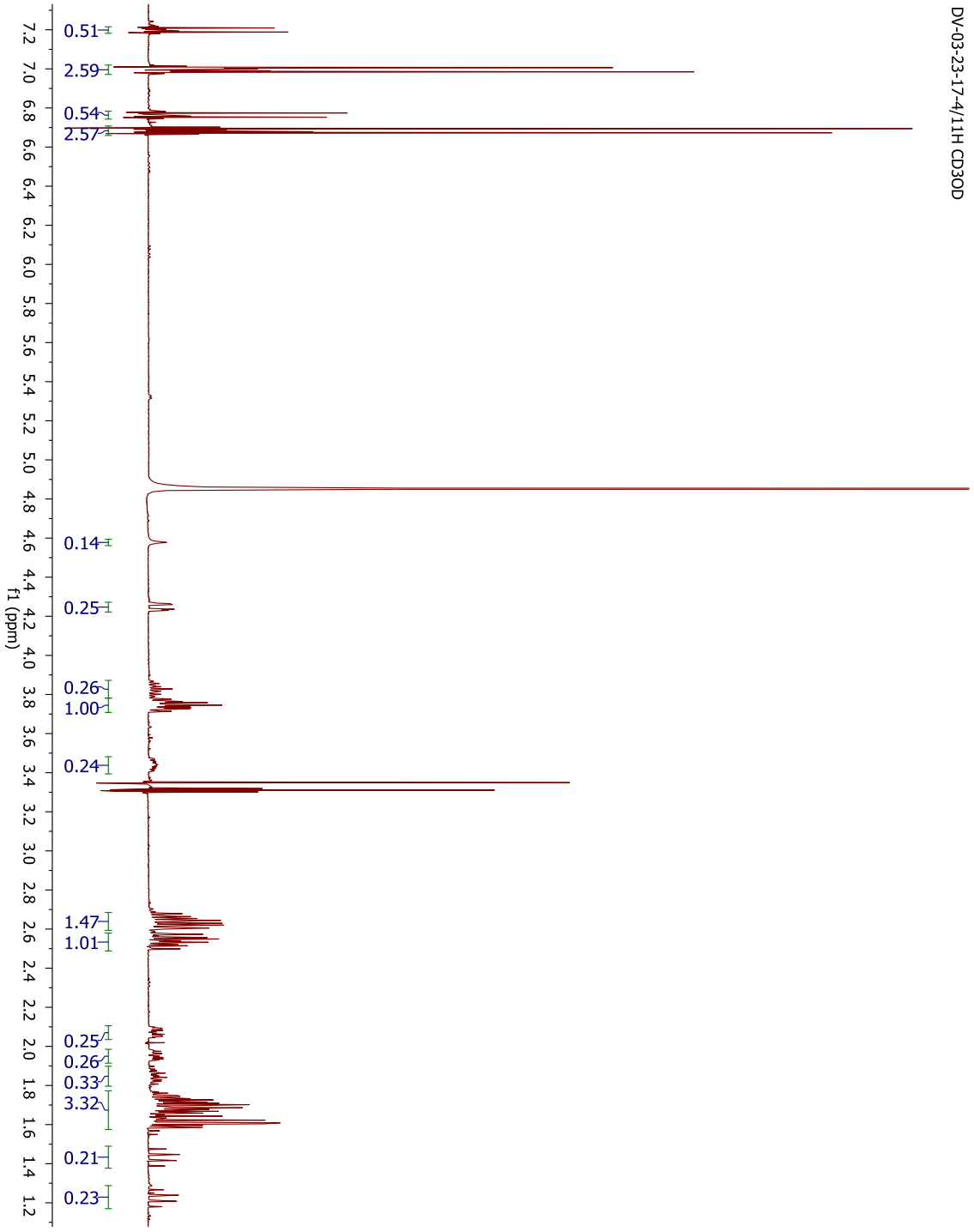

S35. ^{1}H NMR spectrum of **12** in pyridine-d_6

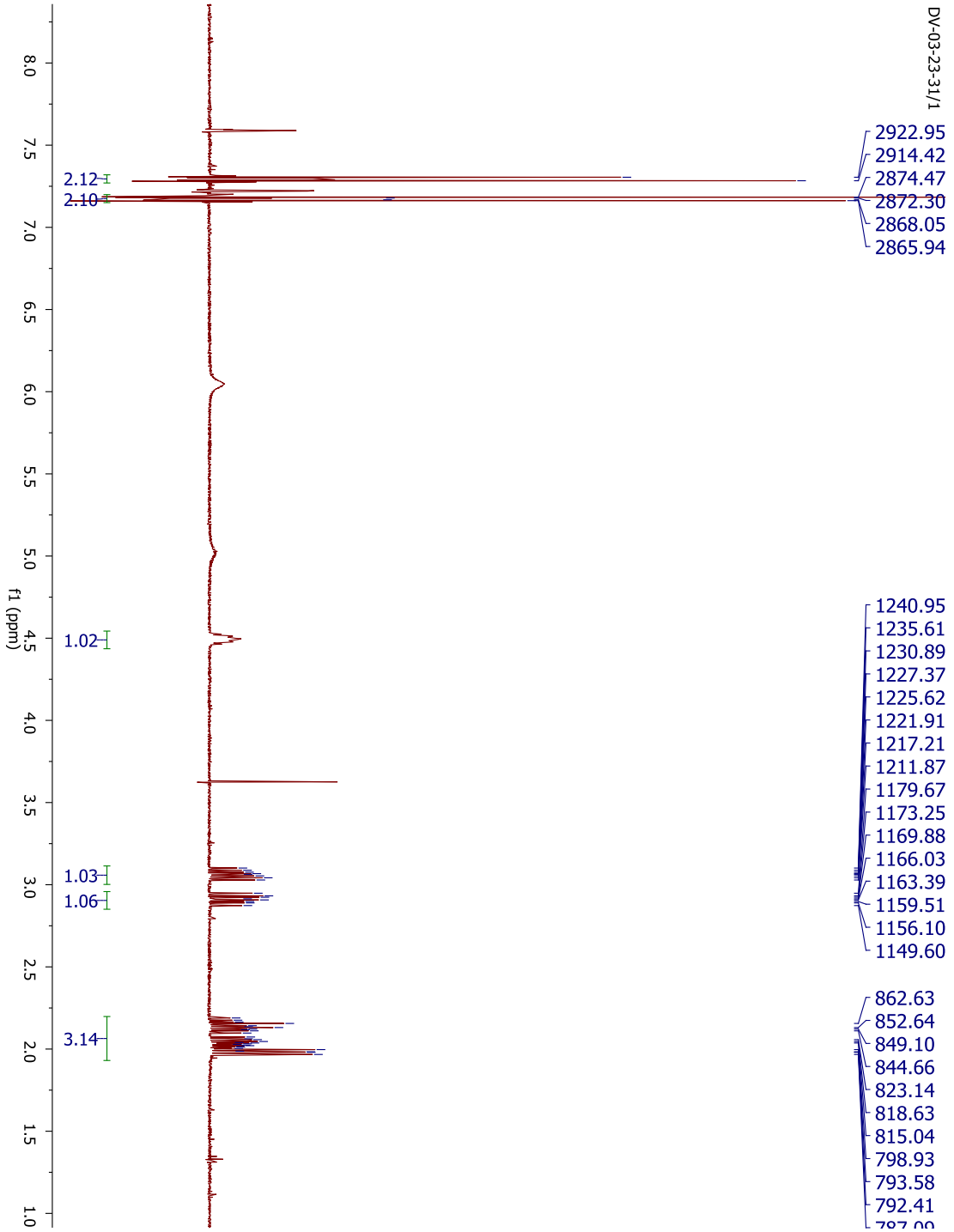

S36. ^{1}H NMR spectrum of **12** in DMSO-d_6

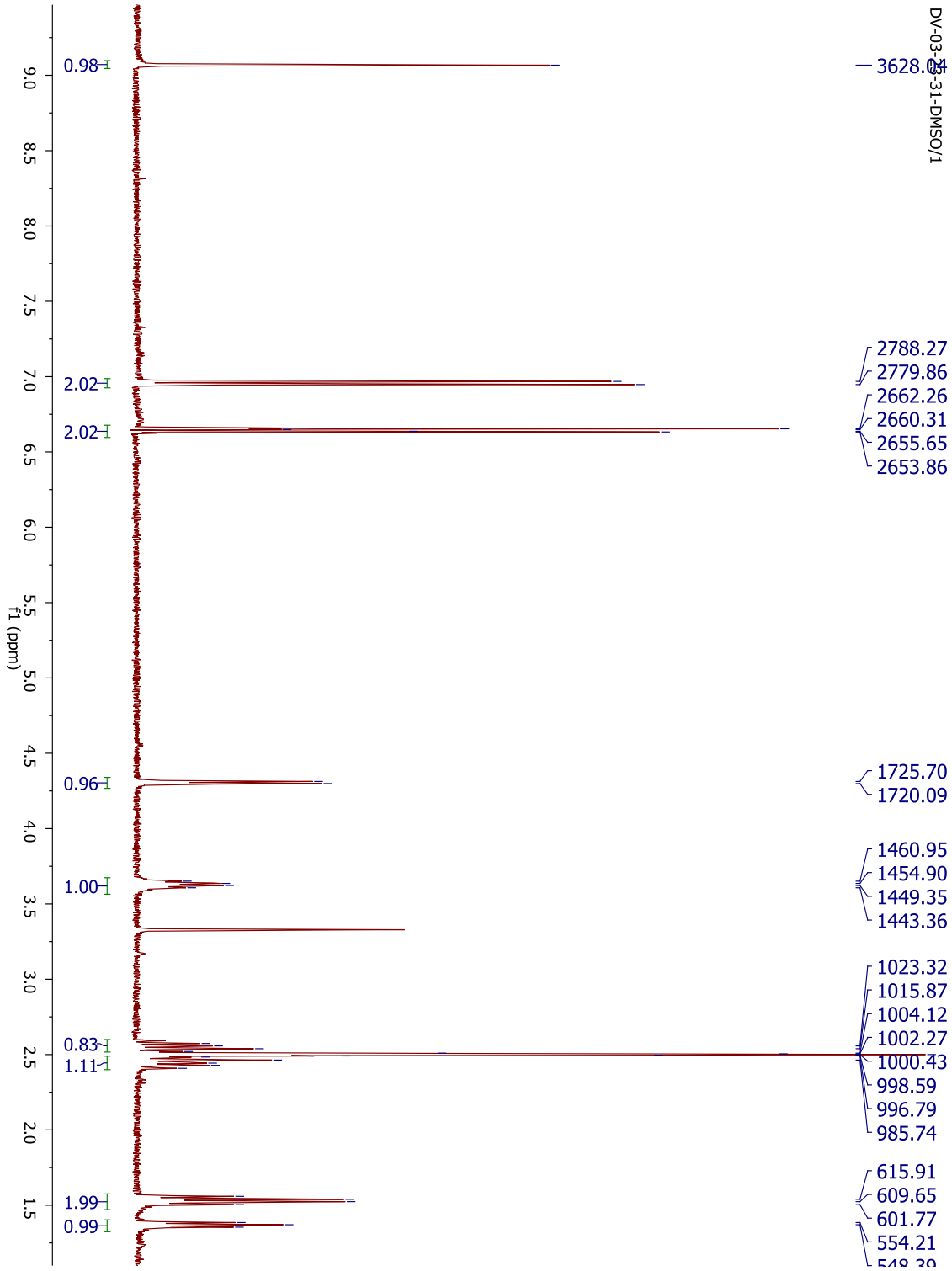

S37. ^{1}H NMR spectrum of **13**/**14** in DMSO-d_6

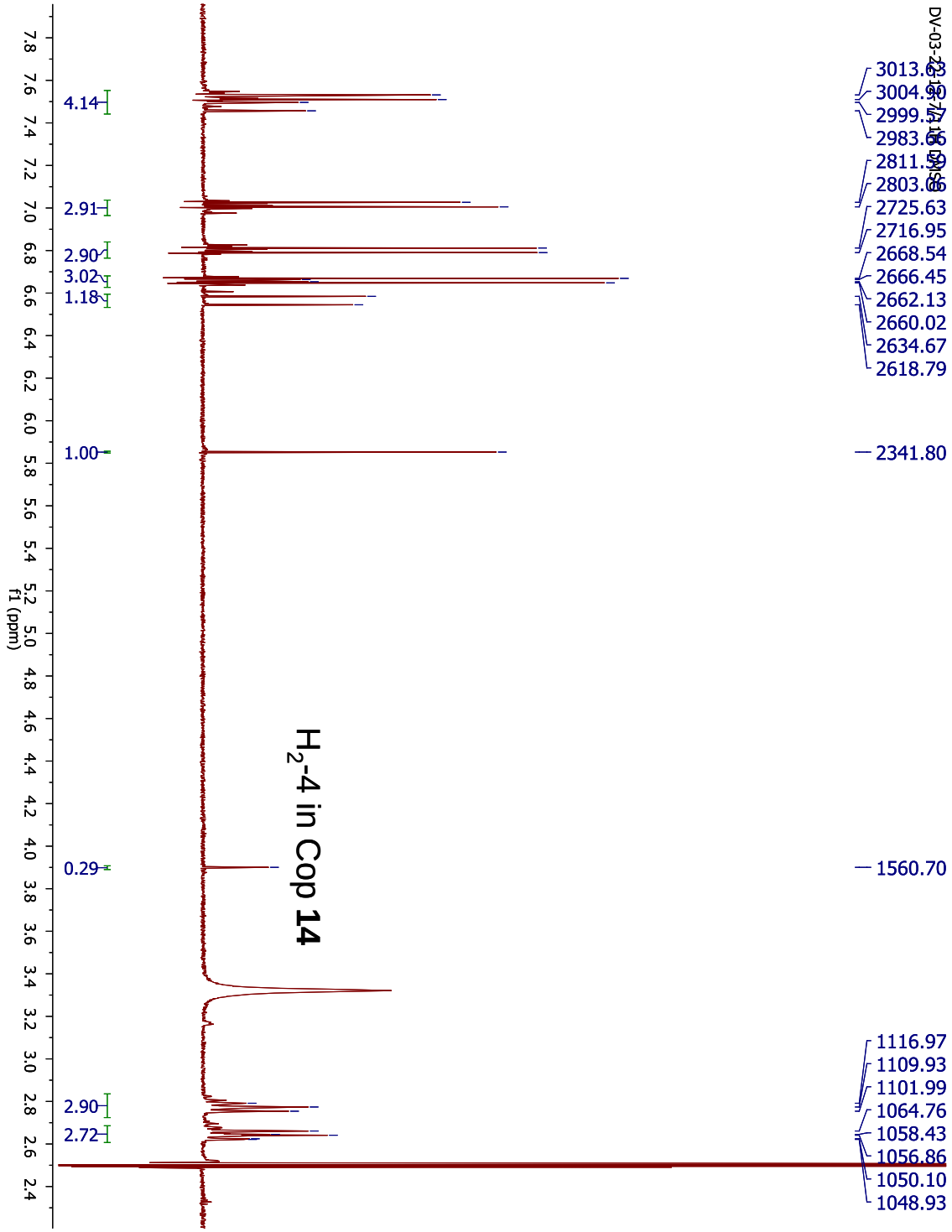

S38. ^{1}H NMR spectrum of the (*R*)-MTPA derivative of **1** in pyridine-d_5

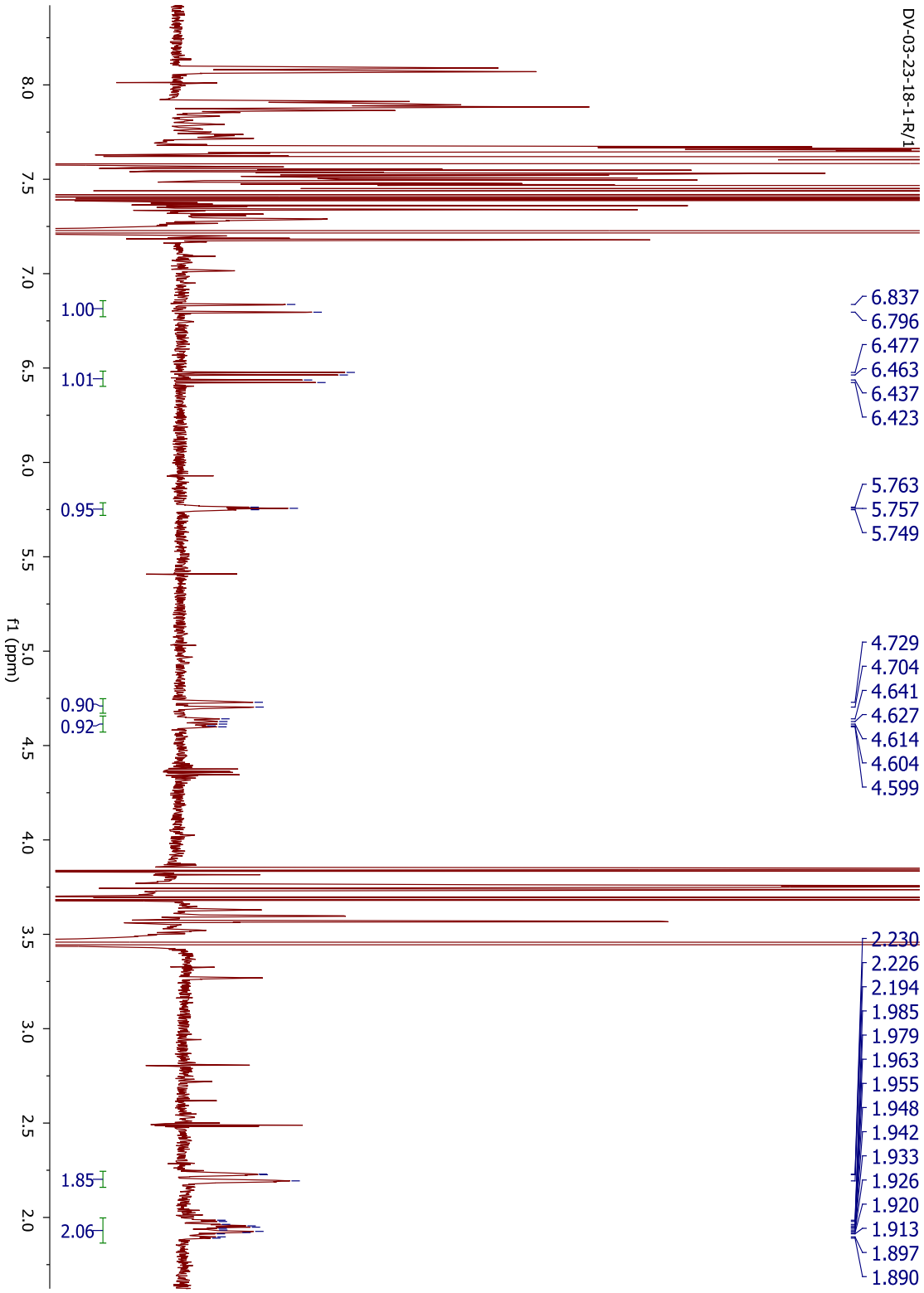

S39. ^{1}H–^{1}H COSY spectrum of the (*R*)-MTPA derivative of **1** in pyridine-d_5

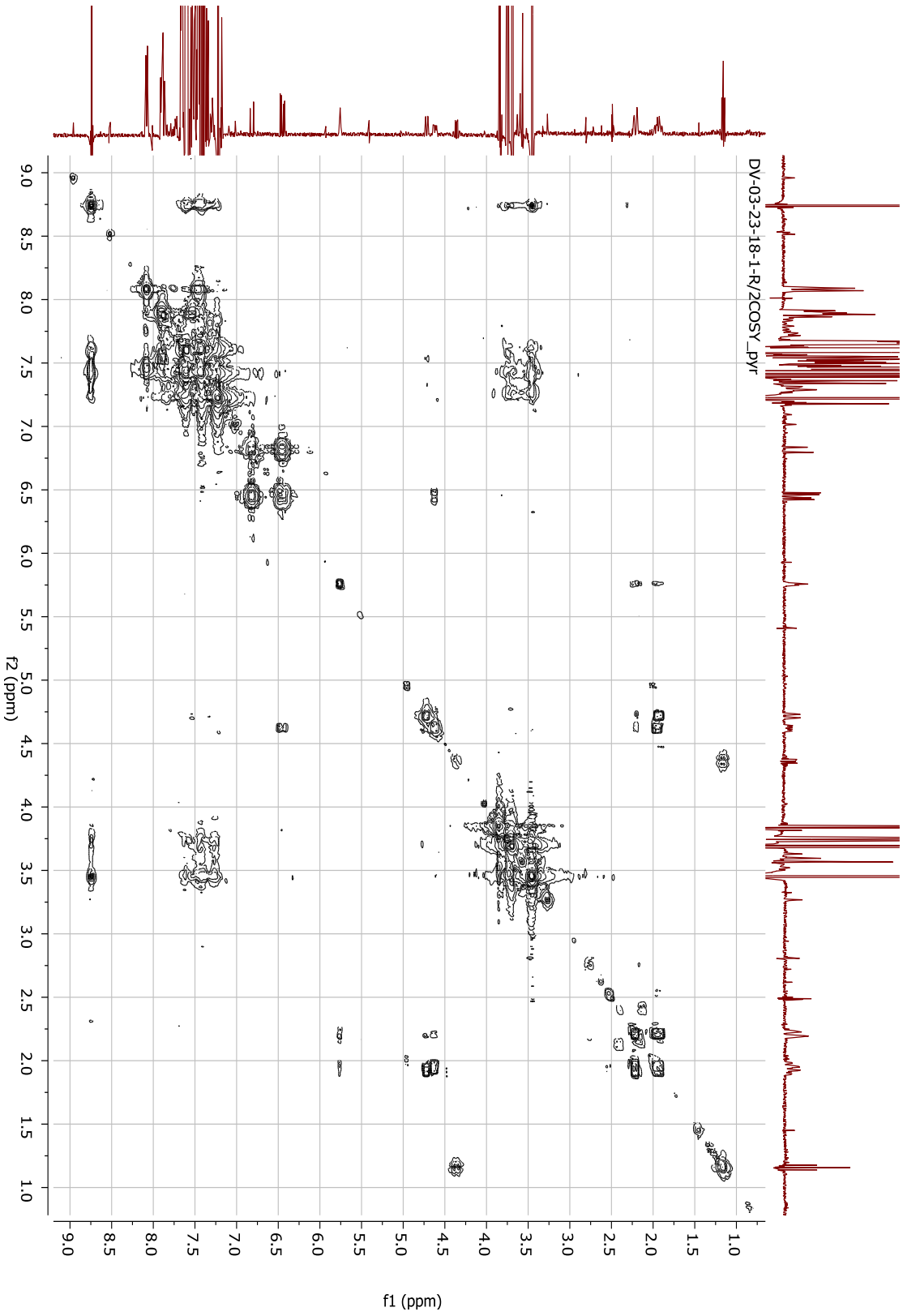

S40. ^{1}H NMR spectrum of the (*S*)-MTPA derivative of **1** in pyridine-d_5

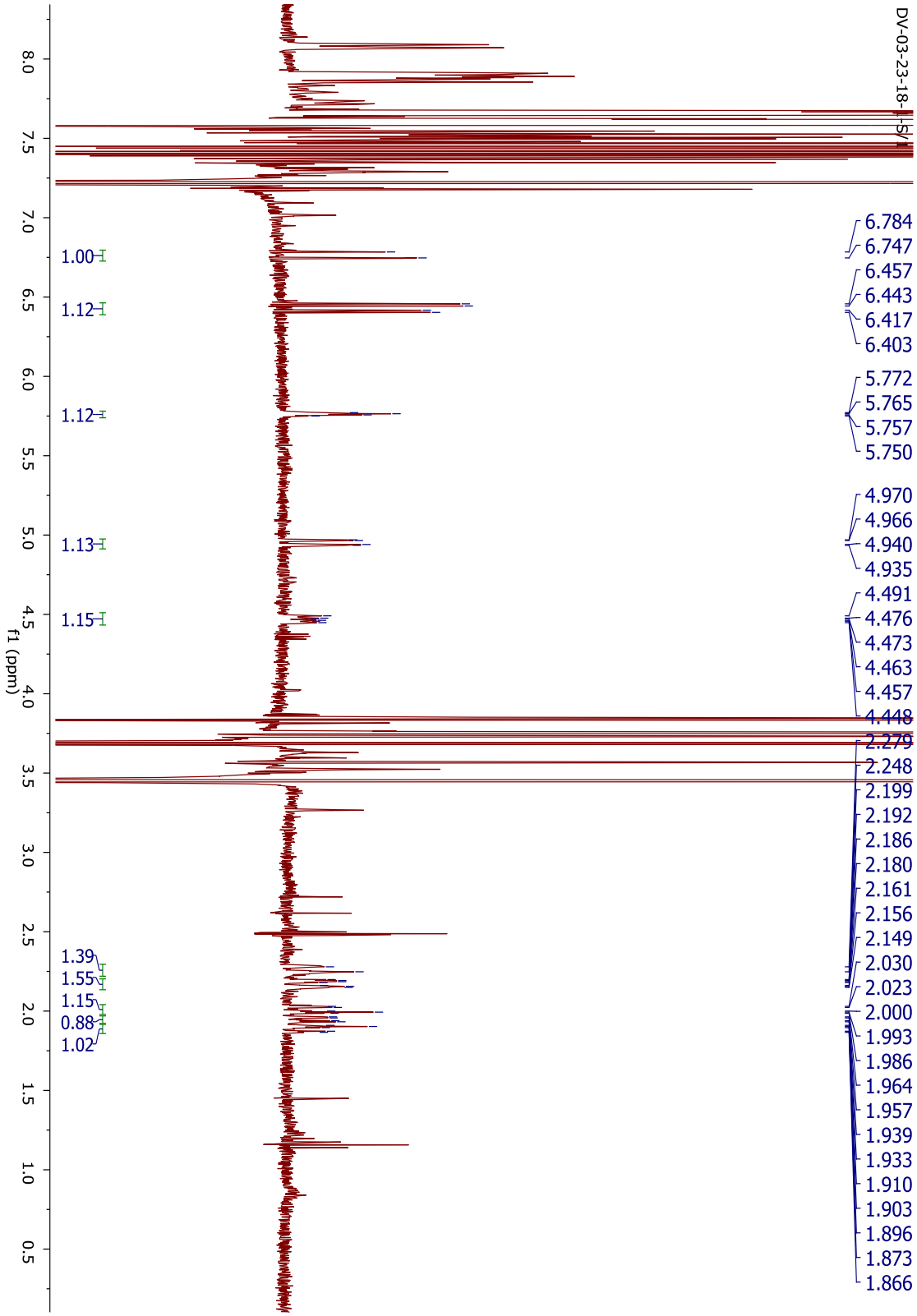

S41. ^{1}H–^{1}H COSY spectrum of the (*S*)-MTPA derivative of **1** in pyridine-d_5

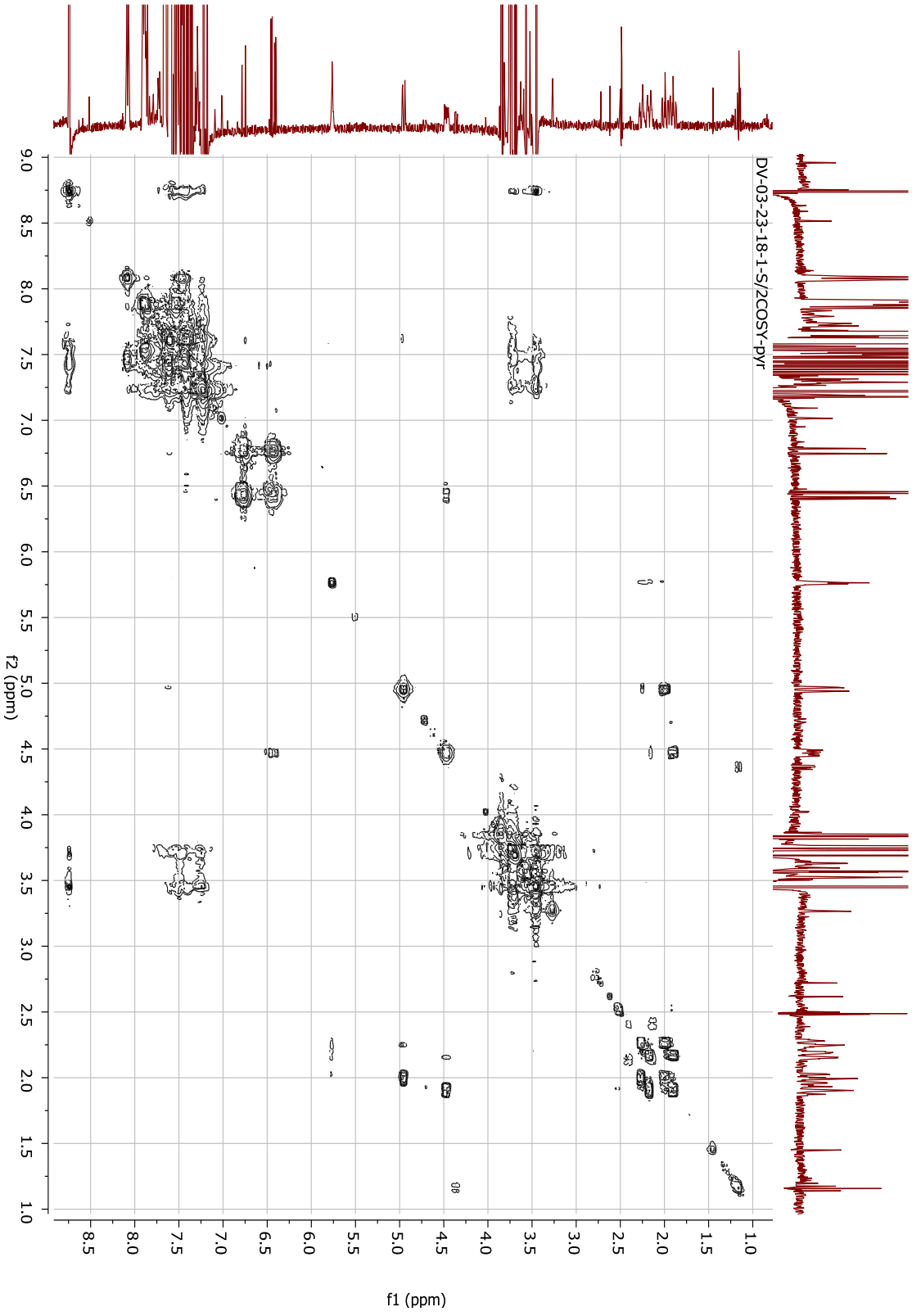

S42. ^{1}H NMR spectrum of the (*R*)-MTPA derivatives of **2**/**3** in pyridine-d_5

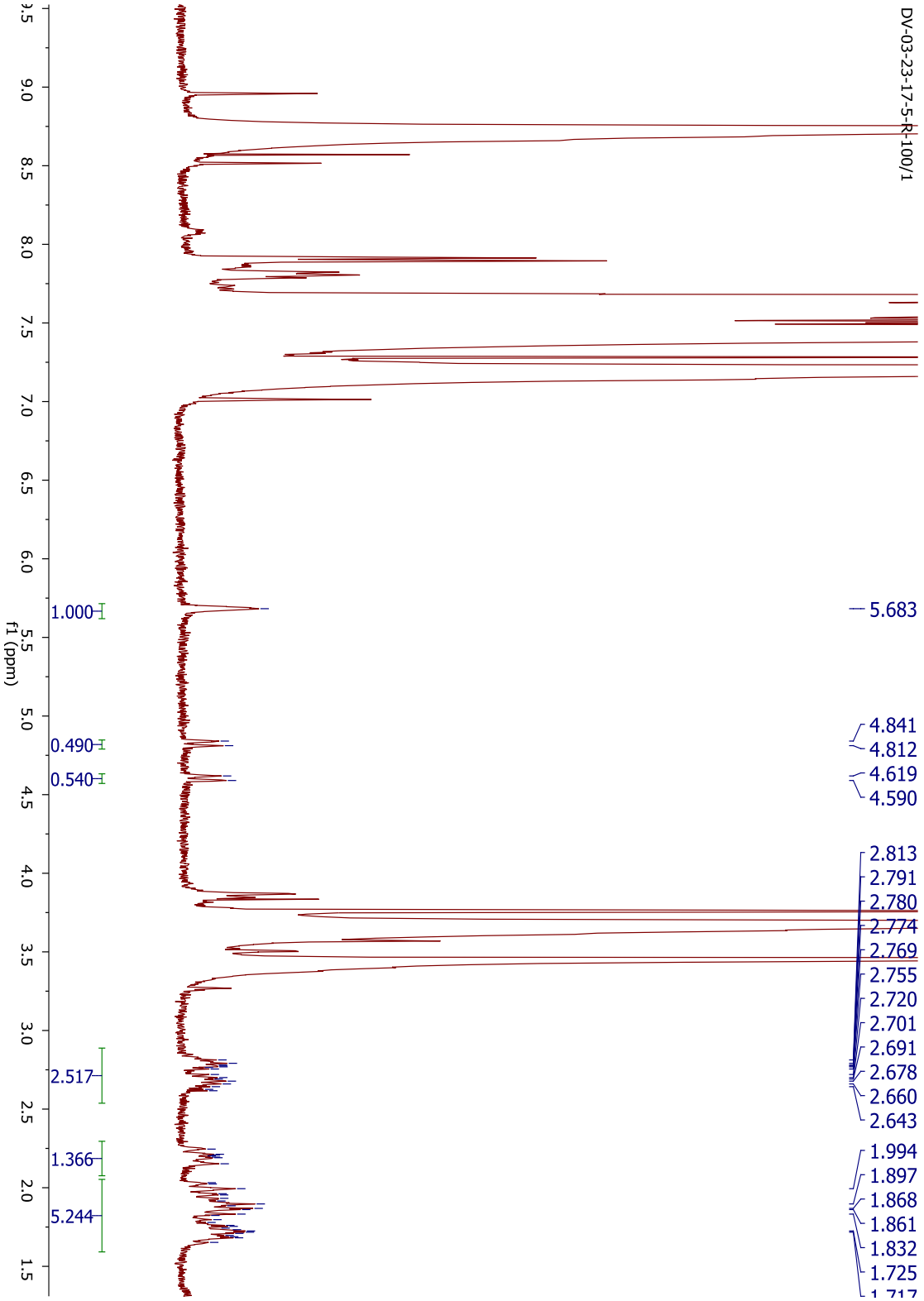

S43. ^{1}H NMR spectrum of the (*S*)-MTPA derivatives of **2**/**3** in pyridine-d_5

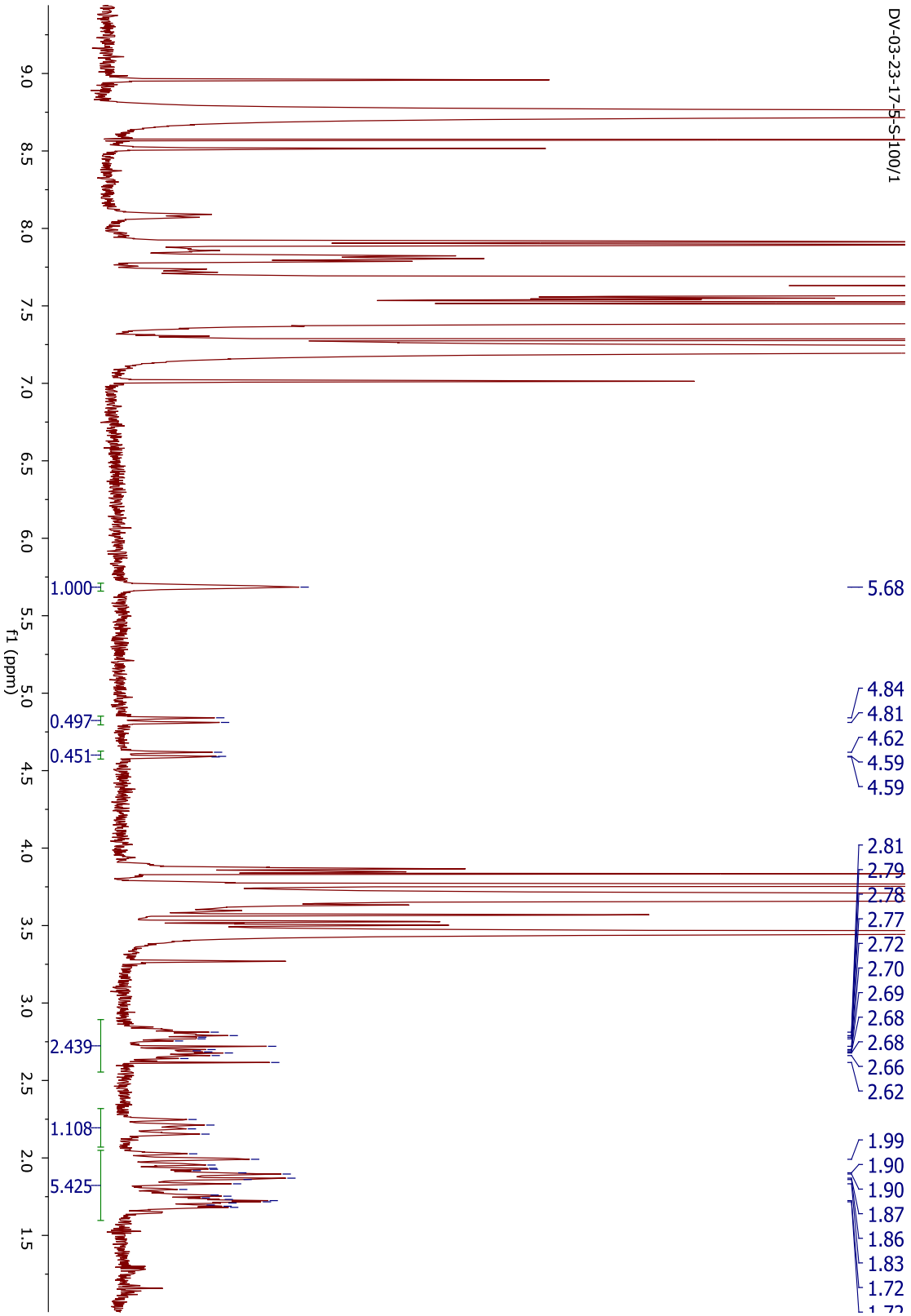

S44. ^{1}H NMR spectrum of the (*R*)-MTPA derivatives of **4**/**5** in pyridine-d_5

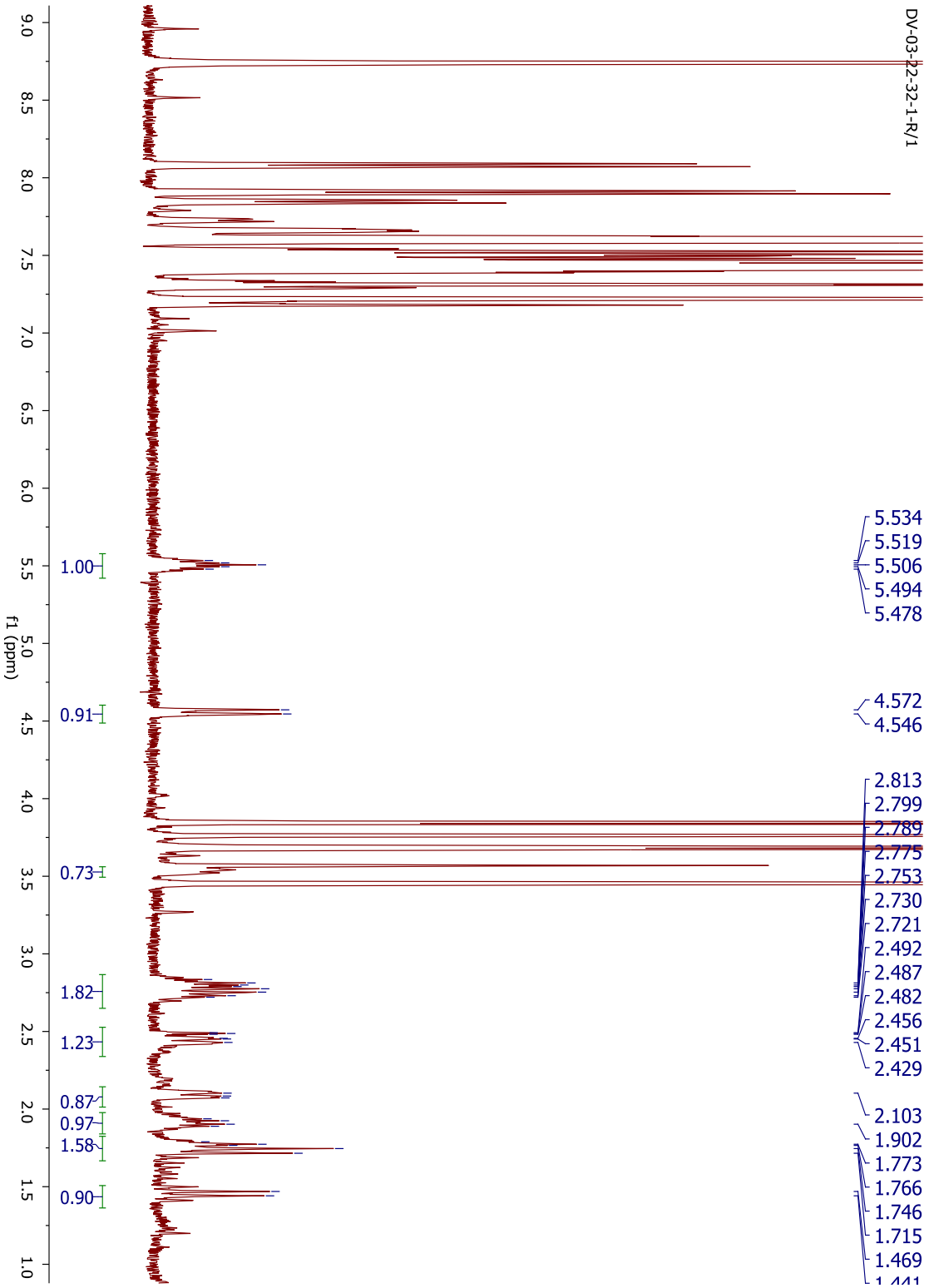

S45. ^{1}H–^{1}H COSY spectrum of the (*R*)-MTPA derivatives of **4**/**5** in pyridine-d_5

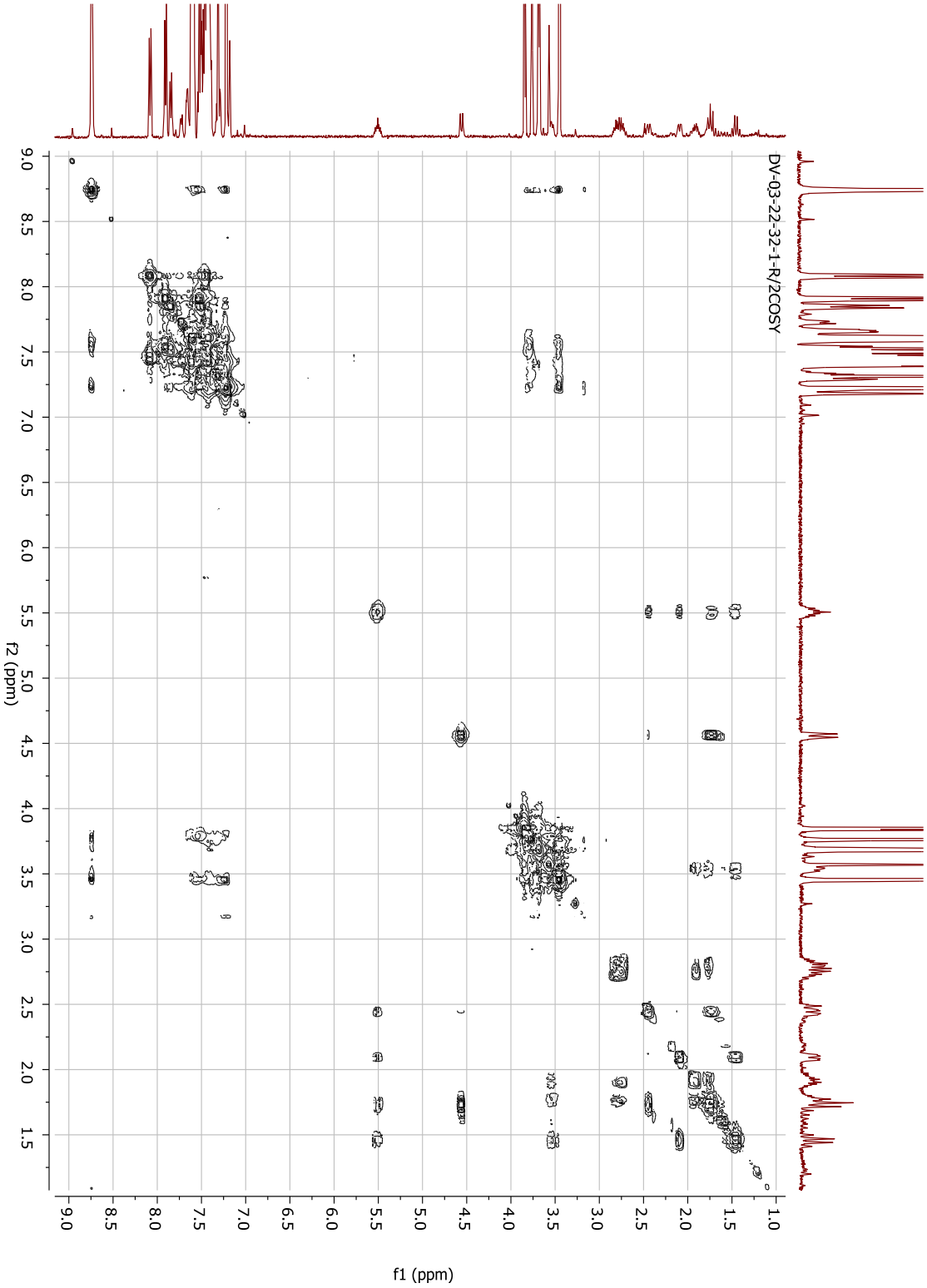

S46. ^{1}H NMR spectrum of the (*S*)-MTPA derivatives of **4**/**5** in pyridine-d_5

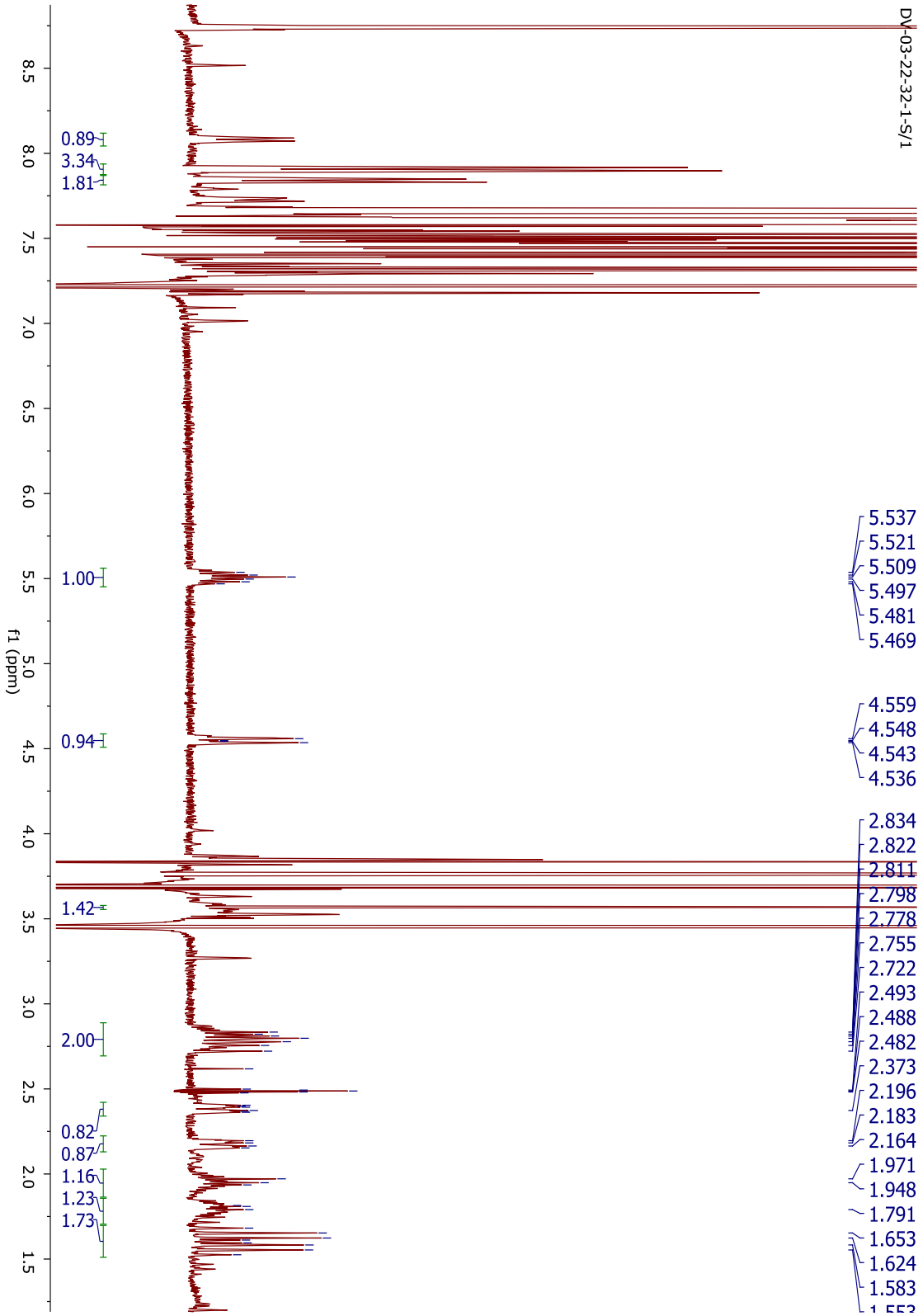

S47. ^{1}H–^{1}H COSY spectrum of the (*S*)-MTPA derivatives of **4**/**5** in pyridine-d_5

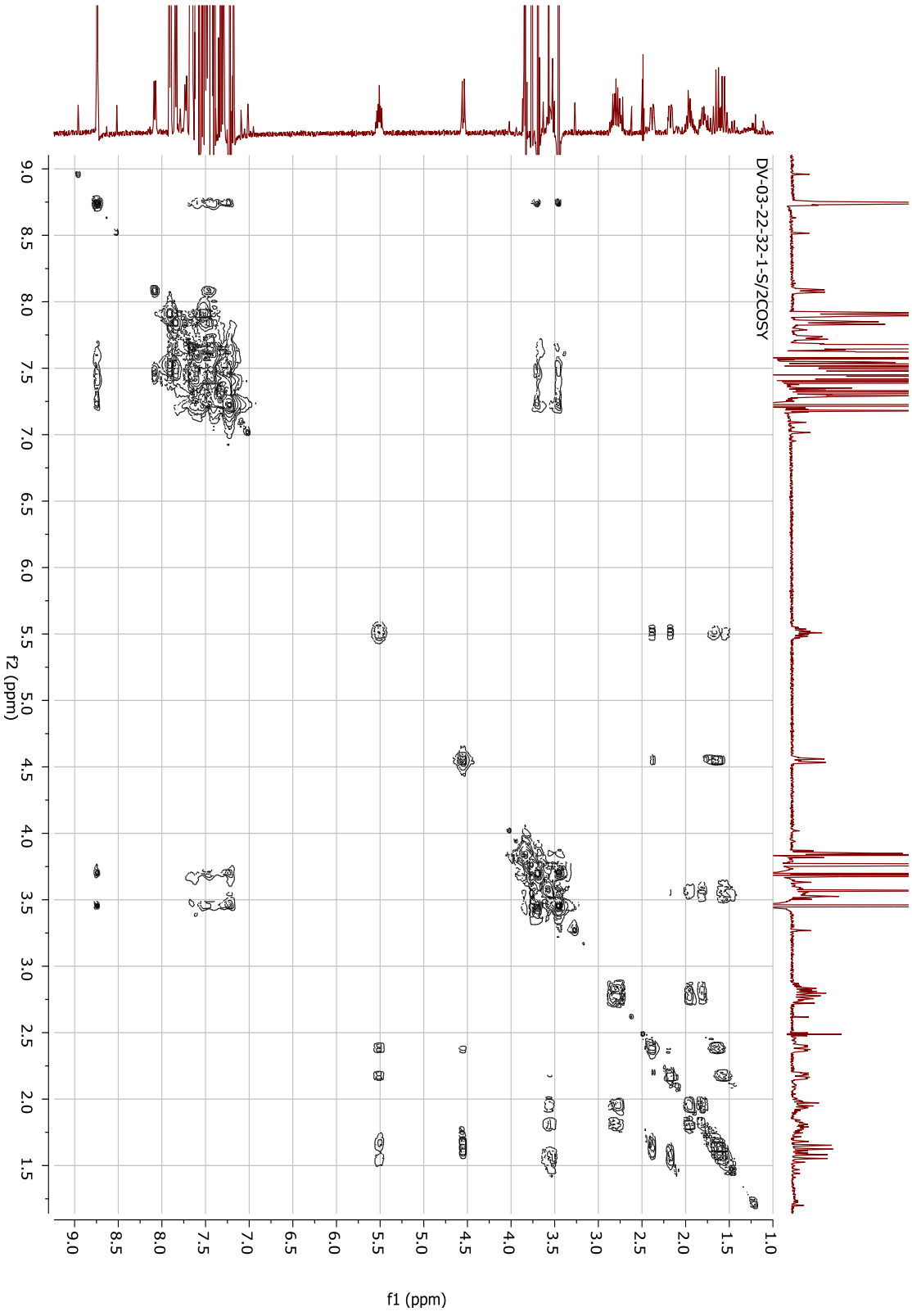

S48. ^{1}H NMR spectrum of the (*R*)-MTPA derivative of compound **6** in pyridine-d_5

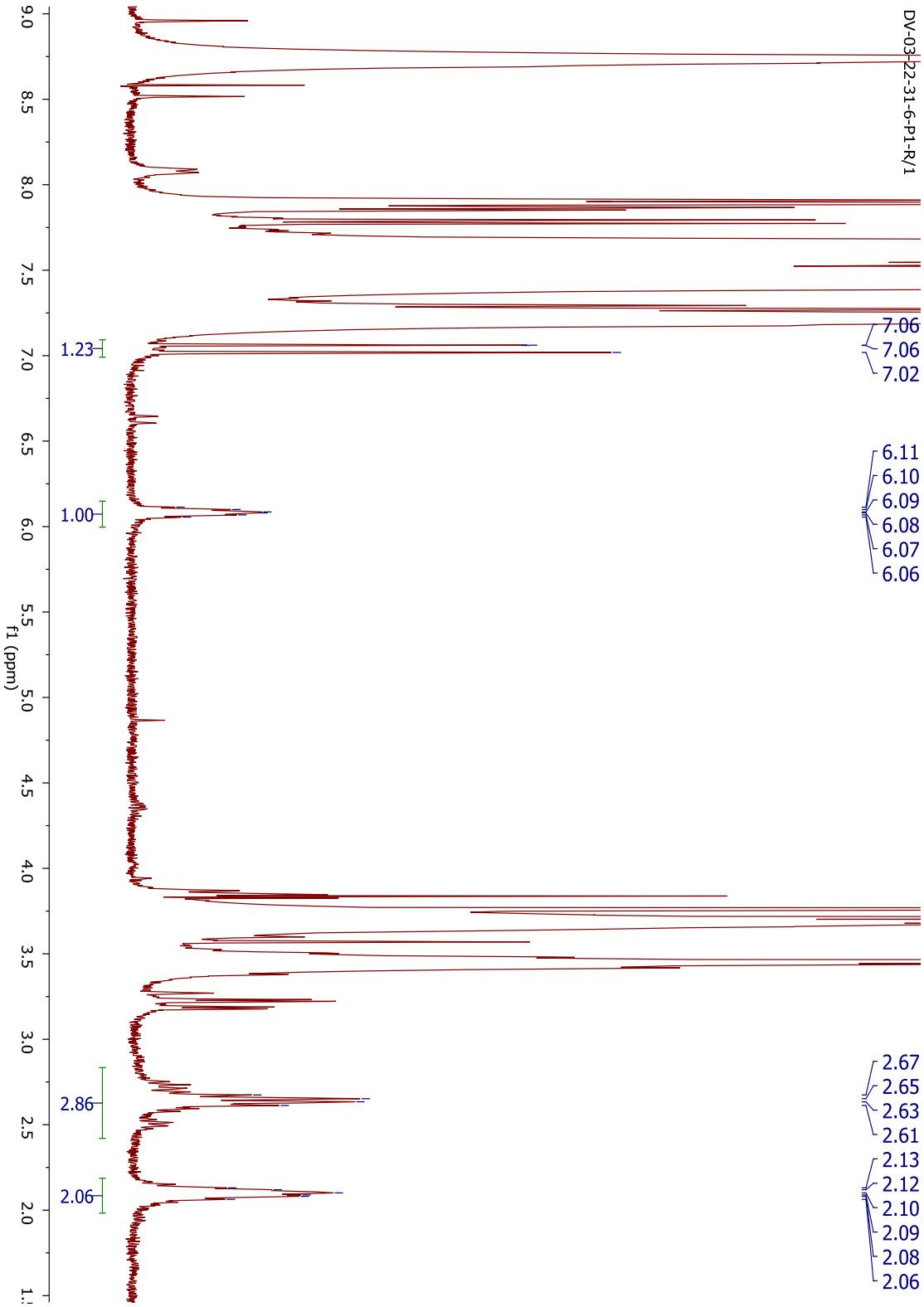

S49. ^{1}H–^{1}H COSY spectrum of the (*R*)-MTPA derivative of **6** in pyridine-d_5

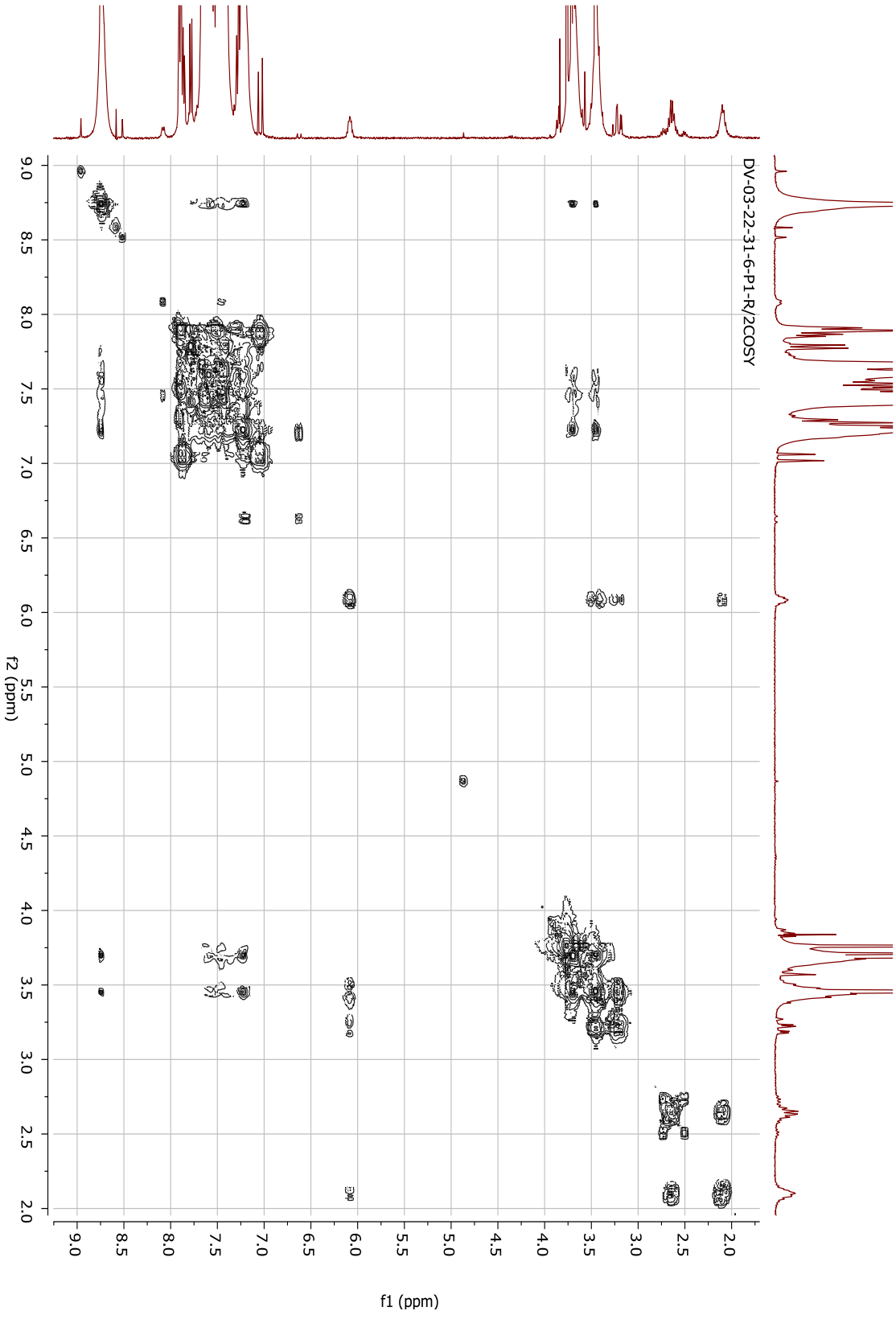

S50. ^{1}H NMR spectrum of the (*S*)-MTPA derivative of compound **6** in pyridine-d_5

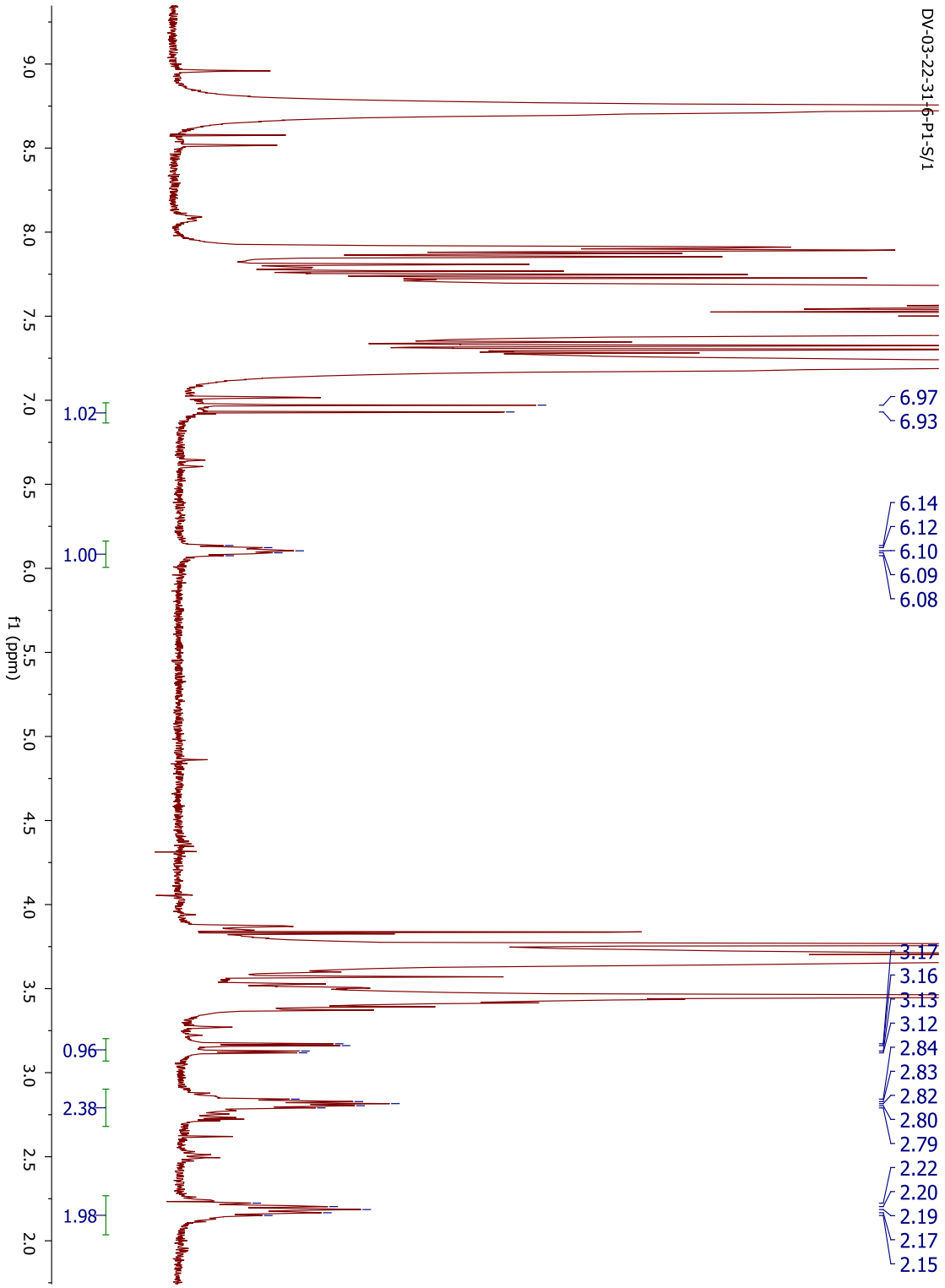

S51. ^{1}H–^{1}H COSY spectrum of the (*S*)-MTPA derivative of compound **6** in pyridine-d_5

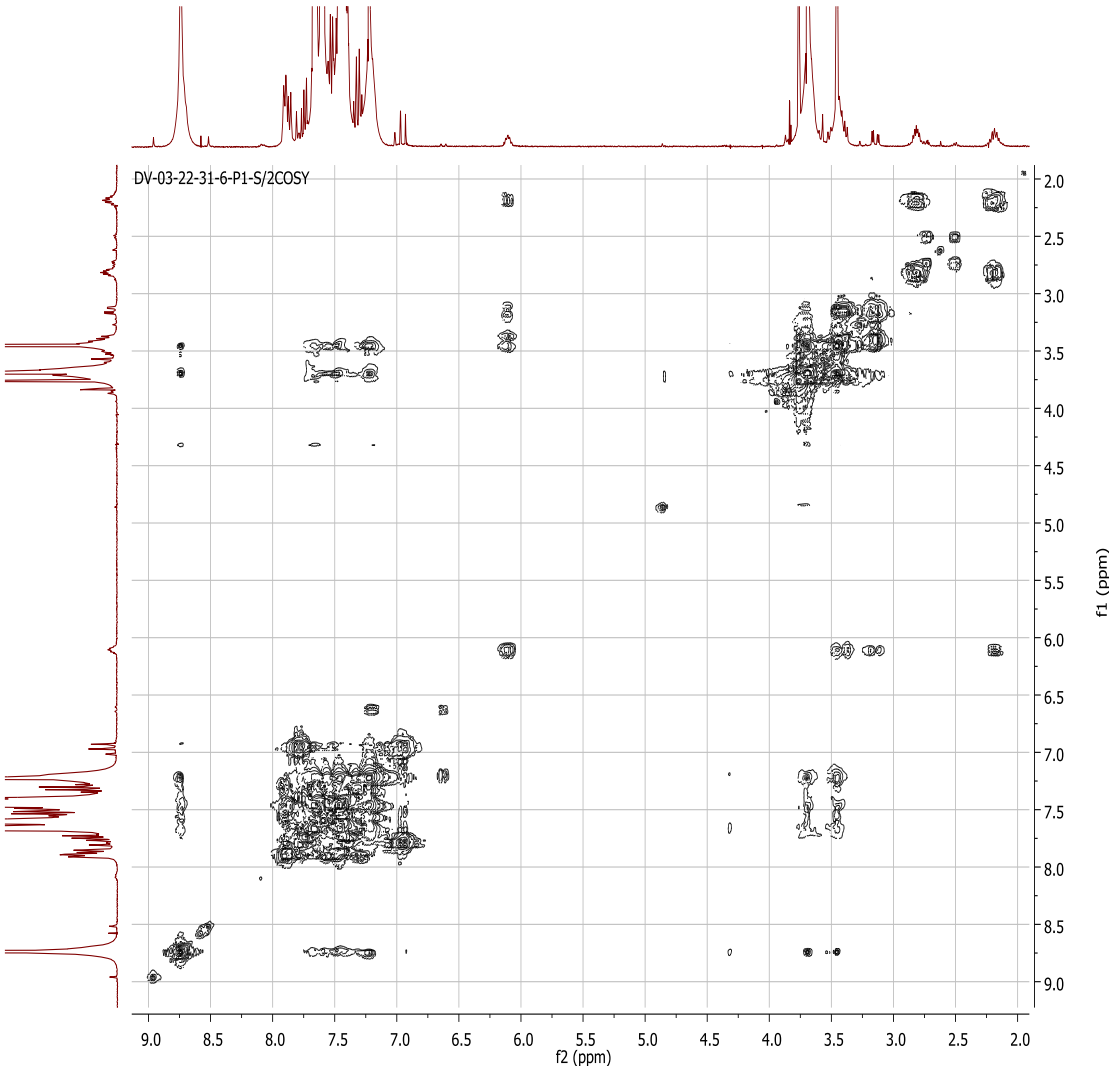

S52. ^{1}H NMR spectrum of the (*R*)-MTPA derivative of **8**/**9** in pyridine-d_5

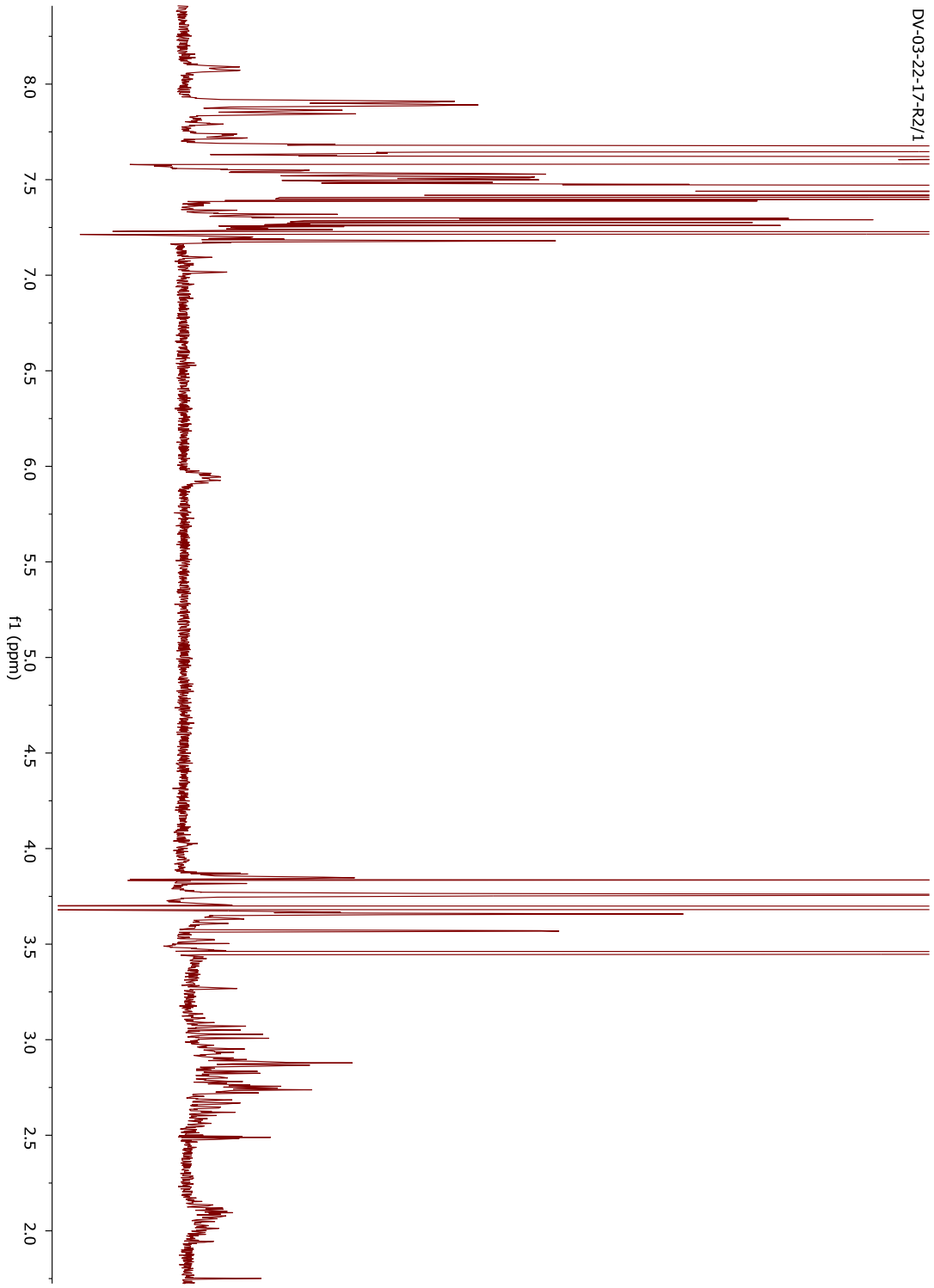

S53. ^{1}H–^{1}H COSY spectrum of the (*R*)-MTPA derivative of **8**/**9** in pyridine-d_5

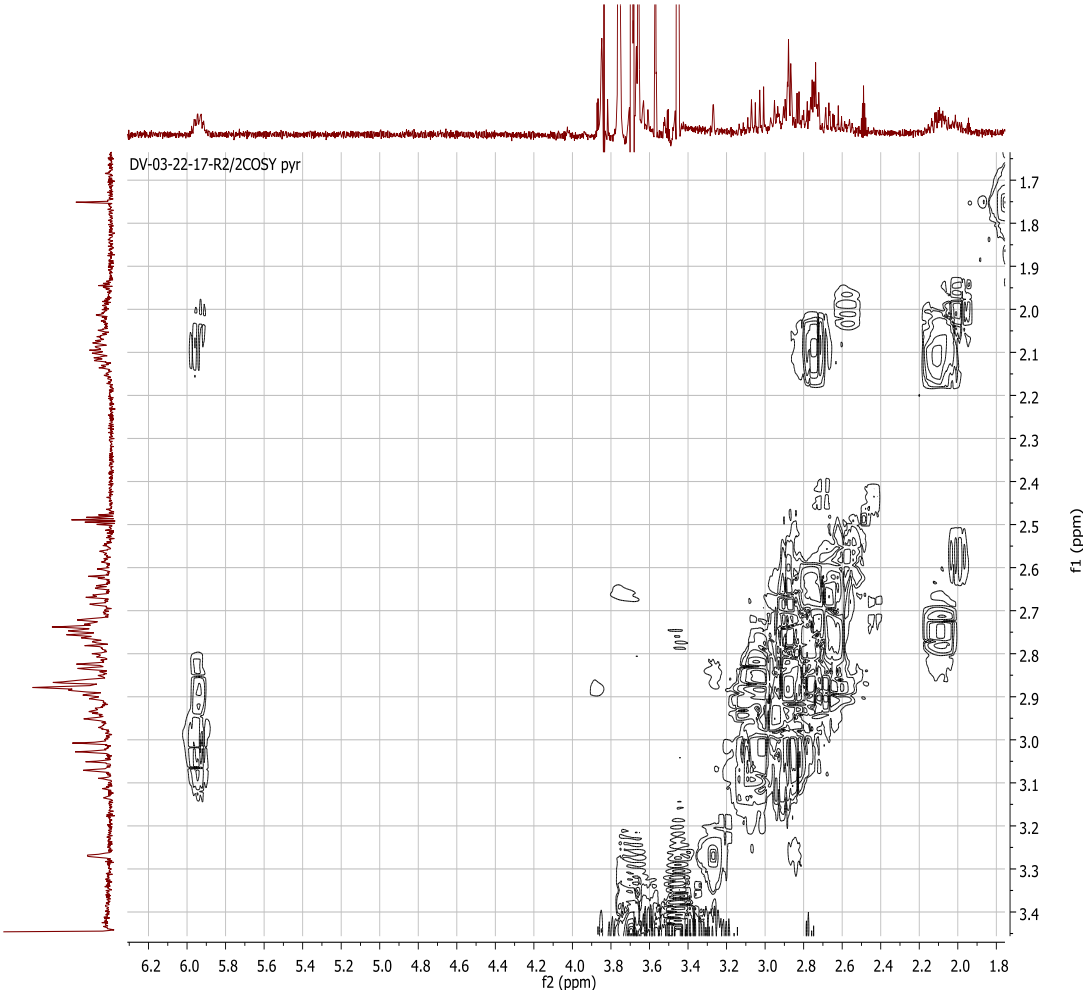

S54. ^{1}H NMR spectrum of the (*S*)-MTPA derivative of **8**/**9** in pyridine-d_5

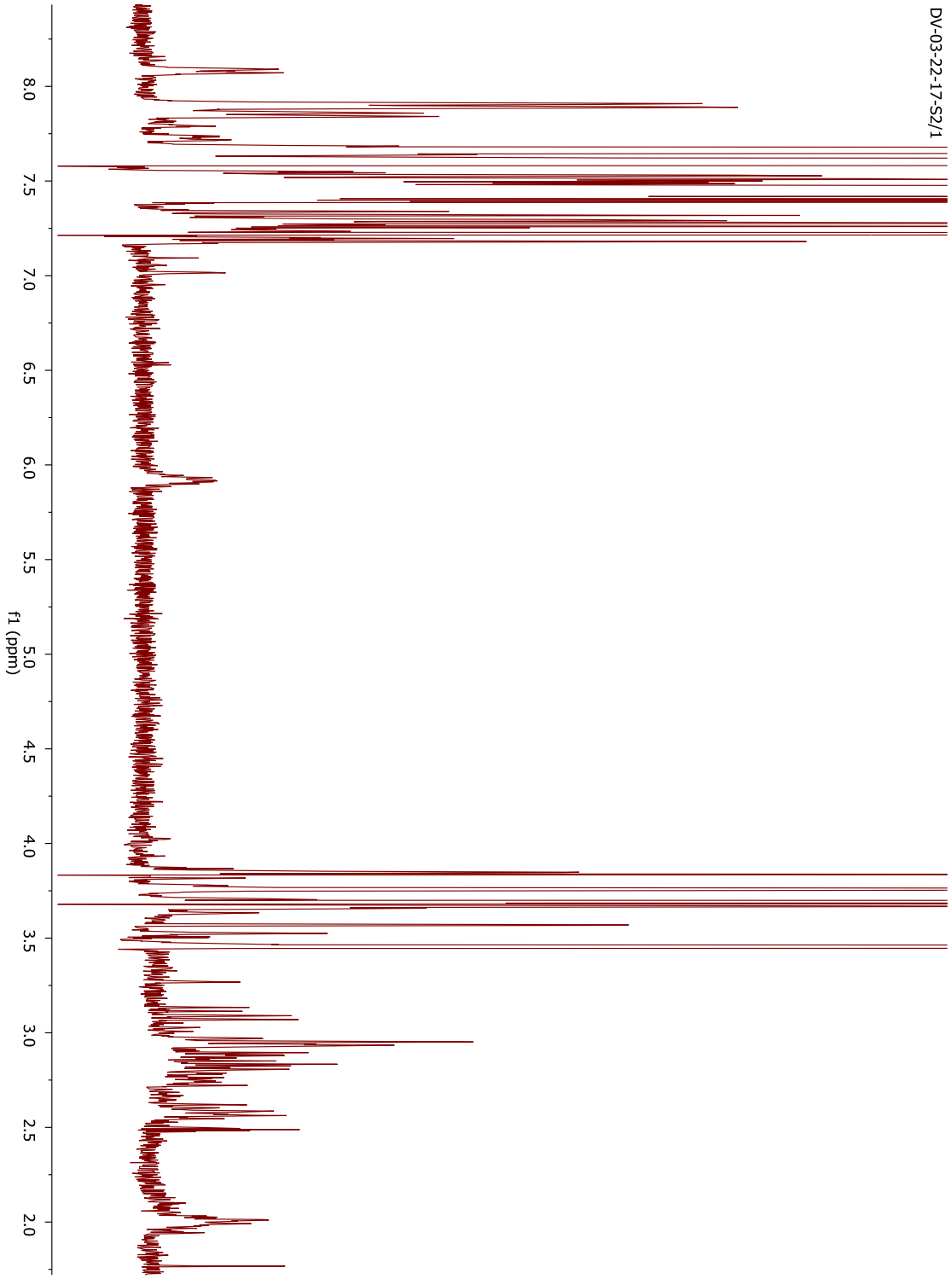

S55. ^{1}H–^{1}H COSY spectrum of the (*S*)-MTPA derivative of **8**/**9** in pyridine-d_5

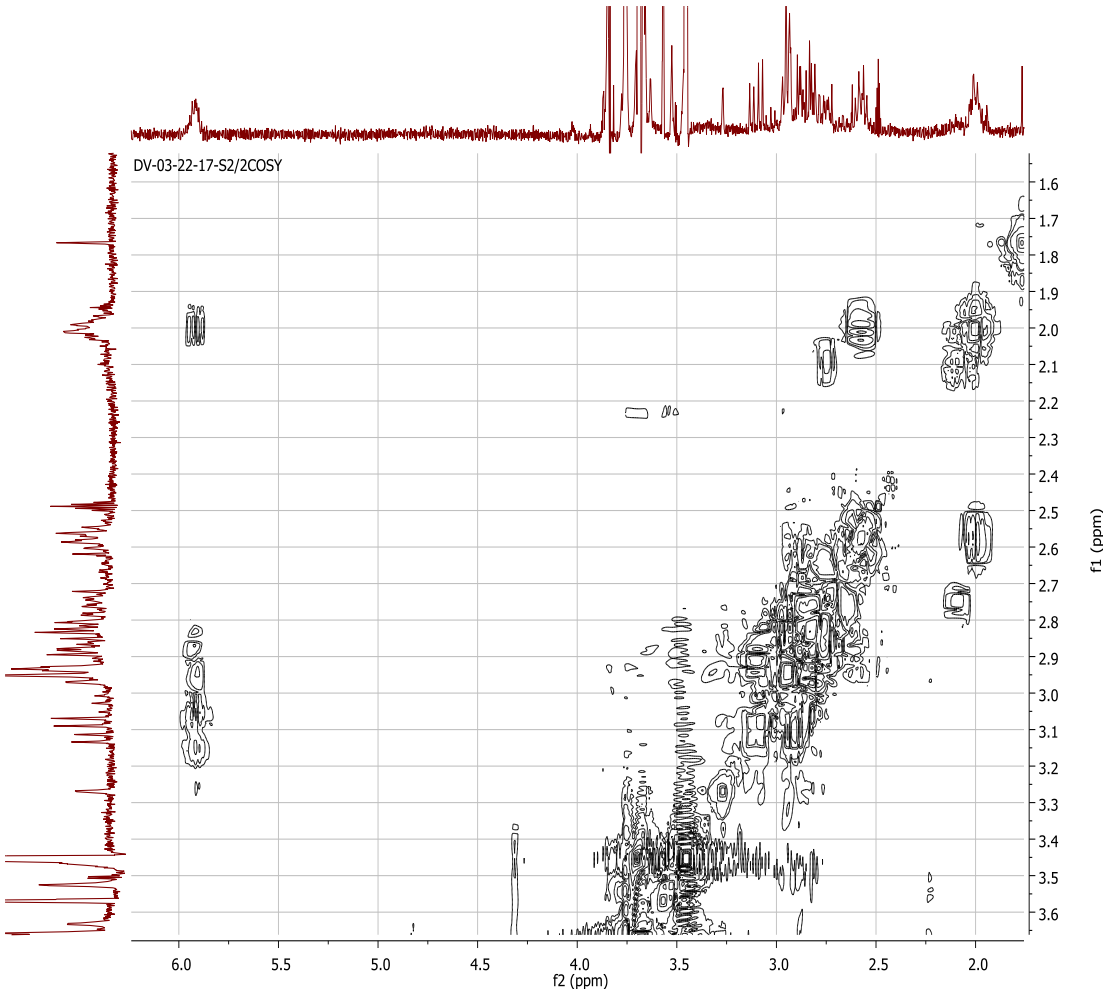

S56. ^{1}H–^{1}H COSY spectra of **1**, **10**, and **12** and the crude extract of BC-601 (6.0-8.5 ppm)*

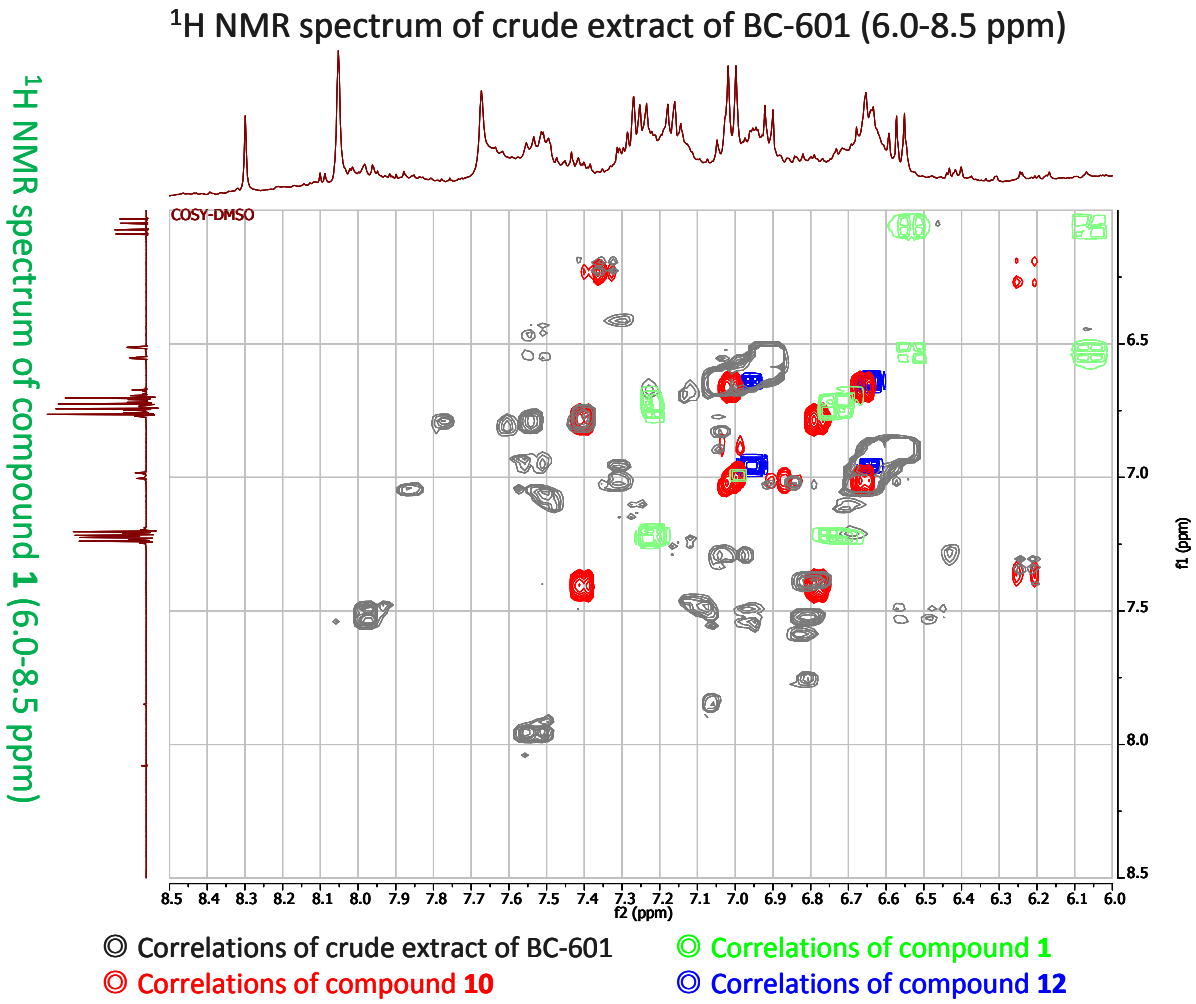

* Diagonal Suppression was applied on BC 601 spectrum